INVESTIGATING THE THERAPEUTIC EFFICACY OF A NOVEL INHIBITOR GAP-107B8 ON OVARIAN CANCER CELLS

By

Fu Jian Yan

This thesis is submitted to the Faculty of Graduate and Postdoctoral Studies at the University of Ottawa in partial fulfillment of the requirements for the degree of

Master of Science (Cellular and Molecular Medicine)

Department of Cellular and Molecular Medicine
Faculty of Medicine
Ottawa, Canada

June 2011

TABLE OF CONTENTS

ACKNOWLEDGEMENTS

Many people have been instrumental in helping me complete the requirements of my Master's degree program. First, I would like to thank my supervisor, Dr. Barbara Vanderhyden, for giving me an opportunity to work in her lab, and for encouraging me and guiding me through all aspects of my project. Many thanks also to Dr. Ken Garson, who was a great resource and with his help has made it possible to complete many aspects of this project. As our collaborators on this project, I would like to thank some PharmaGap personnel. Thanks to Simon Goulet and Isabella Steffensen for being great collaborators with us in the early phases of this project. Thanks to the current PharmaGap staff including Ricardo Mojica, Miranda Gonzalez, Jaclyn Chabot, and Ken Sokoll for their continued guidance on the project. I also want to extend my appreciation to my fellow members in the Vanderhyden lab who have been great colleagues and friends during my time in the lab: Lisa Turchet, Kendra Hodgkinson, Behnam Azadi, Kholoud Al-Wosaibai, Safa Alhejaily, Sara Rafferty, Laura Laviolette, David Pépin, Elizabeth Pitre, François Paradis, Valerie Bourada, Warren Meyers, Maria Merziotis, Emma Graham, and Sarina Scaffidi Argentina, and Zahra Sharif. I would like to thank Valerie Bourada for helping me get started in the lab and to Olga Collins, Elizabeth Macdonald, and Colleen Crane for using your various expertise to help my project along. Thanks to François Paradis for providing many handy suggestions during the time he was here. Thanks to Tom Tang for setting an admirable high ceiling for work ethic and helping me practice my Chinese. Thank you all for allowing me to be part of such an inclusive, supportive, and enthusiastic lab. I would not rather have been anywhere else. All of the students, scientists, and staff of the 3rd floor of the Cancer Centre all deserve

mention for contributing to such a great work environment. Last but not least, a giant thank you goes out to my family. Big thanks to my mom and dad, Xiaoyi and Ming. Mom, I really appreciate your continuous love and support and your awesome meals! Thanks to Donglin for all your support over the years and thanks to my brother Jeff, who has kept me grounded and focused on the right things.

ABSTRACT

Ovarian cancers often develop resistance mechanisms against the standard platinum and taxane chemotherapy, which indicates the need for novel therapeutics to improve patient outcome. *In vitro* assays were performed to assess the effects and mechanism of action of a novel peptide, GAP-107B8, on ovarian cancer cell viability. Xenograft models were used to determine GAP-107B8's effects on tumour burden in immune-incompetent mice. GAP-107B8 significantly reduced cell viability in ovarian cancer cell lines, although no synergistic effects with carboplatin were observed. This reduction in cell viability was due in part to apoptosis and may involve mechanisms leading to decreased pAKT, but without any change in pPKC levels. *In vivo,* GAP-107B8 had no effect on ovarian tumour burden, but significantly reduced ascites volume. The findings suggest that GAP-107B8 can reduce some malignant characteristics of cancer cells *in vitro* and *in vivo* and should be evaluated further as a potential therapeutic for ovarian cancer.

LIST OF FIGURES

LIST OF TABLES

LIST OF ABBREVIATIONS

α	alpha
β	beta
γ	gamma
δ	delta
ε	epsilon
ζ	zeta
η	eta
θ	delta
ι	iota
κ	kappa
λ	lambda
μ	mu
ν	nu
α-MEM	alpha minimum essential medium
Ac	acetate
A-loop	activation loop
aPKCs	atypical protein kinase Cs
ATM	aurothiomalate
ATP	adenosine-5'-triphosphate
BrdU	5-bromo-2-deoxyuridine
CA-125	cancer antigen 125
cDNA	complementary DNA
CD3	cluster of differentiation 3
cm	centimetre(s)
CO_2	carbon dioxide
cPKCs	conventional or classical protein kinase Cs
DAB	diaminobenzidine
DAG	diacylglycerol
DAPI	4', 6-diamidino-2-phenylindole
DBS:FBS	donor bovine serum: fetal bovine serum
ddH_2O	double distilled H_2O
D-MEM	Dulbecco's minimum essential medium
DMSO	dimethylsulfoxide
DN-Akt	dominant-negative Akt
DNA	deoxyribonucleic acid
EGFR	epidermal growth factor receptor
EOC	epithelial ovarian cancer
EpCAM	epithelial cell adhesion molecule

FBS	fetal bovine serum
FITC	fluorescein isothiocyanate
GAP-107B8	PharmaGap lead compound
GAP-107B8-D-Ac	PharmaGap lead compound (D-Isomer) with a acetate counterion
GAP-107B8-D-TFA	PharmaGap lead compound (D-Isomer) with a trifluoroacetate counterion
GAP-107B8-L-Ac	PharmaGap lead compound (L-Isomer) with a acetate counterion
GAP-107B8-L-TFA	PharmaGap lead compound (L-Isomer) with a trifluoroacetate counterion
GAP-107X8-L-TFA	PharmaGap lead compound (L-Isomer) without the protein transduction domain
H_2O	water
HM	hydrophobic-motif
HRP	horseradish peroxidase
IP	intraperitoneal
IT	intratumoural
IV	intravenous
kg	kilogram
µg	microgram(s)
µl	microlitre(s)
µm	micrometre(s)
µM	micromolar
M	molar
mAb	monoclonal antibody
mg	milligram(s)
MISIIR	Müllerian-inhibiting substance type II receptor
MISIIR-TAg	cell line derived from the ovarian tumour of a tgMISIIR-TAg mouse
ml	millilitre(s)
mm	millimetre(s)
mM	millimolar
MTORC2	mammalian target of rapamycin complex 2
MTT	microtetrazoline
NF-κB	nuclear factor kappa B
nm	nanometer
nPKCs	novel protein kinase Cs
PARP	poly (ADP-ribose) polymerase

PB1	Phox Bem 1
PBS	phosphate buffered saline
PDK1	phospho-dependent kinase 1
PDZ	PSD-95, disheveled and ZO1
PI	propidium iodide
PI3K	phosphatidylinositol 3-kinase
PICK1	protein Interacting with C Kinase 1
PKC	protein kinase C
PNA	peptide nucleic acid
PTD	peptide transduction domain
RACKS	receptors for activated C kinase
SCID	severe combined immunodeficiency
SEM	standard error of the mean
STICKS	substrates that interact with C kinase
TAg	large and small Simian virus 40 T antigens
TBST	tris-buffered saline Tween-20
TFA	trifluoroacetate
tgMISIIR-TAg	transgenic MISIIR-TAg mouse model of ovarian cancer
TM	turn-motif
TUNEL	terminal deoxynucleotidyl transferase dUTP nick end labeling
TVS	transvaginal sonography
VEGF	vascular endothelial growth factor
VEGF-A	vascular endothelial growth factor A
wt	wild type

Chapter 1: INTRODUCTION

1.1 Ovarian cancer: General overview

About one of every 70 women develops ovarian cancer, making it the sixth leading cause of death and the most lethal gynaecological malignancy in women (Canadian Cancer Society, 2011). The low survival rate is attributed to a lack of specific symptoms in addition to a lack of an effective screening method. Symptoms such as bloating, nausea, early satiety and abdominal distension are shared with many other common gastrointestinal conditions (Bankhead et al., 2008; Bast et al 2009). Screening tools such as transvaginal sonography (TVS) and monitoring of cancer antigen 125 (CA-125) are available, but these are only reliable methods to detect advanced or recurrent disease. These factors result in the majority of ovarian cancer cases to be diagnosed at a late stage, when metastasis has occurred, and when treatment is more difficult.

Ovarian cancer is characterized by the presence of solid intra-peritoneal tumours and the accumulation of ascites. Malignant ascites is defined as an abnormal accumulation of fluid in the peritoneal cavity occurring in association with a wide variety of neoplasms, including ovarian cancer (Runyon et al., 1994). There are multiple causes of malignant ascites in ovarian cancer, but a detailed molecular understanding is still incomplete. Obstruction of lymphatic vessels, increases in vascular permeability, and secretion of vascular endothelial growth factor (VEGF) by tumour cells are all hypothesized to contribute to the accumulation of fluid in the abdominal cavity (Garrison et al., 1987; Adam and Adam, 2004; Senger et al., 1983; Kobold et al., 2009). The presence of ascites is believed to be the clinical presentation of end-stage disease (Liao et al., 2011).

1.2 Ovarian cancer: Classification

1.2.1 Staging

Ovarian cancer is categorized into four stages of increasing severity: confined to the ovaries (stage I), spread but confined to pelvic organs (stage II), metastasized outside of the pelvic region, mainly in lymph nodes (stage III), or metastasized to distant sites outside of the peritoneal cavity, including the bowel, omentum and liver (stage IV) (Bast et al., 2009; Murdoch and McDonnel, 2002).

1.2.2 Subtypes

Different cell types are known to give rise to cancer of the ovary, resulting in different subtypes. The majority (90%) of ovarian cancers derives from epithelial cells and is called epithelial ovarian cancer (EOC) (Bast et al., 2009; Ji et al., 2008). Unlike most cancers, EOC becomes more differentiated as it progresses, resulting in four main subtypes that each resembles a particular section of the female reproductive tract. The serous, mucinous, endometrioid and clear cell tumours resembles fallopian tube, cervical, endometrium and vaginal epithelium, respectively (Auersperg et al., 2001; Bast et al., 2009; Bell, 2005; Bowtell, 2010; Kobel et al., 2008). Each subtype of EOC differs in its risk factors, gene expression, and response to therapy (Bast et al., 2009; Kobel et al., 2008).

1.2.3 Grading of serous EOC

The most common subtype, serous EOC, is subdivided into two grades associated with the pathway taken to malignancy (Shih and Kurman, 2004; Vang et al., 2009). In general, Type I progresses slowly in a step-wise fashion from a benign cystadenoma to an invasive low grade serous tumour, while Type II progresses rapidly resulting in high

grade tumours (Shih and Kurman, 2004). Type I is characterized by mutations in *KRAS*, *BRAF*, or *ERBB2*. Type II mutations are characterized by high DNA copy number changes, TP53 mutations, and BRCA1 dysfunction (Bowtell, 2010; Shih and Kurman, 2004; Vang et al., 2009). The two grades of serous EOC differ in age at diagnosis and response to chemotherapy (Vang et al., 2009) and high grade is more common than the low grade EOC (Seidman et al., 2006).

1.3 Diagnosis and treatment of ovarian cancer

1.3.1 Ovarian cancer screening

Ovarian cancer has vague symptoms that are often misattributed or overlooked before a diagnosis is made. The peritoneal location of the ovaries limits the ability to detect any abnormalities early. The disease initially responds well to cytoreductive surgery and chemotherapy, and if the disease is confined to the ovaries (stage I), a 90% cure rate can be attained. However, less than 20% of women with advanced ovarian cancer (stage III and IV) can be cured (Das et al., 2008). To date, there is no reliable method of detecting early ovarian cancer. CA-125 is the most notable serum marker involved in ovarian cancer, but it lacks sensitivity and specificity to be used alone on a single occasion for early detection of ovarian cancer (Bast et al., 1983).

Greater specificity can be achieved by combining CA-125 and TVS, or monitoring CA-125 levels over a period of time. Early data from a large trial in the U.K. suggests that monitoring CA-125 levels to prompt TVS could increase the detection of the disease at early stages and provide adequate sensitivity (89.4%) and specificity (99.8%) (Menon et al., 2009).

Furthermore, since only approximately 80% of ovarian cancers express CA- 125, additional biomarkers are required. Whey-associated four-disulphide core domain protein 2 (WFDC2), which may be transcriptionally upregulated by nuclear factor-κB (NF-κB), is a promising candidate (Bouchard et al., 2006). Another report showed that at the tissue level, combining four or five biomarkers enabled researchers to identify more than 95% of ovarian cancers (Lu et al., 2004), suggesting that the use of a panel of biomarkers could enhance the level of detection.

1.3.2 Current standard of care

Ovarian cancer is one of the few cancers where surgical debulking is still indicated even though it may not be possible to remove all tumours (Bast et al., 2009). After cytoreductive surgery, an intravenous (IV) chemotherapy regimen of taxanes and platinum based agents is currently the first-line treatment option. Although most countries still choose the IV delivery route, a study by the Gynecologic Oncology Group has raised some interesting findings. A randomized, Phase 3 clinical trial comparing IV and intraperitoneal (IP) administration of a combination of standard chemotherapeutic agents showed that the median duration of progression-free survival in the IV-therapy and IP-therapy groups was 18.3 and 23.8 months, respectively, and that the median duration of overall survival in the IP-therapy group was 15.9 months longer than the IV-therapy group (Armstrong et al., 2006). Despite the criticism of the IP study design, the National Cancer Institute reviewed the studies done in 3 large randomized trials which showed significant survival benefits of IP treatment and announced that clinicians should now consider IP chemotherapy as an option for front-line treatment.

Unlike the underlying cancer, there is currently no generally accepted evidence-based guideline for the management of malignant ascites. A number of methods have been practiced, the most commonly used procedures being paracentesis and a combination of diuretics and reducing sodium intake (Lee et al., 1998). Other treatment options include peritovenous shunts and IP chemotherapy. Recently, a new trifunctional monoclonal antibody to cluster of differentiation 3 (CD3) receptor and epithelial cell adhesion molecule (EpCAM) called Catumaxomab given IP has shown symptom relief in patients with ovarian cancer and malignant ascites (Ströhlein et al., 2009). Because of the role of vascular endothelial growth factor (VEGF), VEGF inhibitors like Bevacizumab (Avastin™) have also received attention. The biggest problem facing the potential treatment options is the fact there are no randomized controlled trials evaluating safety and assessing efficacy in malignant ascites. Therefore, there is still a need for evidence supporting agents that can effectively provide symptomatic relief in the treatment of malignant ascites.

1.3.3 Targeted therapies: General

When exposed to chemotherapeutic agents, ovarian cancer cells can alter their gene expression and frequently develop resistance mechanisms (Konstantinopoulos et al., 2008). Therefore, other methodologies to treat these tumours are the focus of current research. Targeted therapies are one of these new methodologies. In contrast with traditional chemotherapeutics, targeted therapies inhibit stroma, vasculature or cell signaling pathways aberrant in tumour tissue, thus enhancing selectivity and reducing toxicity to normal tissue (Blagden et al., 2009). Targeted therapies including small

molecule inhibitors or monoclonal antibodies (mAbs) directed against protein kinases are attractive treatment options either alone or in combination with standard chemotherapy.

Protein kinases play an integral part in the signaling within a cell. The human genome encodes approximately 600 kinases, with 100-200 expressed in any given cell. It is their "druggable" nature that has enabled validation at the biochemical, cellular and *in vivo* levels (Traxler et al., 2003). There have been many successes in the development of small molecule inhibitors, including Imatinib (Gleevec®) and Erlotinib (Tarceva®). Imatinib is a specific tyrosine kinase inhibitor that acts by competitive inhibition of the ATP binding site of Bcr-Abl and is used for the therapy of patients with chronic myelogenous leukaemia and gastrointestinal stromal tumours. Erlotinib is a selective epidermal growth factor receptor (EGFR) kinase inhibitor indicated in pancreatic, lung and head and neck cancers (Traxler et al., 2003).

Monoclonal antibodies have also been used in the clinic. The monoclonal human epidermal growth factor receptor-2 antibody trastuzumab (Herceptin®) has been successfully implemented in breast cancer. The VEGF inhibitor Bevacizumab has improved clinical outcome in a wide spectrum of malignancies, including breast, colon cancer, and ovarian cancer (Frederick et al., 2009; Hurwitz et al., 2004; Miller et al., 2007).

1.3.4 Targeted agents in ovarian cancer therapy

Although many agents have failed to show sufficient efficacy, some notable targeted therapies are currently in clinical trials in ovarian cancer. Anti-VEGF strategies are one of the promising avenues based on molecular understanding of tumour angiogenesis. Angiogenesis refers to the process of new blood vessel formation in order to supply a

growing tumour with adequate oxygen and nutrients. This process is achieved when the tumour upregulates expression of pro-angiogenic growth factors such as VEGF and the VEGF receptor (Hanahan and Folkman, 1996).

Inhibition of VEGF is a proven therapeutic strategy that is most commonly used in conjunction with cytotoxic chemotherapeutic agents. However, single agent anti-angiogenics are quite effective as monotherapies in epithelial ovarian cancers. As mentioned above, Bevacizumab is a monoclonal antibody directed against vascular endothelial growth factor receptor A (VEGF-A). Two Phase II clinical trials using Bevacizumab, the second trial consisting of only platinum resistant patients, demonstrated promising results. The two studies demonstrated objective response rates of 21% and 16% respectively, with 52% and 64% achieving stable disease and a median progression-free survival (PFS) of 4.4 and 4.5 months respectively (Burger et al., 2007; Cannistra et al., 2007).

Another VEGF inhibitor monotherapy study involved the VEGF Trap, which is a fusion protein that acts to bind VEGF-A and neutralize all VEGF-A isoforms. When given to patients with recurring ascites, twice-weekly intravenous administrations of the drug were found to reduce the frequency of paracentesis required in 8 out of 10 patients (Colombo et al., 2008).

An alternative targeted therapy in ovarian cancer takes advantage of the concept of synthetic lethality. While patients with an inherited mutation in the tumour suppressor *BRCA1* are known to be predisposed to breast cancer, it was noted these patients also have a 40% increased risk of developing ovarian cancer by 70 years of age (Sowter and Ashworth, 2005). Among the many functions of *BRCA1* is its role within the DNA

damage repair pathway, in which BRCA1 is involved in recognition and repair of double-strand DNA breaks by homologous recombination (Wang et al., 2000). Poly (ADP-ribose) polymerase (PARP) is an enzyme involved in repair of DNA single-strand breaks using the base excision repair pathway. Synthetic lethality in this instance involves the blocking of PARP in addition to the *BRCA1* mutations, thus not allowing the repair of double strand breaks to occur, leading to chromosomal instability and ultimately, cell death (Tutt et al., 2005; Ashworth et al., 2008). A Phase I trial with the oral PARP inhibitor Olaparib on patients who were largely platinum resistant or refractory to standard therapy, has shown a 44% partial response and a 25% rate of stable disease. Toxicity was mild, consisting of gastrointestinal symptoms and fatigue and a Phase II trial is now ongoing (Yap et al., 2007; Fong et al., 2008).

1.3.5 Targets and pathways in ovarian cancer

Recently, there has been a recognition that targeting specific oncogenes may be less effective than targeting key signaling pathways which are commonly activated in cancer. There at least seven signaling pathways activated in >50% of ovarian cancers. The phosphatidylinositol 3-kinase (PI3K) pathway is activated in the majority of ovarian cancers, and its activation is associated with resistance to cytotoxic chemotherapy. It is involved in mediating an anti-apoptotic response, aiding chemotherapy resistance by interacting with the apoptosis inhibitor survivin and blocking p53 response to pro-apoptotic stimuli (Fraser et al., 2008; Xing et al., 2008). Inhibitors of PI3K and Akt prevent growth of tumours in ovarian cancer xenografts and enhance the effects of both platinum and taxane chemotherapeutic agents (Hu et al., 2002). Other pathways which play a role in ovarian cancer include the IL-6-JAK2-STAT3 and lysophosphatidic acid

signaling cascades, resulting in efforts to develop inhibitors for different components in these cascades (Burke et al., 2011, Beck et al., 2008).

1.4 Rational peptide drug design

Peptide-based therapeutics possess advantages such as specificity and affinity compared to small molecules. However, their low resistance to serum and tissue proteases in the body, rapid clearance by the kidneys, and the difficulty in maintaining potency inside the cell remain as hurdles to commercial interest in peptides (McGregor, 2008; Foerg et al., 2008).

Nevertheless, there are a number of computational methods for the rational design of peptide modulators of protein-protein interactions. Peptides, unlike small synthetic molecules, can be designed using sequence-based strategies. Peptides, however, are large in size and are highly flexible, presenting challenges for the conventional computational docking approaches that rely on the usually small number of rotatable bonds in typical molecules. Both sequence-based and structure-based approaches are used to design peptides. The approaches described below are schematically represented in **Figure 1** (Rubinstein and Niv, 2009).

1.4.1 Sequence-based approaches

Sequence-based strategies involve either mimicking a binding partner, or finding an optimal synthetic peptide by a wide-scale screen. One popular strategy is to mimic the sequence of one of the interacting proteins. Most protein kinase inhibitors are small molecules that disrupt the adenosine-5'-triphosphate (ATP) binding of their target kinase (Sebolt-Leopold and English, 2006; Bozulic et al., 2007). Recently, alternative approaches have considered targeting the protein-protein interactions.

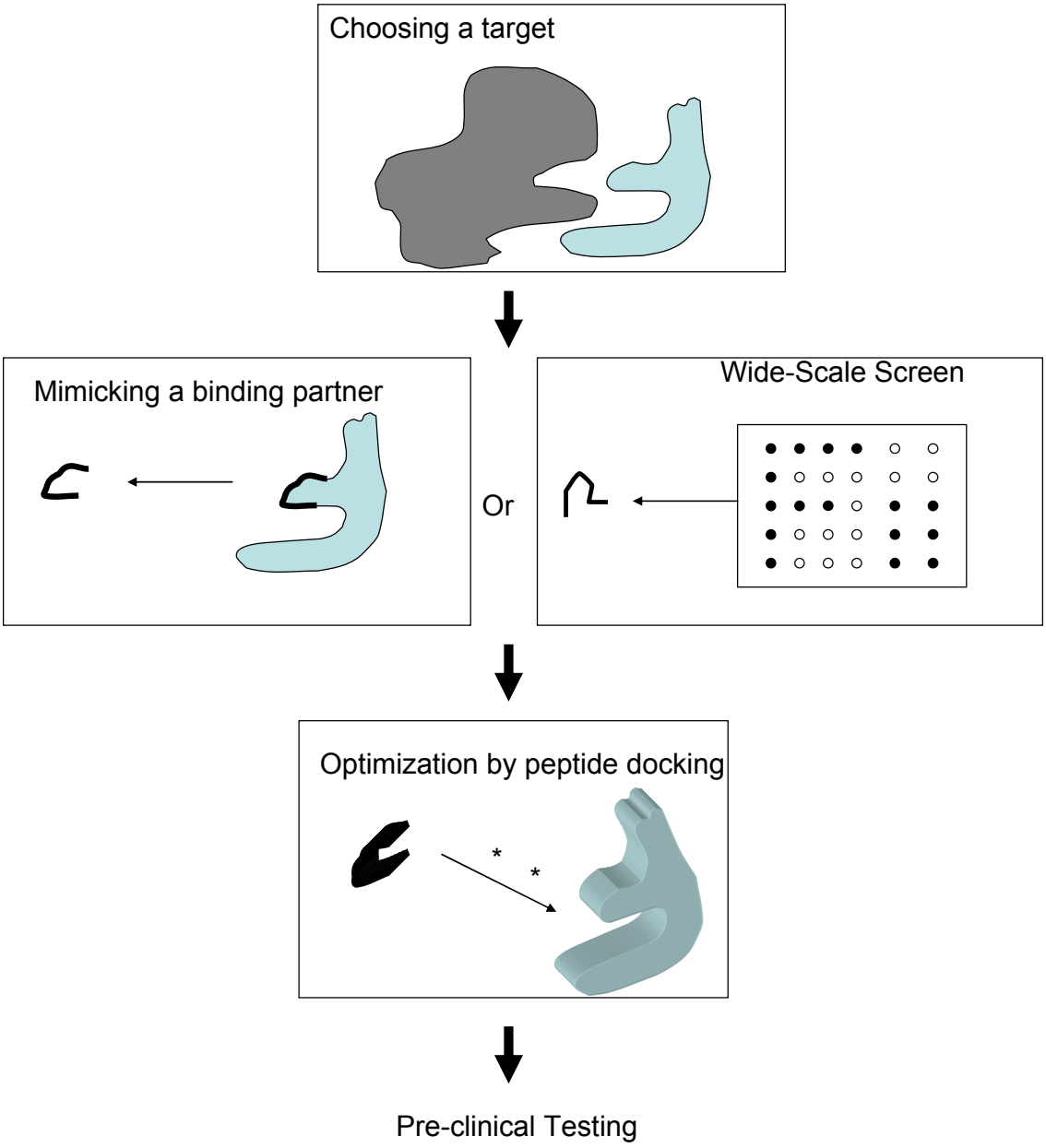

Figure 1. Schematic representation of some approaches used in drug development.

Adapted from Rubinstein and Niv (2009).

Copying either the substrate or the substrate-binding regions of kinases are effective strategies that have been described. For instance, the sequence of the insulin-like growth factor 1 activation loop was used as a pharmacophore template to be mimicked by new macrocyclic molecules (Qvit et al., 2008). Perhaps the best result of this design process is an anti-HIV drug called Enfuvirtide (Fuzeon®). It is a synthetically produced peptide and one of the success stories that reinvigorated research in the design of peptide drugs. It is a Food and Drug Administration approved drug that was derived from a continuous sequence within one of the domains of the gp41 transmembrane protein, which is part of the HIV-1 envelope that mediates HIV-cell fusion (Cooper and Lange, 2004). Enfuvirtide disrupts the fusion process between host and viral membranes (Cooper and Lange, 2004).

A wide-scale screen can also be employed to find an optimal synthetic peptide. These screens can be random (Hong et al., 2008) or biased (Qvit et al., 2008) peptide libraries of up to 20 amino acids in length (Henderson and Bradley, 2007). Here, the protein ligand is allowed to select the best-fitting structures from a large population such as a combinatorial library of diverse molecules. The strategy does not rely on prior structural information, and therefore results in the possibility of new molecules that may not necessarily resemble the native ligands of the protein, but nevertheless are selected to effectively block the protein-protein interaction (Eichler, 2008). This approach develops mimotopes; peptides that mimic antibody epitopes or other protein binding sites. These mimotopes are usually identified using phage display peptide libraries (Sebolt-Leopold and English, 2006).

1.4.2 Structure-based strategies

The use of the resolved 3D structures of signaling proteins, preferably in complex with their ligands, vastly aids the design process of interacting peptides. Furthermore, site-directed mutagenesis helps identify important protein amino acid residues essential for ligand binding. Once a binding site has been located, the challenge of mimicking it lies in being able to present it in a spatial arrangement that is recognized by the ligand. This process often includes attempts to not only mimic the amino acid sequence of the binding site, but also stabilize its ligand-binding conformation. One of the key challenges in structure-based design is that peptides have far greater degrees of freedom than small molecules, so accounting for this in a computational prediction is essential. Conformational plasticity of the protein is also paramount to consider, since some protein-protein interactions stabilize the inactive form of the protein (Rubinstein and Niv, 2009).

1.4.3 Lead compound optimization

Finally, docking of the peptide is also important, particularly for optimization of the peptide, developing it into a lead compound. Docking refers to the interaction between the protein and the peptide when in a complex, an interaction that is predicted based on algorithms evaluating characteristics such as conformation, orientation, and binding affinity between the two molecules (Sousa et al., 2006).

Docking is a complex process because although the process is straightforward for ligands with few rotatable bonds, for highly flexible ligands like peptides, it is not trivial to use an algorithm to assess docking. Ways to limit the conformation space (constraints)

are crucial to successful peptide docking. One way to introduce stereotopic constraints is to cyclize the peptide. For example, Cilengitide is a cyclic ligand-mimicking peptide which binds to and blocks the activities of the integrins, inhibiting endothelial cell-cell interactions and angiogeneisis (Goodman et al., 2002).

The rational design of peptide compounds continues to be important area of research. Computational tools suitable for modeling peptide-protein interactions are now being employed. Further information on the precise interaction between the peptide and the protein in a complex is likely to lead to the greatest advancement in the field and help to develop new compounds that can eventually become drug candidates.

1.5 Kinase inhibitors

1.5.1 Peptide inhibitors: General

ATP competitive small molecule inhibitors were briefly mentioned above. The hydrophobic nature of the ATP binding site makes it an ideal drug binding site. But while the ATP binding sites between kinases are fairly similar, the diversity of peptide substrates across the protein kinase family leads to more variation in the peptide-binding cleft. This diversity presents an opportunity to exploit the peptide substrate site and achieve greater selectivity than is demonstrated by the ATP-competitive inhibitors. There are many types of peptide inhibitors: pseudosubstrate inhibitors, bisubstrate inhibitors, and inhibitors that target domains in signaling proteins or modulate localization of kinases. We will focus on pseudosubstrate inhibitors and bisubstrate inhibitors.

1.5.2 Pseudosubstrate inhibitors

Pseudosubstrate peptide inhibitors mimic natural protein substrates of kinases and can prove to be very effective. Pseudosubstrate inhibitors often contain binding elements making substrates of a particular protein kinase, but with minor alterations that allow them to exercise their inhibitory functions. For instance, protein-serine kinase 1 is a naturally occurring protein kinase A antagonist that is able to bind to the kinase without being phosphorylated, owing to a mutation (Walsh et al., 1971). The lack of a phosphorylatable residue maintains the slow off-rate for the peptide, which is normally enhanced following phosphorylation. In contrast with ATP-competitive inhibitors, a pseudopeptide targeting Protein Kinase C (PKC) α recently screened had over 350 fold selectivity against other PKC isozymes (Li, 2006). One drawback to pseudosubstrate inhibitors is that their potency is usually lower than that of ATP-competitive inhibitors in biochemical assays.

1.5.3 Bisubstrate inhibitors

Bisubstrate Inhibitors represent an alternative strategy for identification of selective kinase inhibitors. This class has interactions in both the kinase ATP and peptide substrate binding sites by mimicking both the phosphate donor (ATP) and acceptor components (serine, threonine or tyrosine containing peptides). While the specificity afforded to a dual-site interaction is good and the constraints on the geometry of the two components will contribute to specificity, the challenge is designing linkers that maintain optimal interaction of both components with the targeted kinase (Harrison et al., 2008).

The compound used in this study was designed as a bisubstrate inhibitor that targets members of the PKC family.

1.6 Protein kinase C

Protein kinases are a part of a superfamily of approximately 600 separate proteins encoded by the human genome. Functionally, these proteins transfer phosphate from ATP to serine, threonine and tyrosine residues of a peptide substrate. The reaction occurs in the cleft formed between the amino-terminal lobe, which contains the glycine rich loop that binds ATP, and the larger carboxy-terminal loop (Taylor et al., 1993).

One class of kinases is PKC. PKC is a family of serine/threonine kinases that controls many cellular processes including cell proliferation, cell cycle control, differentiation, cell polarity and survival (Nishizuka, 1986; Fields and Gustafson, 2003). All PKC isoforms share similar overall structure consisting of an N-terminal regulatory domain and a C-terminal catalytic domain, which is also known as a kinase domain (**Figure 2)**. Functionally, the N-terminal regulatory domain serves two purposes. First, it contains modules which attach the enzyme to various locations in the cell when engaged by lipid second messengers or other interacting proteins. Second, the domain negatively regulates enzymatic activity; it possesses a pseudosubstrate sequence that closely resembles a PKC substrate site. This sequence binds to the substrate binding cavity in the C-terminus and blocks catalytic activity. When lipid second messengers bind to the regulatory domain, the pseudosubstrate sequence is removed from the kinase domain, allowing substrate binding and target phosphorylation.

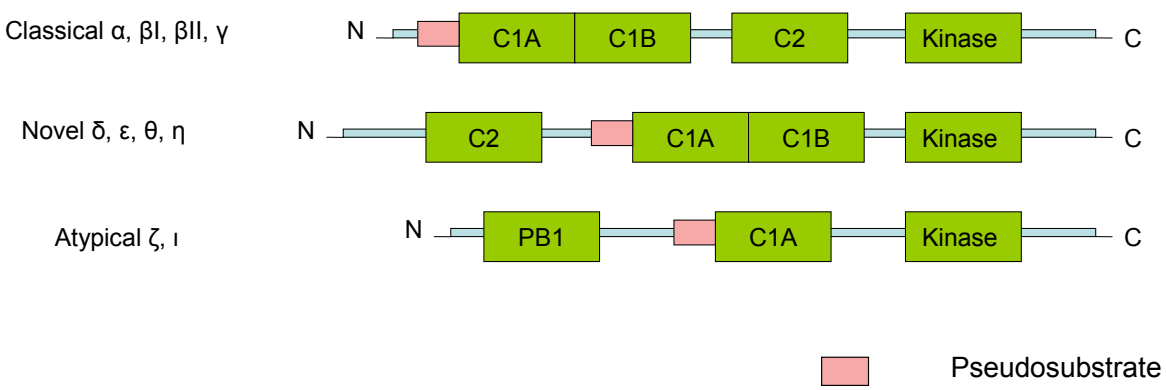

Figure 2. The overall domain structures of the classical, novel and atypical PKC isoforms. Adapted from Newton (2001).

1.6.1 PKC isoforms: Classification

Following the discovery of PKC by Nishizuka and colleagues in the 1970s (Inoue et al., 1977), the subsequent PKC isoforms warranted a classification system. The ten members of PKC are classified into three subgroups; conventional, novel, and atypical PKCs (**Figure 2)**.

Conventional PKCs or classical PKCs (cPKCs) (α, βI, βII and γ) were first discovered in the brain of the cow (Parker et al., 1986). They possess a pseudosubstrate motif, C1 domain, and Ca^{2+} binding site at their C2 region (Roffey et al., 2009). Both C1 and C2 domains can aid in translocation by interacting with the cell membrane. cPKCs can be activated by a combination of Ca^{2+}, diacylglycerol (DAG), and phospholipids (Newton, 1997, 2001).

Other researchers have investigated novel PKCs (nPKCs) such as PKC-δ, ε, η, and θ (Dekker and Parker, 1994). Although similar to cPKCs, they are not activated by Ca^{2+} because novel PKCs have no aspartate residues for Ca^{2+} coordination (Pears et al., 1992). However, to circumvent this problem anionic phospholipids including phosphotidylinositol- 2- phosphate, phosphotidylinositol or phosphotidylserine can bind to the C2 domain. (Pepio and Sossin, 2001). Therefore, translocation to the membrane and activation of nPKCs are dependent on the binding of DAG and anionic phospholipids.

Atypical PKCs (aPKCs) include PKCι and PKCζ. While the catalytic domains of aPKCs are similar to cPKCs and nPKCs, the chief differences lie in the C1 regulatory domain. The C1 domains of atypical PKCs do not bind DAG and also lack calcium

binding pockets, and thus are not activated by either DAG or Ca^{2+}. One study suggested ceramide may directly activate PKCζ *in vitro* (Bourban et al., 2000). There is also a Phox Bem 1 (PB1) domain instead of a C2 domain in aPKCs. The PB1 domain mediates protein-protein interactions. In PKCζ, for instance, the PB1 domain binds to phox and Cdc motifs of the adaptor protein ZIP (protein kinase C ζ interacting protein), an interaction which may be involved in its recruitment to a signaling complex or to potassium channels (Ito et al., 2001). PKCζ also uses its PB1 domain to bind to the PB1 domain of Par6, an interaction involved in establishing polarity in epithelial cells (Noda et al., 2003).

1.6.2 Regulation of PKC

PKC is regulated both structurally and spatially. To be fully functional, the kinase must be phosphorylated at the appropriate residues, have its pseudosubstrate removed, and be localized at the correct intracellular location.

The three key phosphorylation sites on the C-terminus of PKCs are known as the activation loop (A-loop), turn-motif (TM), and hydrophobic-motif (HM). First, phosphorylation of a threonine residue on the A-loop is the rate limiting step. Evidence suggests this phosphorylation event is catalyzed by phospho-dependent kinase 1 (PDK1), with the exception of PKC δ, where studies have shown deletion of PDK1 does not abolish PKC δ A-loop phosphorylation (Wood et al., 2007).

Following the A-loop phosphorylation, autophosphorylation occurs at the TM and HM, which are located at different residues in the different classes of PKC. For conventional PKCs, autophosphorylation occurs at serine 641 and threonine 660; for novel PKCs, at threonine 566, 710, and serine 729; while in atypical PKCs, threonine 410

and 560 are autophosphorylated (Pepio and Sossin, 2001). After these sequential phosphorylation events, the species is able to adopt a self-inhibited, phosphatase resistant conformation and is released from the cell membrane into the cytosol.

1.6.3 Regulation by membrane interaction and anchoring protein

The next step in the regulation of PKC is the translocation from the cytosol to the membrane. The presence of cofactors such as phosphatidylserine, DAG and Ca^{2+} provides the allosteric switch to activate PKC and begin the translocation process. Anchoring proteins such as receptors for activated C kinase (RACKS) and substrates that interact with C kinase (STICKS) facilitate PKC translocation to the membrane sites and allow interaction with cofactors (Dekker, 2004). Phosphatidylserine and DAG can bind to the C1 domain while Ca^{2+} binds to the C2 domain. Binding of one or more ligands provides sufficient energy for the pseudosubstrate to be released from the active site and allow substrate binding and catalysis to occur. (Dekker, 2004).

1.6.4 PKC inhibitors

There are a few classes of PKC inhibitors including small molecule inhibitors and natural modulators of PKC. First, small molecule PKC inhibitors are ATP competitive inhibitors that bind to the kinase domain of the PKC isozymes. The agents in this class have variable specificity for PKC isoforms. Midostaurin inhibits the cPKC and nPKC isozymes while enzastaurin is a PKC-β inhibitor currently being evaluated in a variety of cancers including glioblastoma, lymphoma, and pancreatic cancer (Weisberg and Griffin, 2001; Rizvi et al., 2006).

Natural modulators of PKC also exist. Bryostatin, which is currently being tested in Phase I and II trials, was found from a marine invertebrate and acts as an activator of

PKC in the short term, but as an inhibitor when used over a long period of time (Smith et al., 1985; Philip and Zonder, 1999). Other agents are categorized as nutritional or chemopreventive agents. Curcumin, for instance, is a dietary pigment responsible for the yellow color of curry. It competes with calcium for the chance to bind PKC. It is currently being evaluated in a number of cancers including multiple myeloma, pancreas and colorectal cancer (Kunnumakkara et al., 2008).

1.6.5 PKC and tumourigenesis

PKC became a hot topic in cancer research in the early 1980s when Yasutomi Nishizuka and co-workers provided the first solid evidence of its identification as the target of the phorbol esters, which are natural products with tumour-promoting activity (Castagna et al., 1982). The different isoforms of PKC have both redundant and specific functions that may differ in different types of cancer, increasing the complexity of assigning functions to each isoform. The unique contribution of the various isoforms to cancer development and progression are outlined in **Table 1.**

Although not always the case, there is evidence for opposing roles in tumour biology between different PKC isoforms. For cPKCs, PKC α generally has anti-proliferative effects, as seen in intestinal, breast and pancreatic cells (Slosberg et al., 1999; Detjen et al., 2000). Meanwhile, PKCβI promotes a survival response to chemotherapeutic agents in gastric cancer (Jiang et al., 2002). For nPKCs, the contrasting roles of PKCε and PKCδ in survival and apoptosis, respectively, presents an interesting dynamic. Deregulation in the ratio of apoptotic and survival signals is a hallmark of carcinogenesis. Overexpression of PKCε confers a growth advantage in anchorage independent cultures and produces a tumourigenic phenotype in nude mice (Mischak et al., 1993). For aPKCs, PKCι has been shown to be highly expressed

Table 1. PKC isoform expression in various cancers

	Increased expression in cancer	**Reference**
PKCα	Prostate,	Koren et al., 2004
	Endometrial	Fournier et al., 2001
	Hepatocellular	Tsai et al., 2005
	Hematological	Lahn et al., 2005
PKCβ	Prostate	Koren et al., 2004
	Bladder	Varga et al., 2004
	Colon	Gokmen-Polar et al., 2001
	Ovarian	Zhang et al., 2006
PKCγ	Breast	Mazzoni et al., 2003
	Ovarian	Zhang et al., 2006
PKCδ	Pancreatic	El-Rayes et al., 2008
PKCη	Renal	Brenner et al., 2003
PKCθ	Gastrointestinal stromal tumour	Blay et al., 2004
	Ovarian	Zhang et al., 2006
PKCε	Prostate	Koren et al., 2004
	Brain	Sharif et al., 1999
	Breast	Pan et al., 2005
PKCζ	Follicular Lymphoma	Leseux et al., 2008
	Pancreatic	Peng et al., 2007
	Ovarian	Zhang et al., 2006
PKCι	Non small cell lung	Regala et al., 2005
	Pancreatic	Scotti et al., 2010
	Ovarian	Zhang et al., 2006

	Decreased expression in cancer	**Reference**
PKCα	Basal cell	Neill et al., 2003
	Colon	Kahl-Rainer et al., 1994
	Breast	Kerfoot et al., 2004
PKCβ	Bladder	Varga et al., 2004
PKCγ		
PKCδ	Bladder	Varga et al., 2004
PKCη	Breast	Masso-Welch et al., 2001
PKCθ	Colon	Kahl-Rainer et al., 1994
PKCε		
PKCζ		
PKCι		

in ovarian carcinomas and cooperates with the oncogene mutant Ras (Zhang et al., 2006). Also, observations made in colorectal cancer suggest PKCι and PKC βII cooperate to promote cancer progression (Murray et al., 2009).

1.6.6 PKCs and ovarian cancer

Certain PKC isoforms have been implicated specifically in ovarian cancer. PKCε has been identified as an emerging oncogene in ovarian cancer. It has been shown to phosphorylate claudin-4, which is frequently overexpressed in ovarian cancer (D'Souza, et al., 2007). Claudins are proteins that play a role in forming and maintaining tight junctions. In an array-based comparative genomic hybridization on human ovarian cancer specimens, a select number of PKCs were found to be significantly upregulated, including PKC βI, PKC γ, PKC ζ, and PKC θ, and PKCι. PKCι, in particular, has been the focus of some recent research in the field of ovarian cancer. Among 11 different solid cancers, PKCι was found to be most highly expressed in ovarian cancers (Zhang et al., 2006). The array-based comparative genomic hybridization on human ovarian cancer specimens showed that PKCι DNA copy number exhibited a 43.8% gain, the largest gain reported for any PKC isoform (Zhang et al., 2006). Interestingly, overexpression of PKCι did not seem to affect human ovarian cancer cell proliferation or apoptosis *in vitro.* However, a study done *in vivo* in *Drosophila* suggested that increased PKCι levels correlated with increased cyclin E protein expression, and that this was the cause of increased proliferation in *Drosophila* epithelial cells (Eder et al., 2005). It is possible the effect of PKCι on cell proliferation is not a direct function but rather dependent on *in vivo* growth requirements in cancer.

PKCι has been shown to be activated by K-ras and their co-expression contributes to ovarian epithelium transformation (Zhang et al., 2006). The PKCι inhibitor Aurothiomalate (ATM) is currently in Phase I clinical trials in non small cell lung cancer (NSCLC) patients, but it has not been tested yet in clinical trials of ovarian cancer. ATM was shown to inhibit binding of scaffold proteins par6 and p62 to the PB1 domain of PKCι. (Bratt et al., 2000; Yamashita et al., 2003; Jeon et al., 2000). This leads to downstream effects such as the uncoupling of both Rac1 and NF-κB from PKCι. Rac1 binds to the scaffold protein par6 and the PKCι-par6-Rac1 complex is implicated in transformed growth and invasion in non small cell lung cancer cells (Regala et al., 2005). p62 links PKCι to NF-κB in some cell types and this signaling cascade is implicated in the survival and chemoresistance of chronic myelogenous leukemia cells (Sanz et al., 1999).

1.7 GAP-107B8

1.7.1 GAP-107B8 design

GAP-107B8 (PharmaGap Inc.) is a bisubstrate inhibitor that targets both the ATP binding site and the PSD-95, disheveled and ZO1 (PDZ) binding motif of PKCα. The PDZ motif is a protein-protein interaction module that binds to membrane proteins in addition to lipid molecules (Sheng and Sala, 2001; Zimmermann et al., 2002). GAP-107B8 was designed, in part, to mimic a portion of Protein Interacting with C Kinase (PICK1), allowing it to specifically modulate the function of PKCα in cells. PICK1 is a PKC α binding protein cloned using the yeast-2-hybrid system (Staudinger et al., 1995). PICK1 is a unique gene, being the only gene in the NCBI database that has both a BAR domain and a PDZ domain (**Figure 3A)**.

A

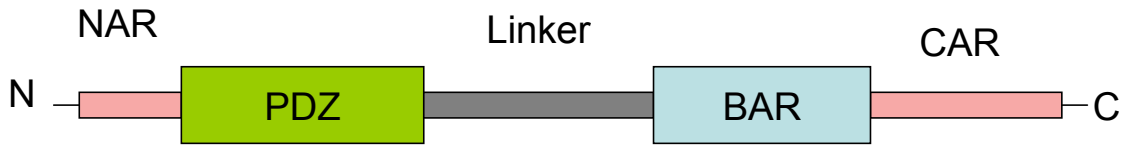

B

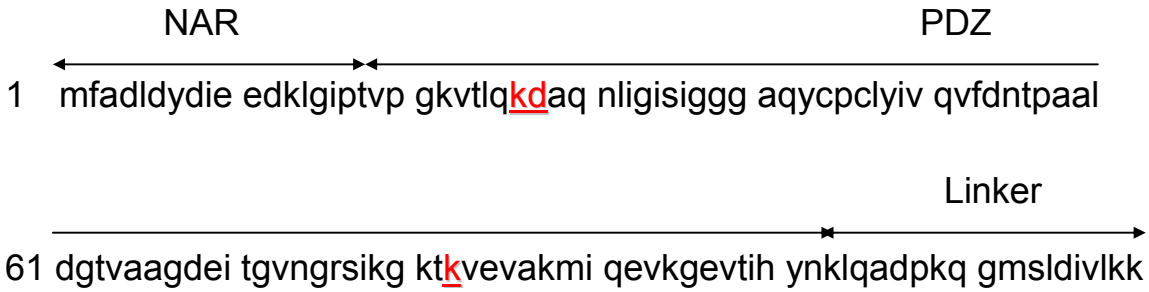

Figure 3. Domain structure of the PICK1 protein. A Diagram of PICK1 domains showing the N-terminal acidic region (NAR), PDZ domain, linker region, BAR domain and the C-terminal acidic region (CAR). **B** Protein sequence of PDZ domain from the human PICK1 protein. Residues K27 and D28 of PICK1, which are critical for binding to PDZ ligands, and residue K83, which determines the preference to different types of PDZ-binding motifs, are underlined and highlighted. Adapted from Xu and Xia (2006).

The BAR domain is a protein module of about 200 amino acids that binds to lipids. It is often found in proteins involved in membrane trafficking and particularly endocytosis.

PICK1's PDZ domain consists of six β sheets and two α helixes with αB and βB forming the binding pocket. **Figure 3B** shows the protein sequence of the PDZ domain of the human PICK1 protein. The lysine (K27) and aspartic acid (D28) residues are very important, as mutation of these residues together completely disrupts PICK1's PDZ interaction (Xia et al., 1999; Staudinger et al., 1997).

The PDZ domain is a modular protein-protein interaction motif that aids to localize proteins to specific subcellular sites (Saras and Heldin, 1996). The PDZ domain of PICK1 is located at its NH2 terminus, which is required for interaction with a PDZ-binding motif (QSAV) at the extreme COOH terminus of PKCα. This PDZ motif is found at the carboxyl end of all PKC isozymes but differs in sequence between isozymes, creating the potential for selective binding.

1.7.2 GAP-107B8 structure

In all forms of GAP-107B8 used in this study, the peptide nucleic acid ($C_{11}N_{14}H_7O_2$) has been linked to the epsilon amino group on a designated Lysine (K) residue and the Protein Transduction Domain (PTD), when present, has always been attached to the amino group of the peptide nucleic acid (PNA). Otherwise, the compound has undergone a number of name changes and structural/synthetic alterations. **Table 2** illustrates these changes. The most significant changes occurred in the counter ion used during production of GAP-107B8. Earlier forms of GAP-107B8 required the lyophilized peptide to be dissolved in DMSO, while later versions of the L and D-isomer permitted dissolution in water. The D-Isomer, in addition to changing each possible amino acid to

Table 2. Evolution of the GAP-107B8 structure.

Name	Compound Name	Structure[a]	PTD[a,b]	Counter Ion	Diluent
GAP-107B8-X-TFA	GAP-107B8.119	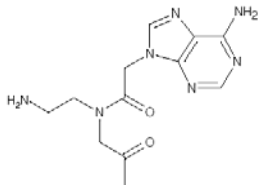 Ac-FRRKFRLGGGGGGKDAQNLIGISI-$CONH_2$	None	Trifluoroacetate	DMSO
GAP-107B8-L-TFA	GAP-107B8-002 GAP-107B8-004	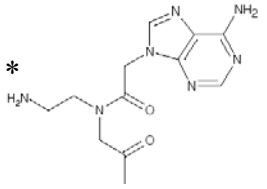 Ac-FRRKFRLGGGGGGKDAQNLIGISI-$CONH_2$	KRRQRRKKR-Ac	Trifluoroacetate	DMSO
GAP-107B8-L-Ac	GAP-107B8.106 GAP-107B8.107 GAP-107B8.108			Acetate	H_2O
GAP-107B8-D-TFA	GAP-107B8-D3-001	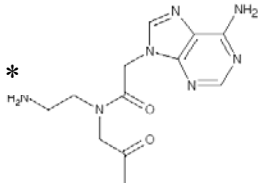 Ac-frrkfrlGGGGGGkdaqnliGisi-$CONH_2$	rkkrrqrrk-Ac	Acetate	H_2O
GAP-107B8-D-Ac	GAP-107B8.301			Acetate	H_2O

a Lower case amino acids are in the D-conformation

b Protein Transduction Domain (PTD) is coupled to the peptide nucleic acid (PNA) moiety at the asterisk (*)

its D-configuration, subtly altered the sequence of the PTD. Addition of the PTD sequence may increase membrane penetration into the cancer cells compared with an earlier version, GAP-107X8-L-TFA.

1.8 Project Rationale

While the current standard of care in the treatment of ovarian cancer following surgical debulking yields high initial response rates, patients often relapse and the need remains to investigate novel therapeutics. A novel peptide inhibitor called GAP-107B8 was developed by PharmaGap Inc. and was tested on several human ovarian cancer cells lines. This study evaluated the effect of two isomers of GAP-107B8 on cell viability in adherent and anchorage independent growth conditions *in vitro*. Also, the effect of GAP-107B8 on the rate of tumour development was assessed *in vivo*. Finally, the mechanism of action of GAP-107B8 on ovarian cancer cells was investigated.

1.9 Hypotheses

At the start of this project, it was hypothesized that:

1) GAP-107B8 inhibits cell viability in adherent and anchorage independent cultures and reduces migration and invasion by ovarian cancer cells in vitro and that GAP-107B8 reduces tumour burden in SCID mice xenografted with ovarian cancer cells in vivo.

2) PKCι is overexpressed in the ovarian cancer cell lines most responsive to GAP-107B8 and its activity is downregulated with treatment of GAP-107B8.

3) GAP-107B8-D-Ac (D-Isomer) causes more potent inhibition of cell viability in adherent and anchorage independent cultures in ovarian cancer cells in vitro and a greater reduction of tumour burden in vivo.

1.10 Project objectives

1) To evaluate the effect of GAP-107B8 on cell viability in adherent and anchorage independent cultures and motility in a panel of ovarian cancer cell lines in vitro in the presence and absence of carboplatin
2) To assess the effect of GAP-107B8 on tumour burden in xenograft models of human ovarian cancer
3) To identify the mechanisms by which GAP-107B8 alters ovarian cancer cell activity
4) To evaluate and compare the effects of L- and D-isomers of GAP-107B8

Chapter 2: MATERIALS AND METHODS

2.1 Tissue culture

2.1.1 Cell lines and maintenance

The cell lines used in this study were obtained from sources cited in **Table 3**. A2780cp, A2780s, C13, OV2008 and ES-2 and OVCAR8 cells were maintained in Dulbecco's minimum essential medium (D-MEM, Hyclone, Logan, UT). HEY, OVCA429, SKOV-3, OVCAR3 and OCC1 cells were maintained in Alpha Minimum Essential Medium (α-MEM, Hyclone). Media were supplemented with either 5% heat-inactivated 3:1 donor bovine serum:fetal bovine serum (DBS:FBS; PAA Laboratories Inc., Etobicoke, ON) or 5% Fetal Bovine Serum Characterized (Hyclone). Cell cultures were maintained in 75 or 175 cm^2 flasks (Corning Inc., Corning, NY) at 37˚C in a humidified incubator equilibrated with 5% carbon dioxide (CO_2). Cells were passaged at or near confluency, washing with phosphate buffered saline (PBS; HyClone, Logan, UT) and then incubating at 37˚C in 0.05% trypsin (Hyclone) for 2-3 minutes. Once cells were detached from the plate, the appropriate medium was added to inactivate the trypsin and cells were centrifuged at 2000 rpm for 4 minutes. The cell pellet was resuspended in fresh medium and a fraction was plated.

Cells were frozen in cryovials (Nalge Nunc International Corp., Rochester, NY) using freezing media composed of 10% dimethylsulfoxide (DMSO, Sigma-Aldrich., Oakville, ON) and 90% FBS. Cells were frozen at -80˚C for temporary storage or transferred to liquid nitrogen for long-term storage. To revive frozen cells, cells were thawed in a 37˚C water bath and then added dropwise into a small amount of warm medium and incubated

Table 3. Human ovarian cancer cell lines used in this study

Cell Line (Source)	Tissue Source	Reference
A2780-s (M. Molepo)	Untreated ovarian cancer patient	Eva et al., 1982
A2780-cp (M. Molepo)	Stepwise exposure of A2780-s cells to up to 70 μM cisplatin	Masuda et al., 1988
C13 (M. Molepo)	Stepwise exposure of OV2008 cells to 0.25-5.25 μM cisplatin	Andrews and Albright, 1992
Hey (G. Mills)	Serous Ad, solid tumor	Buick et al.., 1985
OCC1 (G. Mills)	Ascetic fluid of clear cell carcinoma	Wong et al., 1990
OV2008 (M. Molepo)	Serous Ad, solid tumor, stage IV	DiSaia et al., 1972
OVCAR-8 (J. Bell)	MCF-7/adriamycin resistant	Batist et al., 1986
OVCA 429 (G. Mills)	Ad, ascites	Bast et al., 1981
OVCAR-3 (G. Mills)	Poorly differentiated papillary Ad, ascites	Hamilton et al., 1983b
SKOV-3 (G. Mills)	Ad, ascites	Fogh and Trempe, 1975
ES-2 (ATCC No. RL-1978™)	Ovarian clear cell carcinoma	Lau et al., 1991

at 37˚C in a 5% CO_2 humidified environment. The medium was replaced with fresh medium within 1 day.

2.2 Test compounds

PKC inhibitor GAP-107B8 (PharmaGap Inc, Ottawa, ON) was received in powder form and was subsequently dissolved to a stock concentration of 3.25 -20 millimolar (mM) in DMSO or double distilled water (ddH_2O). The fresh stock solution was then divided into aliquots for each experiment, frozen and stored at -20°C or -80°C until needed. **Table 4** shows the compound name corresponding to the experiments in which it was used.

Carboplatin (Mayne Pharma Inc., Montreal, PQ) was received as a 10mg/mL solution and was stored at room temperature, protected from light.

Wortmannin (Sigma, W1628, Oakville, ON) was received in powder form and dissolved to 23 micromolar (μM) in DMSO.

2.3 *In vitro* experiments

2.3.1 Cell viability assays-adherent cell cultures

Cells were plated in 96-well plates. Cell numbers for plating were determined by a Vi-CELL counter (Beckman-Coulter). Depending on the growth rate of each cell line as determined in preliminary experiments, between 2000-5000 cells were plated in each well. Twenty-four hours later, GAP-107X8-TFA or GAP-107B8-L-TFA (PharmaGap Inc., Ottawa, ON) (1-25 μM) was added to the appropriate wells in the presence or absence of carboplatin (0-2 mM) and/or Wortmannin (0.1 μM). After 48 hours exposure to the drugs, the cell numbers were determined using the CyQuant® fluorescent nucleic acid binding dye, which is a component of the Cyquant Cell Proliferation Assay Kit

Table 4. The different GAP-107B8 compounds used in different experiments

Name	Compound Name	Diluent	Experimental Methods
GAP-107X8-L-TFA	GAP-107B8.119	DMSO	*In vitro* cell viability assays in adherent cultures
GAP-107B8-L-TFA	GAP-107B8-004	DMSO	*In vivo* MTD and efficacy study of intra-peritoneal treatment of intra-peritoneal A2780cp tumours
GAP-107B8-L-Ac	GAP-107B8.106 GAP-107B8.107 GAP-107B8.108	Water	Efficacy study of intra-tumoural treatment of subcutaneous A2780cp tumours; efficacy study of intra-tumoural treatment of subcutaneous HEY tumours; TUNEL; BrdU flow cytometry; western blots; efficacy study of intra-peritoneal treatment of intra-peritoneal A2780cp tumours; *in vivo* MTD and efficacy study of intra-peritoneal treatment of intra-peritoneal OCC1 tumours
GAP-107B8-D- TFA	GAP-107B8-D3-001	DMSO	*In vitro* cell viability assays in adherent cultures
GAP-107B8-D- Ac	GAP-107B8.301	Water	*In vitro* cell viability assays in adherent and anchorage independent cultures; western blots; *in vivo* MTD and efficacy study of intra-peritoneal treatment of intra-peritoneal OCC1 tumours

MTD= maximum tolerated dose

(Invitrogen). CyQuant® labeled cells were detected using the Fluoroskan Ascent FL (Thermo Fisher Scientific). The excitation and emission wavelengths were 485 and 527 nanometers (nm), respectively.

2.3.2 Cell viability assays-anchorage independent cell cultures

Cell viability in anchorage independent cultures was assessed by growth in soft agar using the Cytoselect™ 96-well cell transformation assay (Cell Biolabs, San Diego, CA) following the manufacturer's protocol. Cells (10,000) were plated in soft agar with and without 6.25-25 μM GAP-107B8-L-TFA and in the presence or absence of carboplatin (1.8 μM). The concentration of carboplatin was determined in preliminary experiments such that there would be 25% reduction in the cell viability of A2780s and OV2008 sensitive cell lines. Following 5-14 days of growth at 37°C, the agar was solubilized using Agar Solubilization Solution (Cell Biolabs, San Diego, CA) and the cell numbers quantitated by fluorimetry using the CyQuant® fluorescent nucleic acid binding dye, which is a component of the Cyquant Cell Proliferation Assay Kit (Invitrogen). CyQuant® labeled cells were detected using the Fluoroskan Ascent FL (Thermo Fisher Scientific). The excitation and emission wavelengths were 485 and 527 nm, respectively.

2.3.3 Cell motility assays

Motility assays were performed using the CytoSelect™ 96-Well Cell Migration and Invasion Assay kit (Cell Biolabs, San Diego, CA). All cell lines were first grown overnight in their respective media at 1% serum. After 24 hours, cells with and without GAP-107B8-L-TFA (6.25-25 μM) were plated in 1% serum directly into Boyden chambers in a 96-well format. The Boyden chambers were placed into wells containing media with 5% serum as a chemoattractant. The ability of cells to migrate across the

Boyden membrane during a 24 hour period was measured by dissociating all cells from the underside of the membrane and quantitating cells using the CyQuant® fluorescent dye as directed by the CytoSelect™ 96-Well Cell Migration and Invasion Assay kit.

2.3.4 Protein isolation and western blotting

Cells were lysed using the ProteoJET™ Mammalian Cell Lysis Reagent (Fermentas). Cells were scraped off the plate and collected, while floating cells were collected in all instances except for the flow cytometry experiments. Cells were transferred to a microfuge tube and vortexed and then placed on a shaker for 10 minutes at room temperature. The cells were then centrifuged at 18,000×g for 15 minutes before the supernatant was transferred to a new microcentrifuge tube. The lysate was used immediately or stored at -80ºC. Other Lysis Buffer ingredients include: 1 mM protease inhibitor cocktail (Sigma, #P8340), 1 mM PMSF, and 10X stop solution that was composed of: 0.1 molar (M) sodium pyrophosphate (Sigma, P8010), 0.1 M sodium fluoride (Sigma, S7920), 4 mM sodium orthovanadate (Sigma, S6508), and 25 mM sodium β-glycerophosphate (Sigma, G-6376).

Protein quantification

Five µL of sample and 95 µL of ddH_2O were added into micro-centrifuge tubes. A blank containing 5 µL of lysis buffer and 95 µL of ddH_2O was prepared in a separate micro-centrifuge tube. 900 µL of a 1:5 dilution of Quick Start Bradford 1x Dye Reagent (Bio-Rad Laboratories Ltd.) was added to each sample and blank. The absorbance at 595 nm was measured for each sample using a DU® 640 UV/Visible Spectrophotometer (Beckman Coulter Inc.). The absorbance value and protein concentration of each sample was provided by the instrument.

Running, transferring and visualizing

For a 10 well gel, 30-40 μg of protein per sample was boiled for 5 minutes in 4X protein loading buffer and centrifuged for 1 minute at 14,000 rpm, before being separated on a 4-12% polyacrylamide gel (Invitrogen) in a vertical electrophoresis system and transferred to a nitrocellulose membrane (Hybond C Extra, Amersham, Oakville, Ontario). Antibodies were prepared in 5% milk and added for 90 min at room temperature or overnight at 4°C. The blot was washed three times in 1X tris buffered saline Tween-20 (TBST) in 5% milk before adding the secondary antibody for 90 min at room temperature or overnight at 4°C. Three final washes with 1X TBST were performed before visualization of protein bands by the ECL Advance™ Western Blotting Detection Kit (Amersham) and image acquisition system (Alpha Innotech MultiImage™ II FC Light Cabinet).

Densitometry was performed using the Band Analysis function in the Alpha Innotech AlphaView program. When the blots were to be re-probed with another primary antibody, they were first washed 3 times to remove the residual ECL components, then Restore™ Western Blot Stripping Buffer (Thermo Scientific) was applied for 10-15 minutes. The membranes were then washed again at least 4 times within a 25 minute period in 1X TBST before applying the new primary antibody.

2.3.5 Cell cycle progression

Cell cycle analysis was performed using flow cytometry. Cells ($1x10^6$) were plated for 48 hours prior to the addition of 5-bromo-2-deoxyuridine (30 μM BrdU, Sigma). Following 1 hour incubation with BrdU, cells were washed twice with PBS followed by

treatment with GAP-107B8. Cells were collected at various time points (0-24 hr) and fixed in 70% ethanol and kept at -20°C for at least 30 minutes and up to a week. To analyze the cells, they were treated with sequentially with the following solutions, centrifuging after the addition of each reagent: 0.5mg/mL RNase A solution, 0.1N HCl + 0.7% Triton-X-100, PBS-T (0.5% Tween 20) and HBT Buffer (5% FBS, 0.5% Tween 20). Next, the primary (anti-BrdU, #33281, Pharmingen) and secondary antibodies (anti-mouse FITC conjugate, F-6257, Sigma) were applied sequentially for at least 30 minutes, protected from light at dilutions of 1:100 and 1:20, respectively. Finally, 400-600 microliters (μL) propidium iodide (P4170, Sigma-Aldrich) was added to the cells and kept at 4°C for at least 30 minutes before subjecting them to flow cytometry. Analysis was by two-parameter flow cytometry for fluorescein isothiocyanate (FITC) and propidium iodide (PI) using a Coulter Epics Elite Flow Cytometer. Data presented represents 10,000 events which were subsequently gated to include only single cells.

2.3.6 Apoptosis

Apoptosis was directly assessed using two methods: 1) by the terminal transferase-mediated dUTP-nucleotide-end labeling (TUNEL) assay using the Fluorescein In Situ Cell Death Detection Kit (Roche Diagnostics, Indianapolis, IN, USA), and 2) by western blot detection of PARP using the PARP antibody (Cell Signaling, #9542).

1) TUNEL

A2780cp cells ($6x10^5$) were plated on sterile coverslips in 6-well plates in DMEM + 5% FBS treated with 25 μM GAP-107B8-L-Ac or the equivalent amount of control (ddH_2O) for 30 hours. Cells adhered to coverslips were fixed in 4% paraformaldehyde for analysis by TUNEL according to the manufacturer's protocol. DAPI (4', 6-diamidino-2-

phenylindole) staining was also performed, using the VECTASHIELD® mounting medium for Fluorescence with DAPI (Vector Laboratories Inc., Burlingame, CA). Cells were visualized using fluorescence imaging with the Axioskop 2 MOT fluorescent microscope (Carl Zeiss Canada Ltd. Toronto, ON).

2) PARP cleavage

A2780cp cells were plated and allowed to grow in 100mm plates (BD Falcon™, 353003) until nearly confluent before being treated with 25 μM GAP-107B8.108 or the equivalent amount of vehicle (ddH_2O) and collected after 1, 4, 8 and 30 hours and analysed by western blot. Cells were lysed and 40 micrograms (μg) of total cell proteins of untreated and treated samples were resolved by SDS-PAGE, transferred to a nitrocellulose membrane; and probed with primary antibodies to PARP and GAPDH for 1 hour. The secondary antibody used to detect PARP was donkey anti-rabbit horseradish peroxidase (HRP) (Jackson Immunoresearch Laboratories, Inc., 713-035-147, 1:2500-5000). GAPDH (Abcam, ab8245, 1:60 000) was used as a loading control. The secondary antibody used to detect GAPDH was rabbit anti-mouse (Abcam, ab6728, 1:40,000).

2.3.7 Identification of potential GAP-107B8-L-Ac targets in ovarian cancer cell lines

A2780cp cells were treated with 6.25, 12.5 and 25μM GAP-107B8-L-Ac or vehicle control (ddH_2O) equivalent to the highest concentration of GAP-107B8-L-Ac, and total cellular proteins were collected using lysis buffer at 1 hour post-treatment and analysed by western blot. Western blots were probed with antibodies to pPKCι (Invitrogen, 44968G, 1:1000), PKCι (BD Transduction Labs, 610176, 1:500), pAkt (Cell Signaling, #9271, 1:750), Akt (Cell Signaling, #9272, 1:500), and six antibodies from a pPKC

sampler kit (#9921; all from Cell Signaling), including pPKC(pan) (#9371, 1:1000), pPKCα/βII (#9375, 1:1000), pPKCδ (#9374, 1:1000), pPKCθ (#9377, 1:1000), pPKCμ (#2051, 1:1000), and pPKCζ/λ (#9378, 1:1000). The secondary antibody used to detect the primary antibodies was donkey anti-rabbit HRP (Jackson Immunoresearch Laboratories, Inc., 713-035-147, 1:2500-5000). A GAPDH antibody (Abcam, ab8245, 1:60 000) was used as a loading control. The secondary antibody used to detect GAPDH was rabbit anti-mouse (Abcam, ab6728, 1:40,000).

2.4 *In vivo* experiments

2.4.1 Determination of the maximum tolerated dose (MTD) of GAP-107B8 in severe combined immunodeficient mice (SCID) mice

Female Fox Chase SCID mice (CB-17 SCID from Charles Rivers Laboratories, ages 6-8 weeks) were divided into 5 or 6 groups with 2, 3 or 4 mice per group. Injections were planned for each group of mice using twice daily IP injections for 7 days with the following doses of GAP-107B8: 5, 10, 20, 40, 80 and 160 mg/kg. Each dose of GAP-107B8 was prepared and diluted in PBS to a 500 μL volume. In order to avoid unnecessary toxicity, the 7 day time course of injections was staggered such that the commencement of a higher dose group of mice would not begin until the previous dose of GAP-107B8 was deemed to be tolerated for a minimum of 24 hours. 24 hours after the last treatment of each group, or earlier in the case of acute toxicity, the mice were euthanized and blood and tissues were removed.

2.4.2 Exploratory Efficacy Study of GAP-107B8 in a mouse model of human ovarian cancer

All experiments involving animals were performed in accordance with the *Guidelines for the Care and Use of Animals* established by the Canadian Council on Animal Care, with protocols approved by the University of Ottawa Animal Care Committee.

A Intra-peritoneal (IP) treatment

These studies each used 8-18 female Fox Chase SCID mice (CB-17 SCID from Charles Rivers Laboratories, ages 6-8 weeks). The mice were allowed to accommodate in the animal facility for five to seven days before injection of cancer cells. $1x10^7$ A2780cp or OCC1 human ovarian cells were resuspended in 1 (milliliter) mL of PBS and injected IP. After 5-7 days to allow for the establishment of tumours, the mice were divided into two groups: a control group and GAP-107B8 treated group, and treatments were initiated. Either 20mg/kg (GAP-107B8.108, GAP-107B8-L-Ac, GAP-107B8-D-Ac) or 40mg/kg (GAP-107B8.107) was used, determined previously to be the MTD of each compound. Treatment was given twice daily for up to 14 days continuous or 13 days (5 days on and 2 days off). During the dosing schedule, animals were monitored daily for disease progression using measures of wellness assessment and clinical endpoints including:

1) complete anorexia for >24 hours
2) Dehydration and/or weight loss (>15%) despite fluid therapy >24 hrs.
3) Any evidence of respiratory distress
4) Abnormal neurologic activity (seizures, inability to walk)
5) Diarrhea that is graded as severe for >48 hours.

6) Body weight increase >5 g from the average body weight of control mice at the same age in the same population
7) Presence of a palpable abdominal mass that impairs mobility or affects wellness (points 1-6).
8) Presence of abdominal distension that impairs mobility or affects wellness (points 1-6) or causes significant discoloration evident through the dorsal skin.

B Intra-tumoural (IT) treatment

SCID mice were injected subcutaneously on the flank with 10^6 HEY or A2780cp cells. When the tumours reached 200 mm^3, mice were divided into 2 groups based on weight, size of tumour and growth rate of the tumour, making an attempt to balance all factors between each group. Mice in each group were treated IT daily either with 0 (vehicle control), 20 mg/kg or 40 mg/kg GAP-107B8 in 50 µl volumes, once per day until tumours reached 2 cm^3. Tumour sizes were measured daily with calipers. All mice in the study were euthanized when any mouse had tumours that reached 2 cm^3.

C Necropsy

IP treatment

At necropsy, peritoneal ascites fluid, when present was estimated by comparison to control tubes containing 0-2 mLs of water in 0.1 mL increments. The extent of tumour dissemination was either qualitatively noted or quantified and all tumour tissues were excised and weighed.

2.5 Statistical Analyses

Cell viability assays were performed on two or three independent experiments performed in duplicate or triplicate. Only assays performed three independent times in triplicate were expressed as mean ± standard error of the mean (SEM). Statistical analysis was performed only on assays with three independent experiments. Statistical significance was determined using one-way analysis of variance (ANOVA) in order to compare three or more treatments and a Bonferroni's Multiple Comparison post-test to compare pairs of group means between selected groups. Two-way ANOVA was used to determine if an interaction existed between the effects of two independent variables, GAP-107B8 and carboplatin, was significant between the three or more selected treatment groups. Statistical significance was inferred when $p<0.05$. GraphPad Prism statistical software (version 3.02; GraphPad Software, San Diego, CA) was used for all one-way and two-way ANOVA statistical analyses.

For tolerability and efficacy studies in SCID mice, data are represented as means of independent tumour samples ± SEM, with the number of samples per group indicated in each figure caption. An unpaired t-test was used to identify differences between one group and a control; in our experiments, vehicle treated mice were compared to GAP-107B8 treated mice. Parameters measured include the size of tumours, the average number and average weight of tumours, as well as the volume of ascites.

Densitometry analysis comparing the pAkt/Akt ratio between control and GAP-107B8 treated A2780cp cells was also determined by unpaired t-test. Statistical significance was inferred when $p<0.05$. GraphPad Prism statistical software (version 3.02; GraphPad Software, San Diego, CA) was used for all t-test statistical analyses.

Chapter 3: RESULTS

3.1 Assessing the effects of GAP-107X8-L-TFA and GAP-107B8-L-TFA on ovarian cancer cells *in vitro* and *in vivo*

Note: The cells of adherent and anchorage independent cultures were measured using CyQuant® cell proliferation assays, a fluorometric indicator of cell numbers based on the fluorescence enhancement exhibited by the CyQuant dye upon binding to cellular nucleic acids. These assays showed decreased cell numbers in treated cells compared to control cells. The term "inhibition of cell viability" appears throughout the text based on results obtained to explain the decreases in cell number, although the assays themselves do not directly measure cell viability or cell number, but rather nucleic acid content. This method does not distinguish whether fewer cells are due to a decrease in cell proliferation or cell viability. Although the amount of cells plated is known, this number was not quantitated by fluorimetry and thus there is no baseline fluorimetry measurement of cell number. With only the flow cytometry results suggesting transient inhibition of cell proliferation, the evidence for suppression of growth is incomplete. However, much more evidence exists for apoptosis, including the TUNEL, PARP cleavage and flow cytometry results. Therefore the "inhibition of cell viability" in the presentation of the results will be used, rather than "inhibition of cell proliferation."

3.1.1 GAP-107X8-L-TFA effect on cell viability in adherent cultures in a panel of human ovarian cancer cell lines

The effect of reduction of cell viability in a panel of human ovarian cancer cell lines following treatment with GAP-107X8-L-TFA was investigated *in vitro.* The 9 cell lines are derived from various subtypes of ovarian cancer. Only the C13 cell line showed significant inhibition of cell viability ($p<0.05$) when treated with 25 μM GAP-107X8-L-TFA (**Figure 4)**.

3.1.2 GAP-107B8-L-TFA effect on cell viability in adherent cell cultures in a panel of human ovarian cancer cell lines

A different formulation of GAP-107B8 containing a PTD, called GAP-107B8-L-TFA, was used to assess the effects on cell viability in the same panel of human ovarian cancer cell lines *in vitro.* Addition of the PTD sequence is presumed to increase membrane penetration into the cancer cells versus GAP-107X8-L-TFA. It was found that 6 of the 9 cell lines showed a significant inhibition of cell viability ($p<0.05$) when treated with 25 μM GAP-107B8 in the presence of 5% serum, including the chemoresistant cell lines A2780cp and C13 (**Figure 5)**. In addition, a seventh cell line, OVCAR3 showed significant reduction in cell viability when treated with 25 μM GAP-107B8-L-TFA in the presence of carboplatin (data not shown). However, analysis by two-way ANOVA failed to indicate any interaction between the effects of GAP-107B8 and carboplatin. The percent reductions of viability in adherent cultures by 25 μM GAP-107B8-L-TFA are shown in **Table 5** with 4 cell lines showing a greater than 50% reduction in viability over 48 hours.

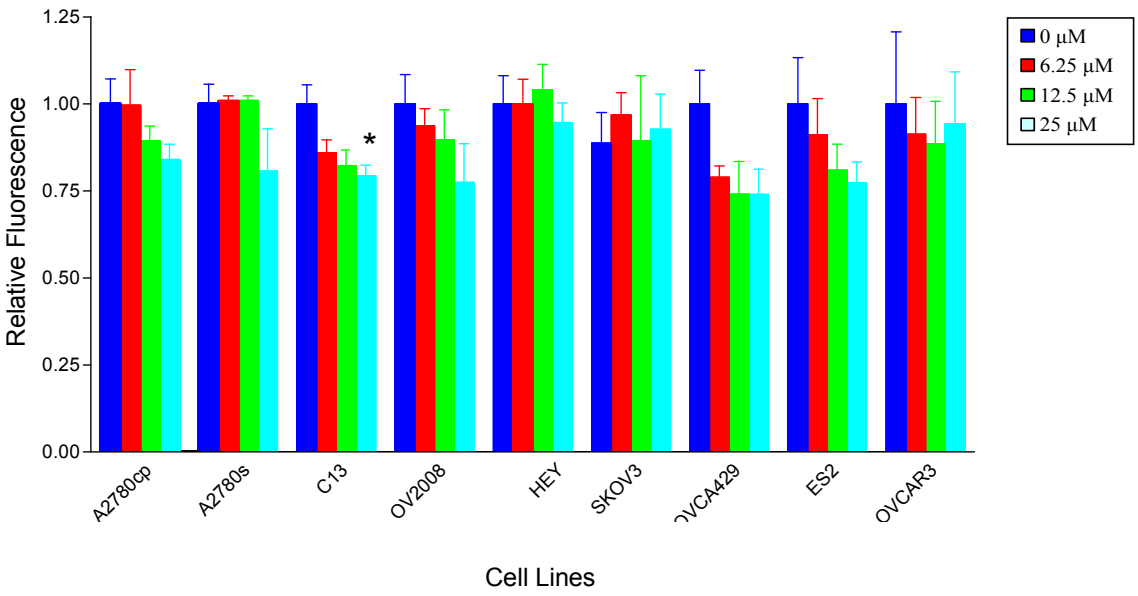

Figure 4. Inhibition of cell viability of ovarian cancer cell lines in adherent cultures in the presence of GAP-107X8-L-TFA. Cells were incubated with the indicated concentrations of GAP-107X8-L-TFA for 48 hours. All data bars represent the means of three experiments performed in triplicate. Error bars show the standard error of the mean (SEM). Bars indicated with an asterisk (*) are treated groups that are significantly different ($p<0.05$) from their respective untreated control cells.

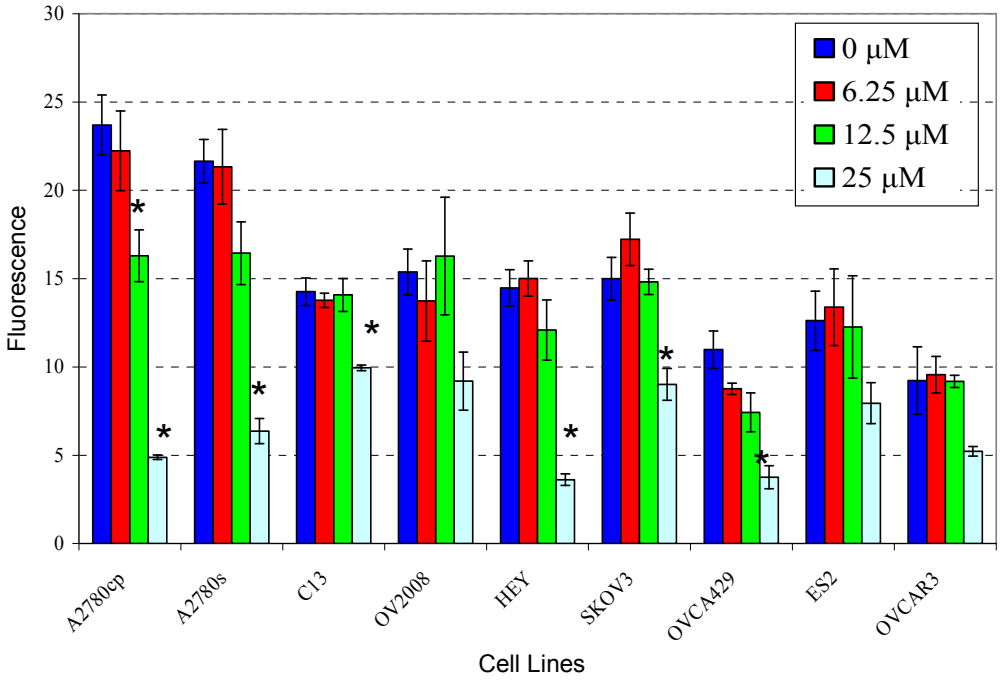

Figure 5. Inhibition of cell viability of 6 of 9 ovarian cancer cell lines in adherent cultures in the presence of GAP-107B8-L-TFA. Cells were incubated with the indicated concentrations of GAP-107B8-L-TFA for 48 hours. All data bars represent the means of three experiments performed in triplicate. Error bars show the standard error of the mean (SEM). Bars indicated with an asterisk (*) are treated groups that are significantly different ($p<0.05$) from their respective untreated control cells.

Table 5. Percent reduction of cell viability and motility by 25 µM GAP-107B8-L-TFA.

	Cell viability		Motility
	Adherent	Agar	
A2780cp	79%	94%	70%
A2780s	71%	86%	74%
C13	30%	91%	67%
OV2008	40%	93%	54%
HEY	75%	84%	50%
SKOV3	40%	50%	17%
OVCA429	66%	40%	24%
ES2	37%	80%	35%
OVCAR3	43%	4%	-

The percentage reduction was based on three independent experiments done in triplicate and statistically significant values ($p<0.05$) are highlighted.

3.1.3 GAP-107B8-L-TFA effect on cell viability in anchorage independent cell cultures in a panel of human ovarian cancer cell lines

Another property of cancer cells is their ability to grow without adhering to a surface, avoiding anoikis, an apoptotic process that is triggered by inadequate cell-matrix contacts (Frisch and Screaton, 2001). Therefore, the effects on cell viability in anchorage independent cultures on the same panel of human ovarian cancer cell lines following treatment with GAP-107B8-L-TFA were investigated *in vitro.* **Figure 6** shows the reduced cell viability of A2780cp, A2780s and HEY cells in soft agar treated with 6.25, 12.5 and 25 μM GAP-107B8-L-TFA. The 3 cell lines tested showed significant reduction of cell viability at all drug concentrations tested. The remaining cell lines required 14 days of culture to achieve measurable growth and were treated only with 25 μM GAP-107B8-L-TFA. The data on these remaining cell lines is summarized in **Figure 7**. Summarizing this data, 7 of the 9 cell lines showed a significant inhibition of cell viability ($p<0.05$) ranging from 50% to 93% when treated with 25 μM GAP-107B8-L-TFA based on one-way ANOVA with all 7 cell lines showing a reduction of cell viability equal to or greater than 50% (**Table 5**). Analysis by two-way ANOVA failed to indicate any interaction between GAP-107B8-L-TFA and carboplatin (data not shown).

3.1.4 GAP-107B8-L-TFA effect on cell motility

GAP-107B8-L-TFA caused a significant reduction in motility ($p<0.05$) ranging from 50% to 74% was observed in 5 of 9 ovarian cancer cell lines (**Figure 8**, **Table 5)**. However, this reduction in motility of cells treated at 25μM could not be interpreted due

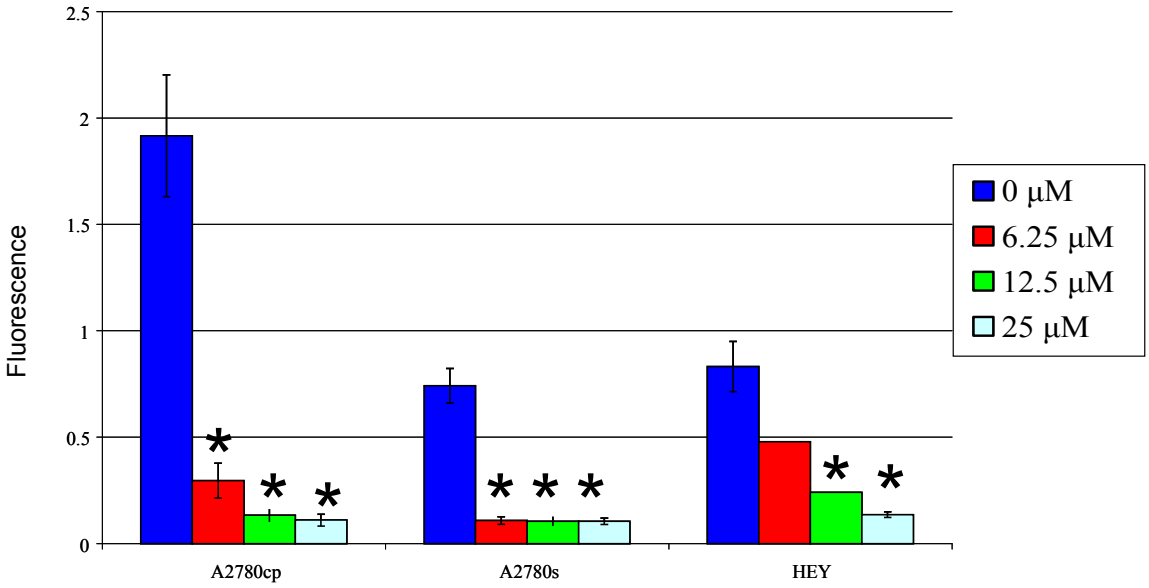

Figure 6. Inhibition of cell viability of A2780cp, A2780s or HEY cells ovarian cancer cell lines in anchorage independent cultures in the presence of GAP-107B8-L-TFA. Cells numbers were measured following 5 (A2780cp and A2780s) or 7 (HEY) days of growth in soft agar in the presence of the indicated concentrations of GAP-107B8-L-TFA. All data bars represent the means of three experiments performed in triplicate. Error bars show the standard error of the mean (SEM). Bars indicated with an asterisk (*) are treated groups that are significantly different ($p<0.05$) from their respective untreated control cells.

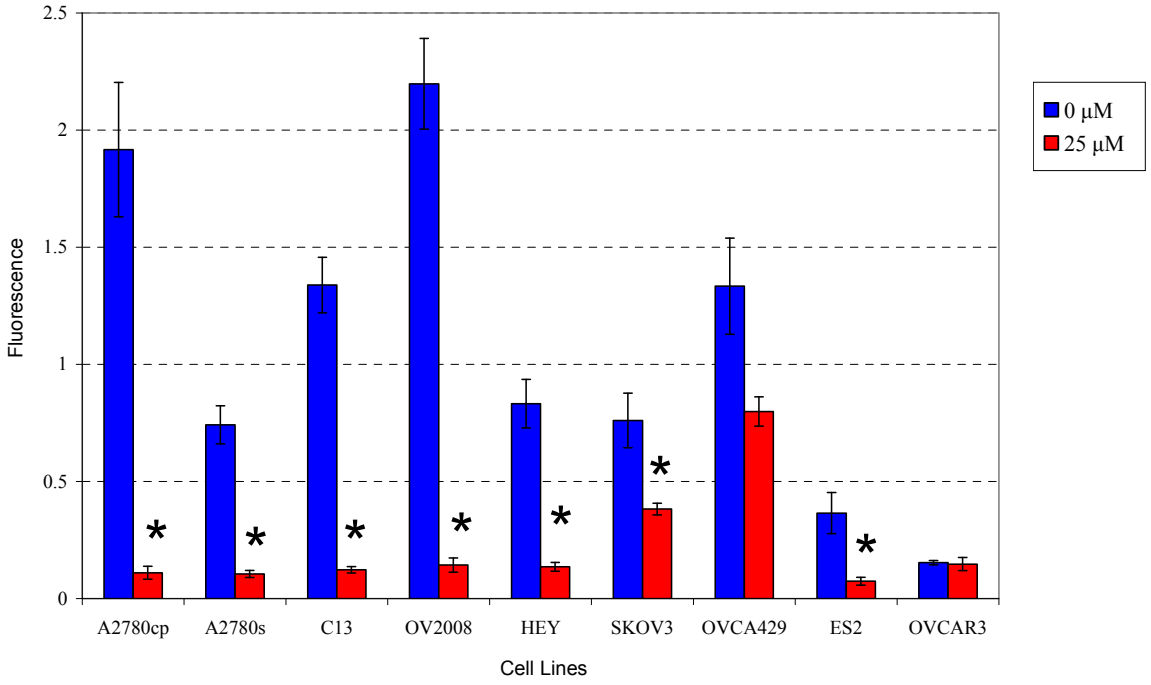

Figure 7. Inhibition of cell viability of 7 of 9 ovarian cancer cell lines in anchorage independent cultures in the presence of GAP-107B8-L-TFA. Cell numbers were determined following 5 (A2780cp, A2780s), 7 (HEY) or 14 (C13, OV2008, SKOV3, OVCA 429, ES2, OVCAR 3) days of growth in soft agar in the presence or absence of 25 µM GAP-107B8-L-TFA. All data bars represent the means of three experiments performed in triplicate. Error bars show the standard error of the mean (SEM). Bars indicated with an asterisk (*) are treated groups that are significantly different ($p<0.05$) from their respective untreated control cells.

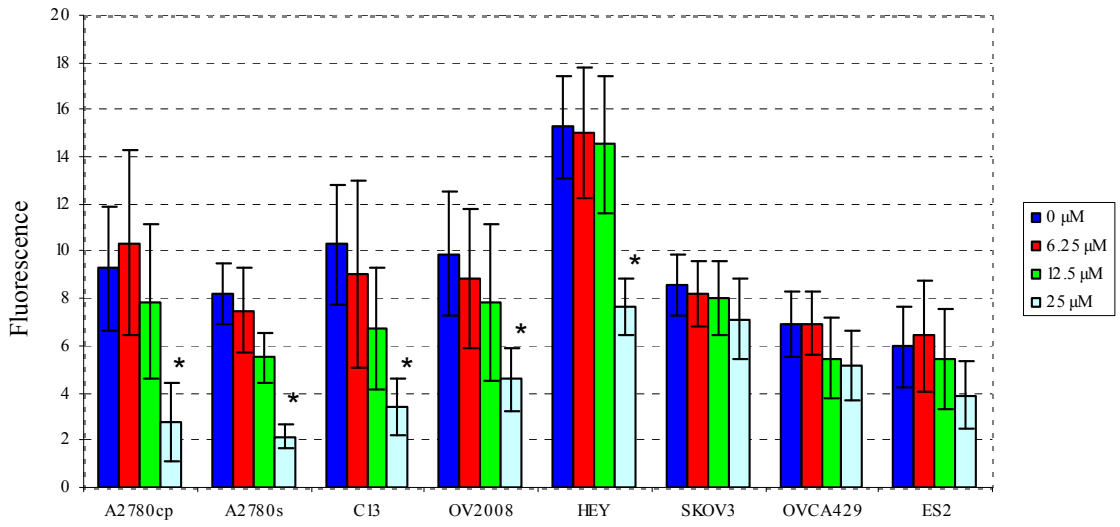

Figure 8. Inhibition of cell motility of 5 of 8 ovarian cancer cell lines in the presence of GAP-107B8-L-TFA. Cells were incubated with the indicated concentrations of GAP-107B8-L-TFA during for 24 hour. All data bars represent the mean of three experiments performed in triplicate. Error bars show the standard error of the mean (SEM). Bars indicated with an asterisk (*) are treated groups that are significantly different ($p<0.05$) from their respective untreated control cells.

to the loss of cell viability at that same concentration of GAP-107B8. Furthermore, doses at which cell viability was not affected did not impact cell motility.

3.1.5 Determining the MTD of treatment of intraperitoneal xenograft tumours with GAP-107B8-L-TFA

The MTD of GAP-107B8-L-TFA delivered IP to SCID mice needed to be determined prior to assessing the effect of GAP-107B8-L-TFA on tumour burden in xenograft models of ovarian cancer. **Table 6** describes the behavior and health of the mice during the course of the study. The lethal dose of GAP-107B8-L-TFA was found to be 160 mg/kg. The highest dose of GAP-107B8-L-TFA administered that did not require premature euthanization was 40 mg/kg. However, successive injections with this concentration of GAP-107B8-L-TFA did result in increasing toxicity with each successive dose. Consequently, while 40mg/kg, may be tolerated for short-term studies, it was determined that the increased toxicity with each administration might limit longer-term administration of GAP-107B8-L-TFA in a xenograft model. For this reason, the twice daily IP injections of 20 mg/kg was determined to be the MTD of GAP-107B8-L-TFA for future xenograft studies in SCID mice.

3.1.6 Treatment of intraperitoneal xenograft tumours with GAP-107B8-L-TFA

Using the MTD as a guideline for treatment, the ability of GAP-107B8-L-TFA to inhibit cancer cell viability *in vivo* and reduce tumour burden was investigated. Eight mice were injected with $1x10^7$ A2780cp cells. After 7 days to allow for the establishment of tumours, the mice were separated into 2 groups of 4 and each mouse was injected

Table 6. Health status of SCID mice in each group during the course of the GAP-107B8-L-TFA maximum tolerated dose study.

Group (Dose)	Status
Group1 (5mg/kg)	Well hydrated throughout study, normal behavior, no hunching
Group2 (10mg/kg)	Well hydrated throughout study, normal behavior, no hunching
Group3 (20mg/kg)	Seemed to behave normally throughout the study, one mouse lost quite a bit of weight, but still appeared quite active and otherwise normal. Both mice exhibited at times a slight hunch and erect pilus, still relatively well hydrated
Group4 (40mg/kg)	Beginning on Day 1 of injections for Group 4, mice did not appear to feel well after each injection, crowding water bottle and hunched over but would return to normal behavior after 30 minutes to an hour. However, they took progressively longer to bounce back as days went on.
Group5 (80mg/kg)	Exhibited hunched posture, similar to Group 4 but was visibly sluggish on Day 1 of injections for group 5. On Day 2 of injections for Group 5, hair became erect-a sign of poor hydration, and still sluggish. Survived two days of injections, but were euthanized after completing injections on Day 2
Group6 (160mg/kg)	Did not survive first injection, pronounced dead before the afternoon injection

Mice were injected twice daily IP for 7 days. To avoid unessecssary toxicity, the 7 day time course of injections was staggered to allow higher doses to be administered only after the animals treated at the lower dose were shown to tolerate their treatment.

twice daily IP with a dose of GAP-107B8-L-TFA for 14 days. Mice in the GAP-107B8-L-TFA treated group, but not the control group, exhibited a hunched posture with squinting of the eyes immediately after the initial injection of GAP-107B8. As the dosing schedule progressed, mice in the GAP-107B8-L-TFA treated group seemed to display successively less of an adverse reaction to GAP-107B8-L-TFA. Towards the end of treatment, the control mice appeared to exhibit more signs of severe disease, including being visibly sluggish with evidence of respiratory distress in addition to visible abdominal distension and palpable tumours.

In agreement with this observation, the control mice reached a loss of wellness endpoint first, which resulted in early termination of the experiment. Large visible and palpable tumours were present in mice from the GAP-107B8-L-TFA treated group as well, although it affected their mobility and well being less than the mice in the control group near the end of the study. Consequently, all mice were euthanized at the same time after 14 days of GAP-107B8-L-TFA injections in order to permit a comparison of tumour burden in both groups of mice at the same time point.

Figure 9 shows the mean tumour burden of SCID mice xenografted with A2780cp cells in the treated and control arms of the experiment. One control mouse failed to develop IP tumours and was removed from the analysis. Interestingly, qualitative observations revealed that control mice had smaller and more numerous nodules attached to many different organs, while the GAP-107B8-L-TFA treated mice had fewer but larger, more solid nodules. Nevertheless, the mean tumour burden of animals from both groups was not statistically different ($p>0.05$) from each other.

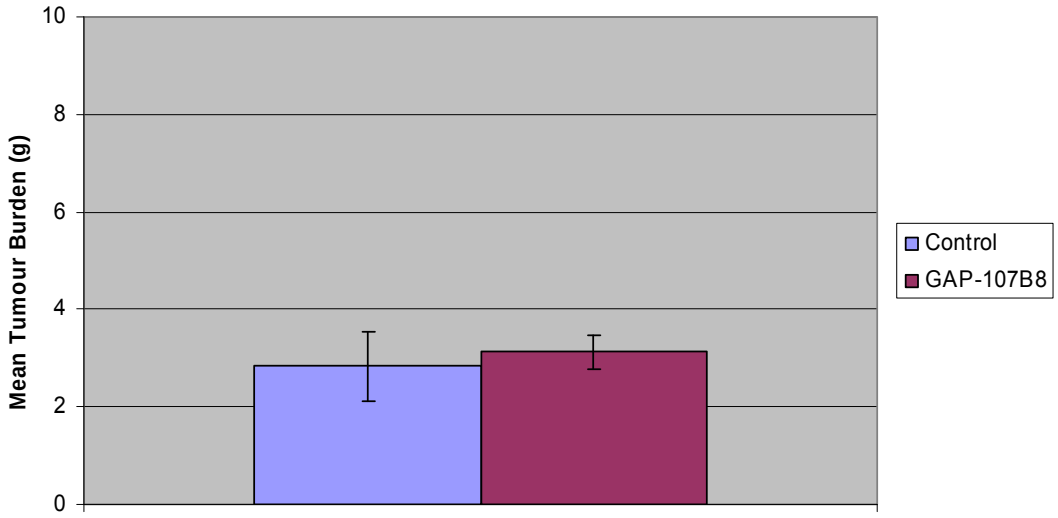

Figure 9. Mean tumour burden of SCID mice xenografted with A2780cp cells. Mice were injected IP with 1 mL of PBS buffer containing 10^7 A2780cp human ovarian cancer cells. After 7 days to allow tumour initiation, the 8 mice were divided into control (*n=4)* and treatment (*n=4)* groups. One control mouse failed to develop IP tumours and was removed from the analysis. Error bars show the standard error of the mean (SEM).

Two issues that needed to be addressed as a result of this study were the contributing toxicity of DMSO and the efficacy of the IP route of delivery. The following chapter aimed to address these concerns.

3.2 Assessing the effect of GAP-107B8-L-Ac on ovarian cancer cells *in vitro* and *in vivo*

From the previous chapter, questions regarding confounding toxicity parameters were raised with the GAP-107B8-L-TFA compound used in the IP studies. The peptide GAP-107B8-L-TFA had a trifluoroacetate counter ion, which required it to be dissolved in DMSO. Although injection of DMSO into control animals was not found to induce toxicity, DMSO toxicity has been documented and its presence was considered a confounding factor in our experiments due to the possible combined toxicity of GAP-107B8-L-TFA and DMSO. Therefore, we repeated the experiment using GAP-107B8-L-Ac, which possesses an acetate counter ion and allows it to be dissolved in water, eliminating any confounding toxicity parameters.

3.2.1 GAP-107B8-L-Ac effect on cell viability in adherent and anchorage independent cell cultures in A2780cp human ovarian cancer cell line

The effect of cell viability of A2780cp cells adherent and anchorage independent cultures in the new formulation GAP-107B8-L-Ac in was determined As shown in **Figure 10A,** cell viability in adherent cultures was significantly inhibited in A2780cp cells treated with 25 μM GAP-107B8-L-Ac as determined by one-way ANOVA

A

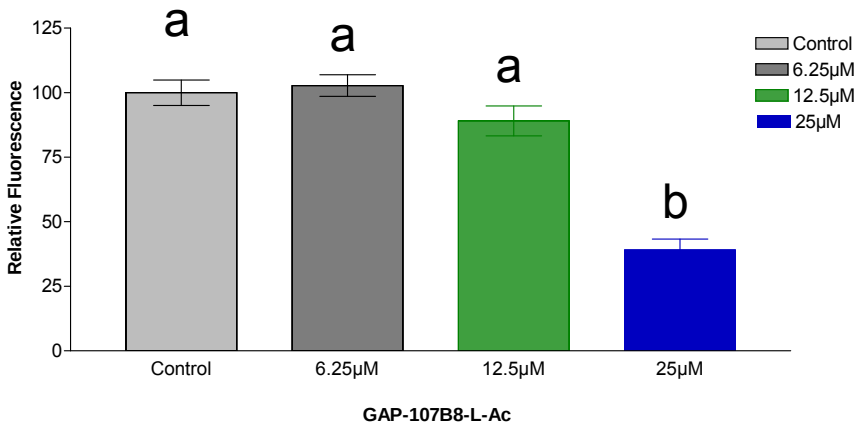

B

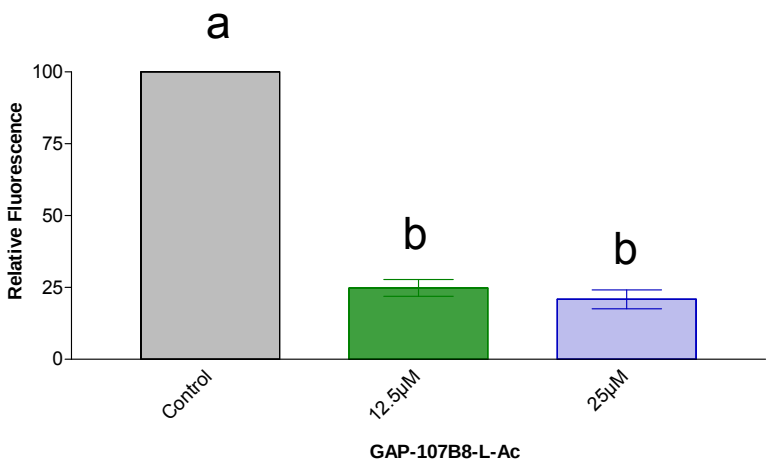

Figure 10. Inhibition of cell viability of A2780cp cells in adherent (A) and anchorage independent (B) cultures in the presence of GAP-107B8-L-Ac. A A2780cp cells were incubated with the indicated concentrations of GAP-107B8-L-Ac for 48 hours. **B** A2780cp cells were incubated with the indicated concentrations of GAP-107B8-L-Ac for 5 days. All data bars represent the means of three experiments performed in triplicate with values normalized to yield a mean control value equal to 100. Error bars show the standard error of the mean (SEM). Means with different letters indicate statistical differences (Bonferroni, $p<0.05$).

($p<0.05$). In anchorage independent conditions, cell viability was significantly inhibited at both doses of GAP-107B8-L-Ac ($p<0.05$) (**Figure 10B)**.

3.2.2 Treatment of intraperitoneal xenograft tumours with GAP-107B8-L-Ac

Twelve SCID mice were injected with $1x10^7$ A2780cp cells. After 7 days to allow for the establishment of tumours, the mice were separated into 4 groups of 2 and each mouse was injected twice daily IP with a dose of GAP-107B8-L-TFA for 14 days. Throughout the duration of the experiment, mice in the GAP-107B8-L-Ac treated group did not exhibit signs of toxicity immediately after injection of GAP-107B8-L-Ac. This is in contrast to the initial IP efficacy study where mice in the treatment group exhibited a hunched posture with squinting of the eyes immediately after the first and subsequent injections. Since both groups in that study received injections containing DMSO, the toxicity seen in the treated animals may be related to the combination of GAP-107B8-L-TFA and DMSO.

Most of the treated animals and some of the control animals reached a loss of wellness endpoint on Day 12 post-treatment of the study due to high tumour burden. During the final 2 days of treatment, the loss of wellness presented as impairment of movement due to increased tumour burden. Consequently, all mice were euthanized at the same time, on Day 12, in order to permit a comparison of tumour burden in both groups. **Figure 11A** shows once again there is no significant difference in mean total tumour burden between the control and treatment groups. One control mouse failed to develop IP tumours and was removed from the analysis.

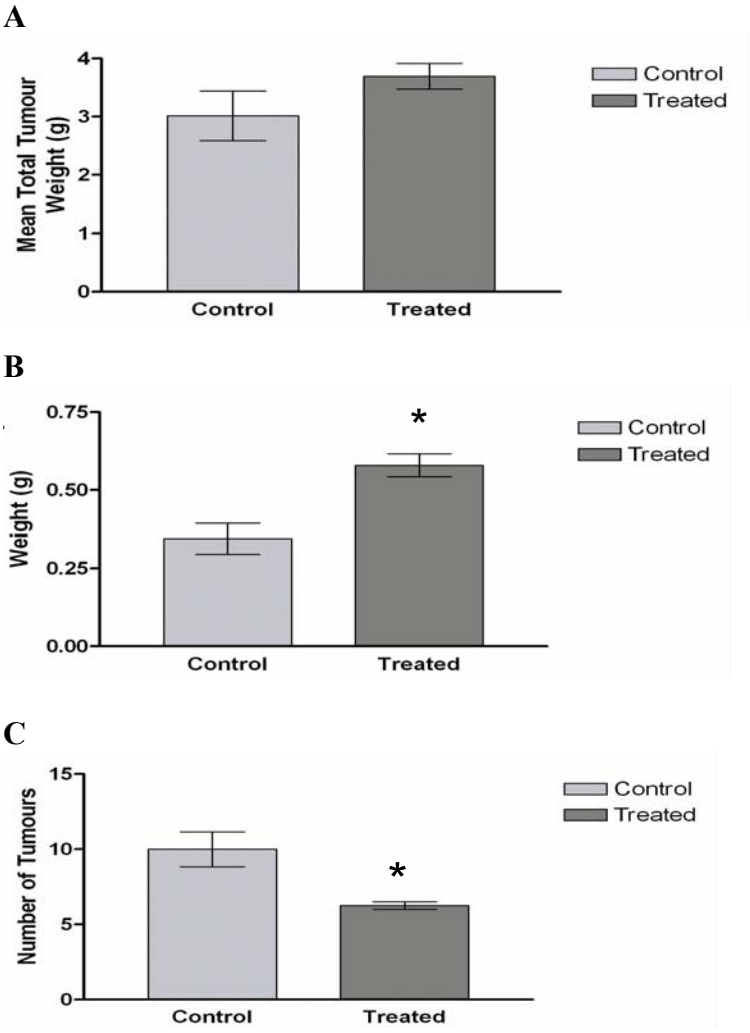

Figure 11. IP treatment of A2780cp IP tumours. Mice harboring A2780cp IP tumours were treated with GAP-107B8-L-Ac twice daily IP for 12 days. **A)** Mean tumour burden expressed as mean total tumour weight from control (*n*=5) and GAP-107B8-L-Ac treated mice (*n*=6). **B)** Total tumour weight divided by the number of tumours was used to calculate average weight of each tumour per mouse. **C)** Number of tumours was counted manually. Mean weight of the individual tumours and the mean number of tumours were determined from control (*n*=3) and GAP-107B8-L-Ac treated (*n*=4) animals. Bars indicated with an asterisk (*) are treated groups that are significantly different ($p<0.05$) from controls. Error bars show the standard error of the mean (SEM).

Interestingly, similar to the initial efficacy study, mice in the GAP-107B8-L-Ac treated arm of the study appeared to have larger and fewer tumours compared to control mice. Quantification of the tumours revealed that the mean weight of the individual tumours in treated animals was significantly larger than the control animals ($p<0.05$) (**Figure 11B).** In addition, **Figure 11C** shows there is a significantly greater mean number of tumours per mouse in the control animals compared to the treated animals ($p<0.05$).

3.2.3 Treatment of subcutaneous xenograft tumours with GAP-107B8-L-Ac

Since it was determined that GAP-107B8-L-Ac was not able to reduce mean tumour burden *in vivo* in an IP xenograft model, the objective of this study was to determine whether GAP-107B8-L-Ac is able to reduce ovarian tumour burden *in vivo* following intratumoural (IT) injection into a subcutaneous tumour. This route of delivery would allow the drug to have a direct opportunity to target the cancer cells and with a higher local bioavailability. A second cell line, HEY, was included in the study to rule out cell line specific effects.

A2780cp IT xenograft

Fifteen mice were injected subcutaneously on the flank with 10^6 A2780cp cells. When the tumours reached 200 (millimeter) mm^3, mice were divided into 2 groups based on weight, size of tumour and growth rate of the tumour. Mice in each group were treated daily IT either with 0 (vehicle control) or 20 mg/kg GAP-107B8-L-Ac in 50 µl volumes, once per day until tumours reached 2 cm^3. All mice that developed tumours were euthanized after 11 days of treatment with GAP-107B8-L-Ac when it was

determined that the size of the tumour in the control animals exceeded the planned endpoint targets. **Figure 12A** shows the tumour sizes of the control and GAP-107B8-L-Ac treated mice at various days post-treatment. To permit a comparison of tumour burden in both groups of mice at the same time point, tumour burden in each animal at Day 10 after initiation of treatment was used (**Figure 12B**). A significant (45%) reduction in average tumour size was observed between mice in the control group and mice treated with GAP-107B8-L-Ac by unpaired t-test ($p<0.01$). The mean tumour size of the control group was 4412 ± 617.1 mm^3 (mean ± SEM), while the mean tumour size of the treatment group was 2407 ± 250.6 mm^3.

HEY IT xenograft

Six mice were injected subcutaneously on the flank with 10^6 HEY cells. When the tumours reached 200 mm^3, mice were divided into 2 equivalent groups based on weight, size of tumour and growth rate of the tumour. Mice in each group were treated daily either with 0 (vehicle control) or 40 mg/kg GAP-107B8-L-Ac IT in 50 µl volumes, once per day until tumours reached 2 cm^3. All mice were euthanized at day 7 post-treatment due to the formation of lesions in the skin of the tumour in the GAP-107B8-L-Ac treated animals. **Figure 13A** shows the tumour sizes of the control and GAP-107B8-L-Ac treated mice at various days post-treatment. To permit a comparison of tumour burden in both groups of mice at the same time point, tumour burden in each animal at day 7 post-treatment was used (**Figure 13B**). A significant (75%) reduction in average tumour size was observed between mice in the control group and mice treated with GAP-107B8-L-Ac by unpaired t-test ($p<0.001$). The mean tumour size of the control group

A

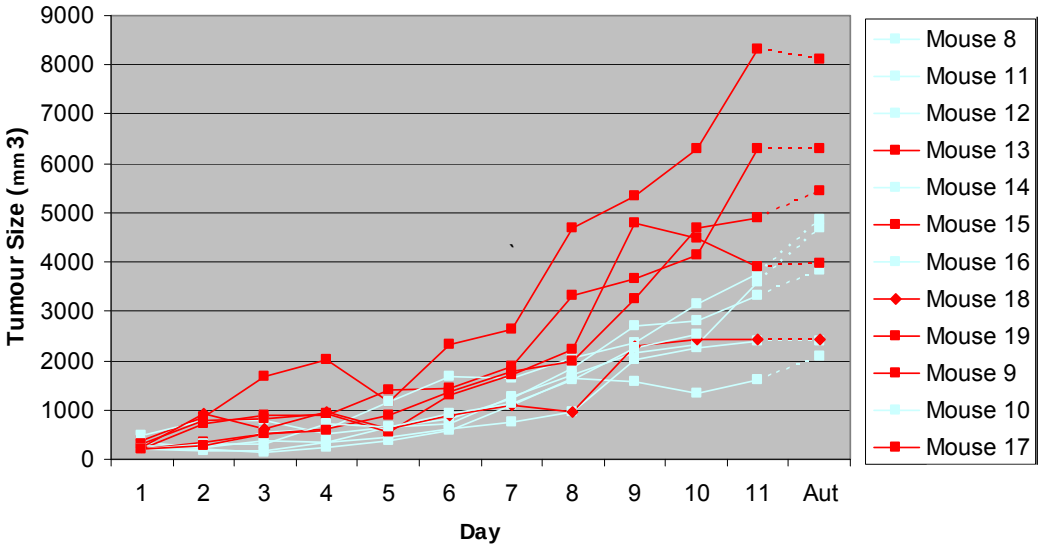

B

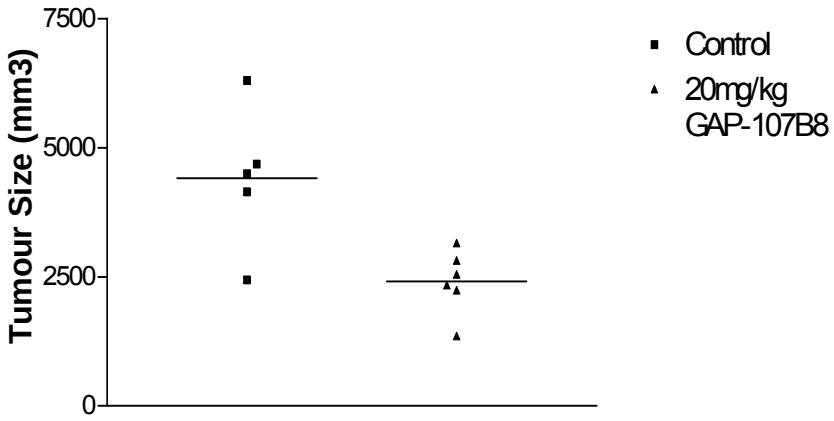

Figure 12. Intra-tumoural treatment of A2780cp subcutaneous tumours with GAP-107B8-L-Ac for 11 days. Fifteen SCID mice were injected subcutaneously on the flank with 10^6 A2780cp cells. When the tumours reached 200 mm^3, mice were divided into 2 groups and treated daily either with 0 (vehicle control) or 20 mg/kg GAP-107B8-L-Ac intra-tumourally in 50 µl volumes, once per day for 11 days. Tumour sizes were measured daily with calipers. **A** Daily tumour sizes are shown for the control (red) and GAP-107B8-L-Ac treated (blue) mice. The dashed line signifies that the last measurement was made during autopsy (Aut). **B** Tumour size comparison between control (n=5) and GAP-107B8-L-Ac (n=6) treated animals at Day 10 of the treatment schedule.

A

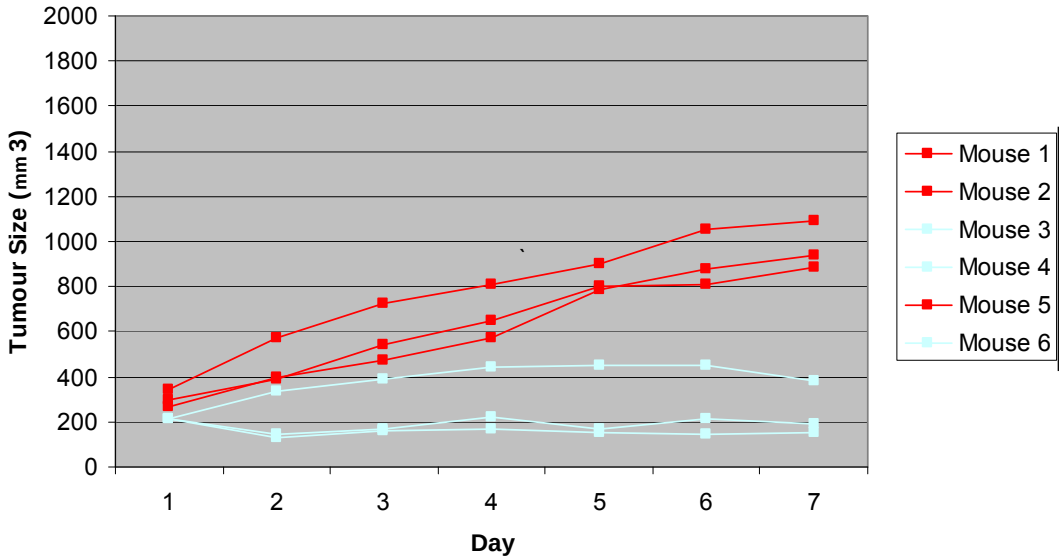

B

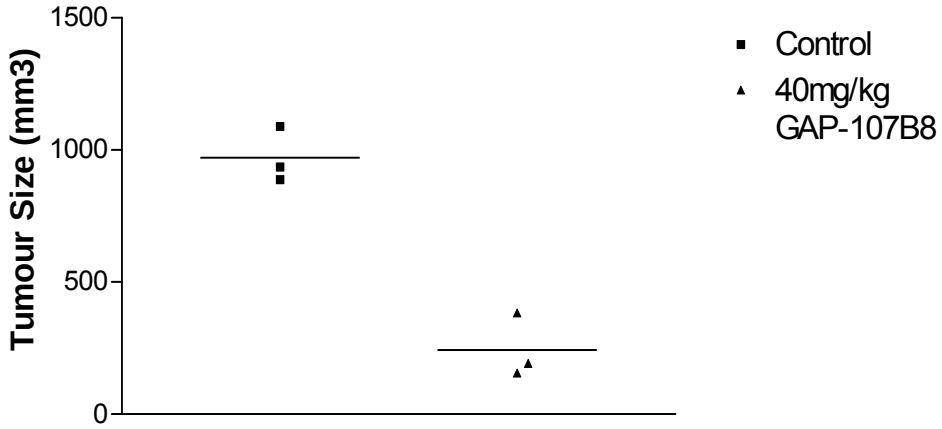

Figure 13. Intra-tumoural treatment of HEY subcutaneous tumours with GAP-107B8-L-Ac for 7 days. Six SCID mice were injected subcutaneously on the flank with 10^6 HEY cells. When the tumours reached 200 mm^3, mice were divided into 2 groups and treated daily either with 0 (vehicle control) or 40 mg/kg GAP-107B8-L-Ac intra-tumourally in 50 µl volumes, once per day for 7 days. Tumour sizes were measured daily with calipers. **A** Daily tumour sizes are shown for the control (red) and GAP-107B8-L-Ac treated (blue) mice. **B** Tumour size comparison between control (n=3) and GAP-107B8-L-Ac (n=3) treated animals at Day 7 of the treatment schedule.

was 971.1 ± 60.55 mm^3, while the mean tumour size of the treatment group was 243.5 ± 70.27 mm^3.

3.3 Determining the mechanism of action of GAP-107B8-L-Ac

3.3.1 Effects of GAP-107B8-L-Ac on apoptosis in A2780cp human ovarian cancer cells

Apoptosis was directly assessed using two methods: by the TUNEL assay and by detection of cleaved PARP. A2780cp cells treated with 25μM GAP-107B8-L-Ac for 30 hours showed increased numbers of apoptotic cells as determined by the observation of increased numbers of treated cells having condensed nuclei by DAPI staining and being TUNEL positive compared to untreated samples (**Figure 14**).

PARP is involved in the DNA base-excision-repair system and can be cleaved by various caspases (Satoh and Lindahl, 1992; Lazebnik et al., 1994; Cohen, 1997). Therefore, PARP helps to maintain the viability of cells and its cleavage is a marker for apoptosis. GAP-107B8-L-Ac treated A2780cp cells showed a decrease in PARP and an increase in cleaved PARP over a period of 30 hours (**Figure 15)**. These results confirm the induction of apoptosis in A2780cp cells treated with GAP-107B8-L-Ac.

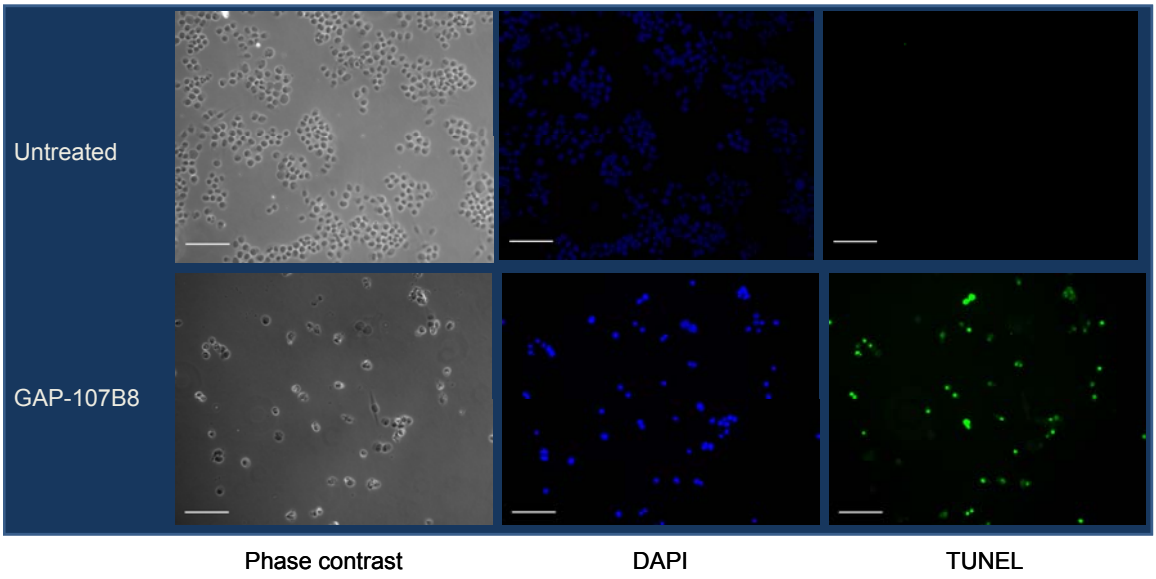

Figure 14. TUNEL and DAPI staining of GAP-107B8-L-Ac treated A2780cp cells. A2780cp cells were collected after 30 hours treatment with ddH2O or 25 µM GAP-107B8-L-Ac. Data are representative of three independent experiments. The white scale bar indicates 100µm.

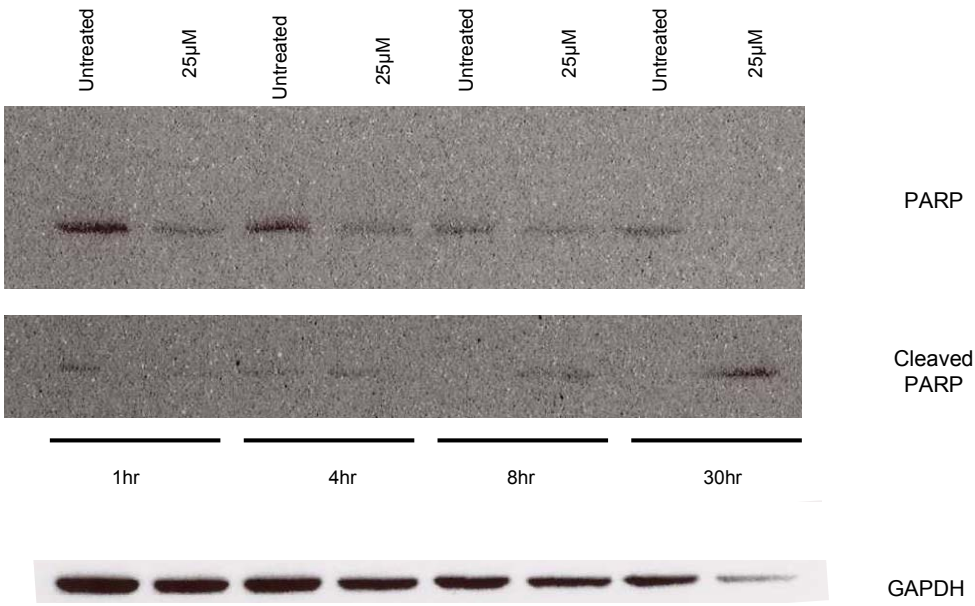

Figure 15. Western blot analysis of PARP and cleaved PARP in A2780cp cells treated with GAP-107B8-L-Ac. A2780cp cells were treated with GAP-107B8-L-Ac and collected at the indicated times and analysed by western blot. Cells were lysed and 40μg of total cell extracts of untreated and treated samples were resolved by SDS-PAGE, transferred to nitrocellulose membrane and probed with an antibody to PARP, cleaved PARP and GAPDH. GAPDH was used as a loading control. Data are representative of three independent experiments.

3.3.2 GAP-107B8-L-Ac effects on the cell cycle progression in A2780cp cells

In addition to inducing active apoptosis, it was possible that GAP-107B8-L-Ac is inhibiting the growth of cells through other mechanisms. Therefore, it was investigated whether GAP-107B8-L-Ac caused the inhibition of growth of A2780cp cells through the induction of cell cycle arrest, apoptosis, or a combination of both processes. Cells were labeled with BrdU, treated with GAP-107B8 or vehicle, and collected at various time points. Cells were then analyzed by flow cytometry to determine the impact of the drug on steady state levels of apoptotic cells, cells residing in G_1/G_0, S phase cells or cells in G_2/M. As shown in **Figure 16**, treatment with GAP-107B8-L-Ac increases the proportion of sub-G_1 (apoptotic) cells by 4 hours and delays the proportion of cells progressing through the G_2/M stage of the cell cycle at the 8 hour time point. The delay in progression of the cell cycle is transient as indicated by the 14 hour time point, where both the untreated and treated cells have returned to the G_1 phase of the cell cycle. This data suggests that GAP-107B8-L-Ac may be unstable in culture media in prolonged experiments or indicate the presence of a resistant population of cells to GAP-107B8-L-Ac.

3.3.3 GAP-107B8-L-Ac effects on the activity of PKCs in A2780cp cells

Given the literature on the role of PKCι in ovarian cancer cells and the initial design of GAP-107B8-L-Ac as a PKC inhibitor, it was anticipated that GAP-107B8 would have an impact on the phosphorylation status of PKCι, and perhaps other PKCs also. However, western blot analysis did not reveal any difference in either the abundance of PKCι or its phosphorylation status (threonine 555) between untreated and treated cells

Untreated **Treated**

A B

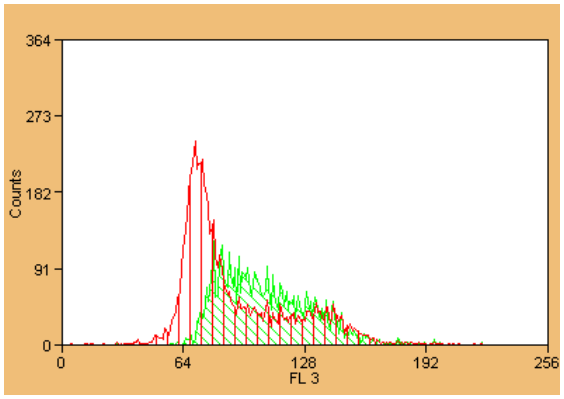

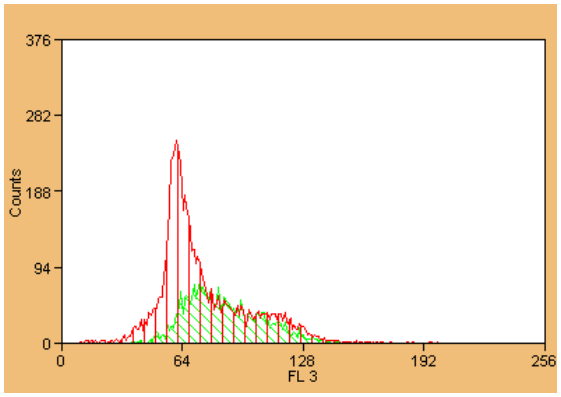

1hr

C D

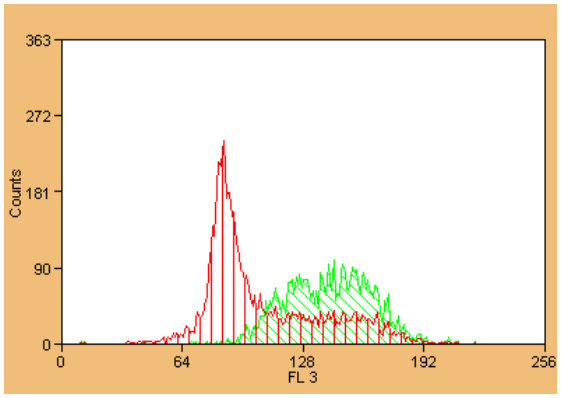

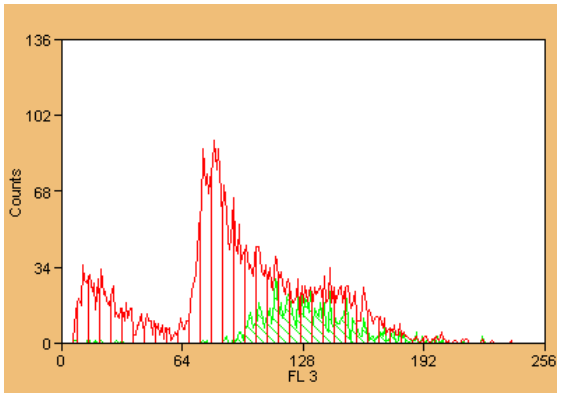

4hr

E F

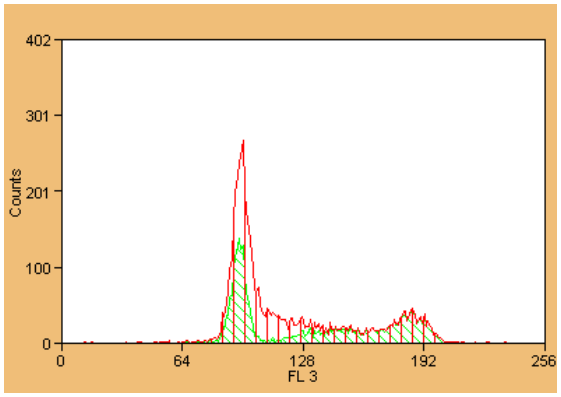

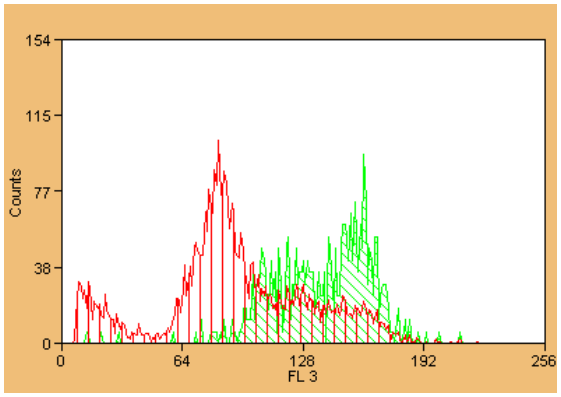

8hr

G H

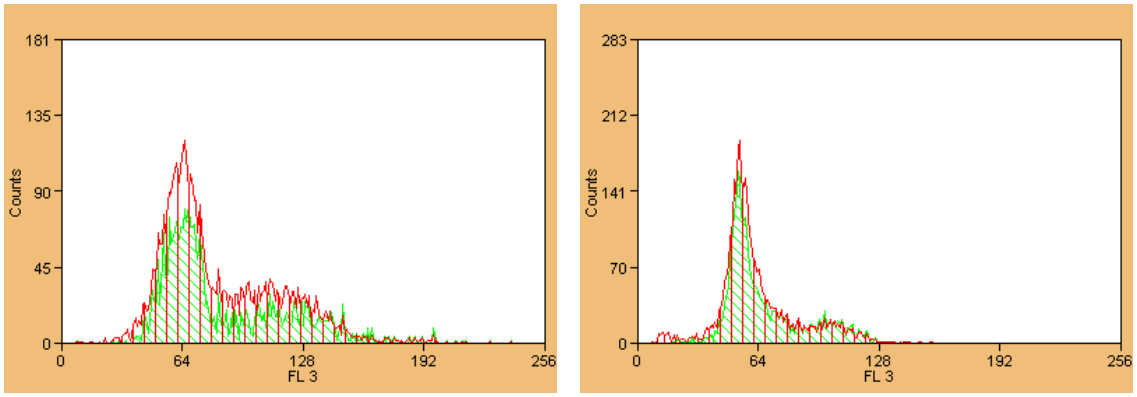

14hr

Figure 16. Flow cytometry analysis of A2780cp cells treated with GAP-107B8-L-Ac. Cells were labeled with BrdU (green) for 1 hour prior to GAP-107B8-L-Ac treatment. Red indicates the total cells present. Cells were either untreated (control) or treated with 25 µM GAP-107B8-L-Ac and collected at 1 (A, B), 4 (C, D), 8 (E, F) or 14 hours (G, H) after treatment. Data are representative of three independent experiments.

(**Figure 17A**), suggesting that GAP-107B8 does not inhibit the baseline level of PKCι activity in A2780cp cells, at least after one hour.

Subsequent experiments explored the possibility that other isoforms of PKC may be targets of GAP-107B8-L-Ac. As shown in **Figure 17B**, there is no apparent inhibition in the phosphorylation status of any PKC investigated, as detected using antibodies against the phosphorylated forms of pan-PKC (Ser 660), PKCα/βII (Ser 744/748), PKCδ (Thr 505), PKCμ (Ser 916), and PKCζ/λ (Thr 410/403). There were no bands detected when probing for pPKCθ.

3.3.4 GAP-107B8-L-Ac effects on the phosphorylation of Akt at Ser 473 in A2780cp cells

Akt is a central signaling molecule that plays a critical role in the survival of ovarian cancer cells. While not predicted to be a direct target of GAP-107B8, it was of interest to see whether impingement of this signaling pathway might be implicated in GAP-107B8-L-Ac induced apoptosis. As seen in **Figure 18A**, GAP-107B8-L-Ac treated A2780cp cells showed a dramatic decrease in phosphorylation of Akt at Ser473 at all three concentrations tested (6.25, 12.5 and 25 μM). There was no dose-response effect for the range of concentrations tested. Densitometry analysis of three independent western blots showed a significant 62%, 58% and 58% decrease in the ratio of pAkt/Akt in A2780cp cells treated with 6.25, 12.5 and 25 μM GAP-107B8, respectively (**Figure 18B**; *$p<0.001$). The suppression of Ser473 phosphorylation of Akt was sustained over 30 hours when A2780cp cells were treated with 25 μM GAP-107B8-L-Ac (**Figure 19**).

A: PKCι

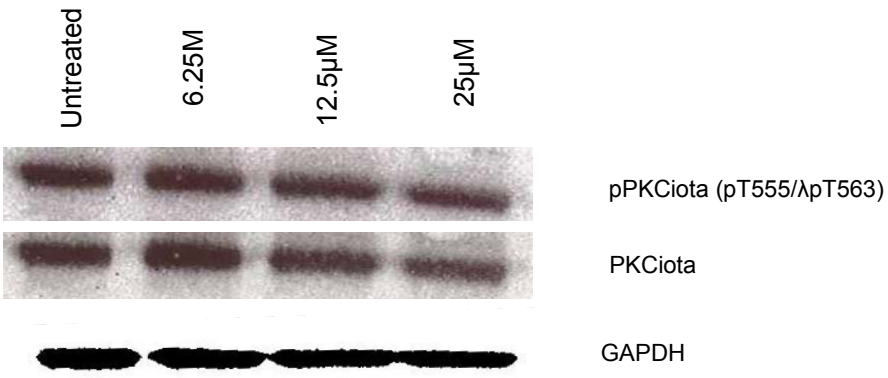

B: Other PKCs

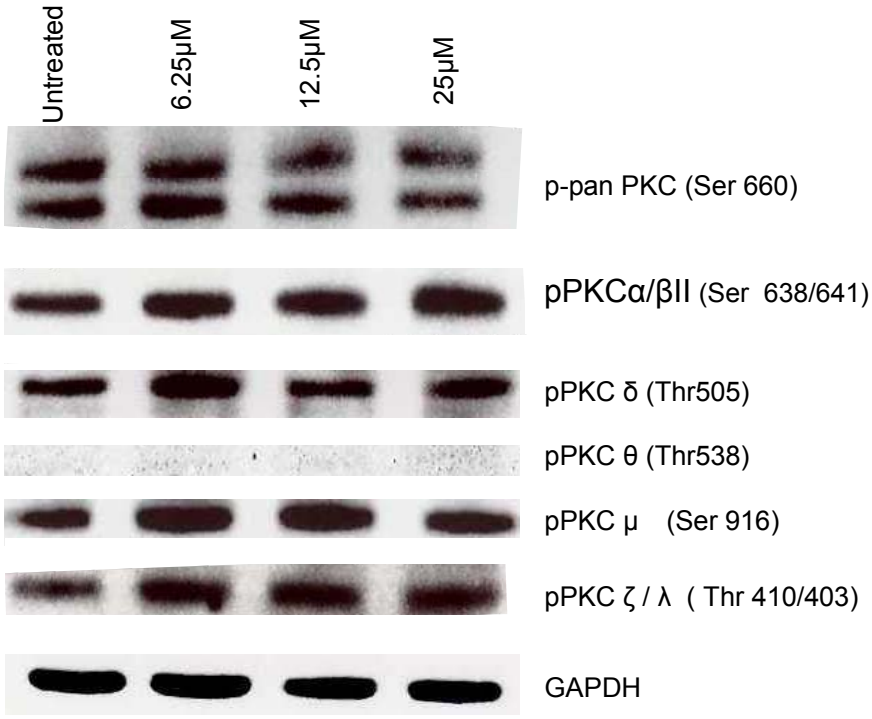

Figure 17. GAP-107B8-L-Ac effect on various PKC isoforms in A2780cp cells. A2780cp cells were treated with the indicated concentrations of GAP-107B8 for 1 hour. Cells were lysed and 40 μg of total protein of untreated and treated cells were resolved by SDS-PAGE, transferred to nitrocellulose membrane, and probed with antibodies to pPKCι and PKCι (**A**) and p-panPKC, pPKCα/βII, pPKCδ, pPKCθ, pPKCμ, pPKCζ/λ (**B**). GAPDH was used as a loading control. The data is representative of two independent experiments.

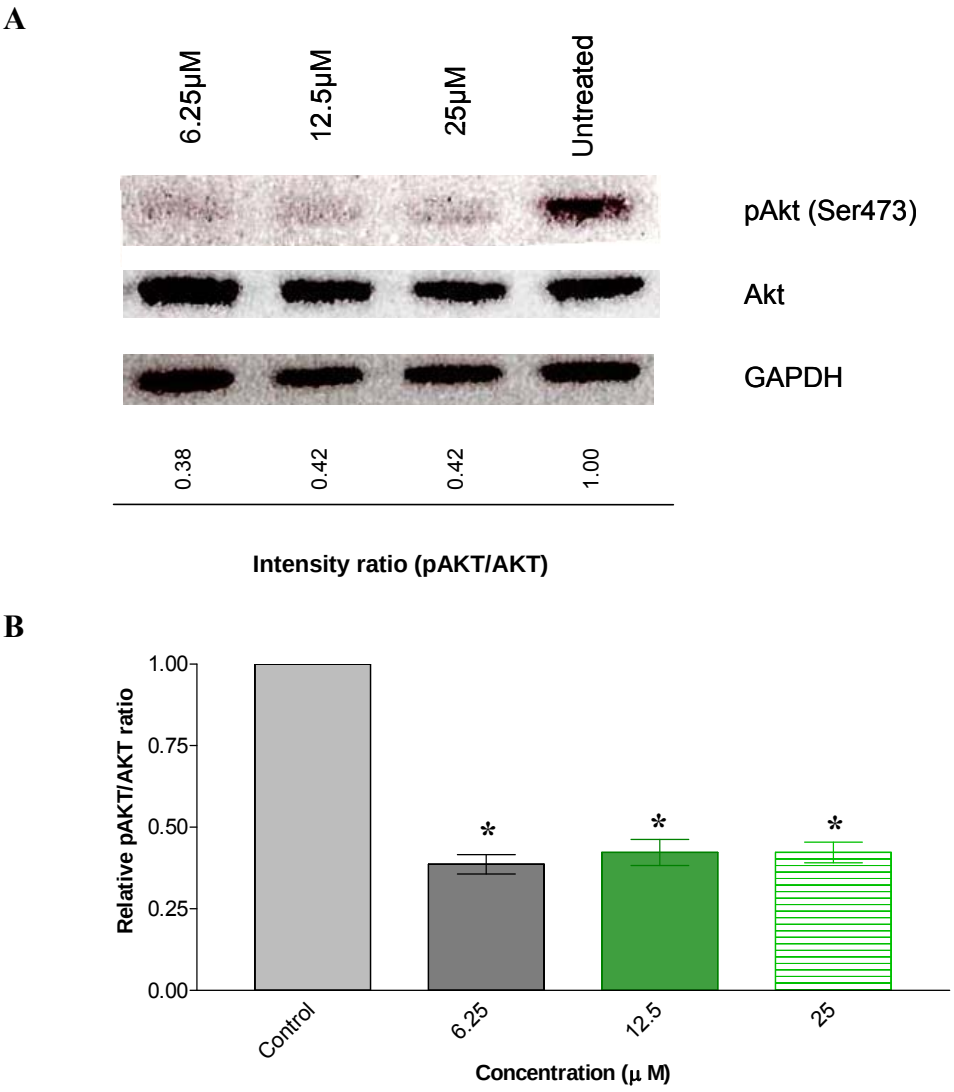

Figure 18. A2780cp cells were treated with the indicated concentrations of GAP-107B8-L-Ac for 1 hour. Cells were lysed and 40 µg of total cell proteins of untreated and treated cells were resolved by SDS-PAGE, transferred to nitrocellulose membrane, and probed with antibodies to pAkt, Akt and GAPDH (**A**). GAPDH was used as a loading control. Band intensities were quantified by densitometry analysis of blots from three independent experiments, and values for the pAkt/Akt mean ratio +/- SEM are shown relative to control A2780cp cells, which were assigned an intensity ratio of 1.0 (**B**). Asterisks (*) indicate statistical significance ($p<0.001$) between the treated samples and the untreated control.

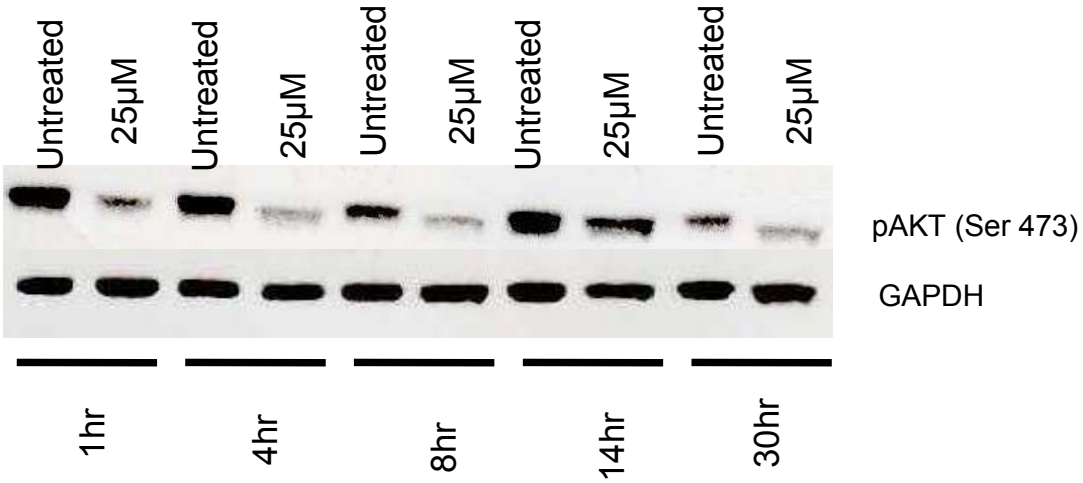

Figure 19. Time course of GAP-107B8-L-Ac treated A2780cp cells. A2780cp cells were treated with GAP-107B8-L-Ac and collected at the indicated times and analysed by Western blot. Cells were lysed and 40 μg of total cell extracts of untreated and treated samples were resolved by SDS-PAGE, transferred to nitrocellulose membrane and probed with an antibody to pAKT. GAPDH was used as a loading control. The blot is representative of three independent experiments, except the 30 hour time point, which has been performed twice.

Although treatment of A2780cp cells with the lower dose of 6.25 μM GAP-107B8-L-Ac led to loss of phosphorylation of Akt at Ser473 one hour after treatment (**Figure 18**), this response was transient as partial inhibition was seen at 4 hours and no inhibition was evident at 8 hours (**Figure 20**).

3.4. Comparative effects of GAP-107B8-L-Ac and GAP-107B8-D-Ac

Previously, GAP-107B8-L-TFA and GAP-107B8-L-Ac were shown to effectively inhibit the cell viability of a variety of ovarian cancer cell lines in both adherent and anchorage independent cultures (**Figure 5-8, 10**). More recently, PharmaGap Inc. developed a D-isomer analogue of the GAP-107B8, a compound that bears the name GAP-107B8-D-Ac. It was of interest to compare the efficacy in this compound in similar assays using several of our ovarian cancer cell lines.

3.4.1 GAP-107B8-L-Ac and GAP-107B8-D-Ac effect on cell viability in adherent cell cultures

The reduction in cell viability in adherent cultures of the A2780cp, OCC1 and OVCAR8 ovarian cancer cell lines following treatment with GAP-107B8-L-Ac or GAP-107B8-D-Ac are summarized in **Figure 21 A, B,** and **C,** respectively. The inhibition of cell viability in adherent cultures was significant in two of three cell lines treated with 25 μM GAP-107B8-L-Ac by one-way ANOVA ($p<0.05$). In addition, all three cell lines showed significant inhibition of cell viability at 12.5 μM, and for two of the three cell lines, at 6.25 μM when treated with GAP-107B8-D-Ac by one-way ANOVA ($p<0.05$). The mean percent reductions of cell viability by GAP-107B8-L-Ac and GAP-107B8-D-

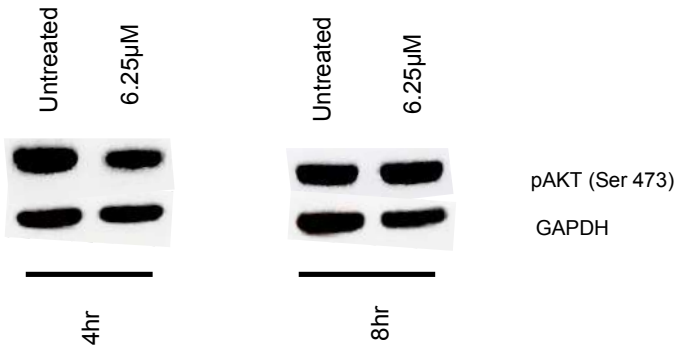

Figure 20. Western Blot analysis of pAkt status in A2780cp cells after 4 and 8 hours treatment with GAP-107B8-L-Ac. A2780cp cells were treated with GAP-107B8-L-Ac and collected at the indicated times and analysed by Western blot. Cells were lysed and 40μg of total cell extracts of untreated and treated samples were resolved by SDS-PAGE, transferred to nitrocellulose membrane and probed with an antibody to pAkt and GAPDH. GAPDH was used as a loading control. Data is from one experiment.

A: A2780cp

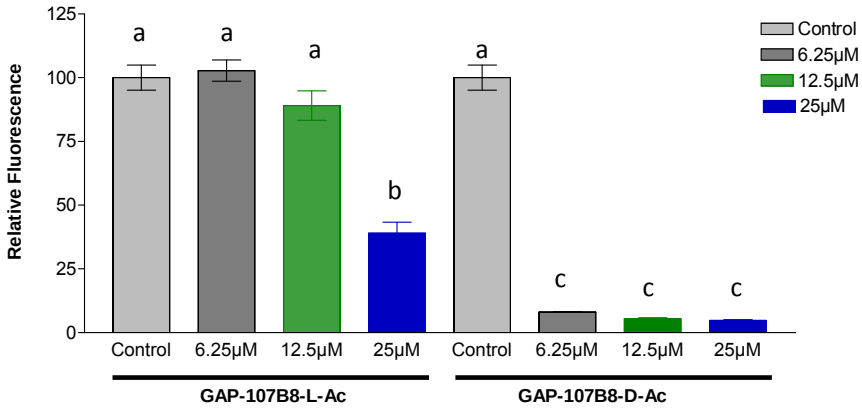

B: OCC1

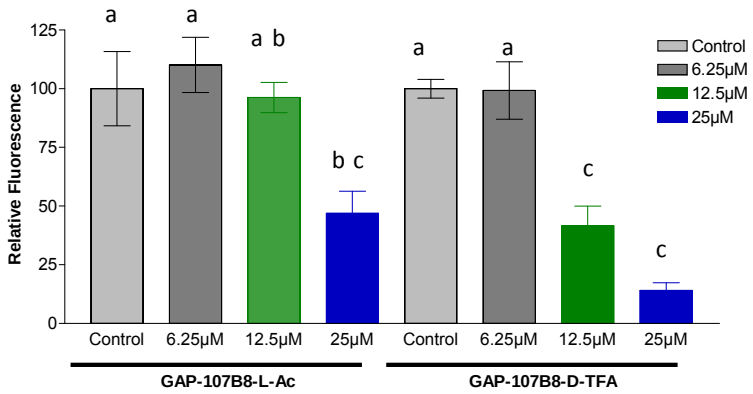

C: OVCAR8

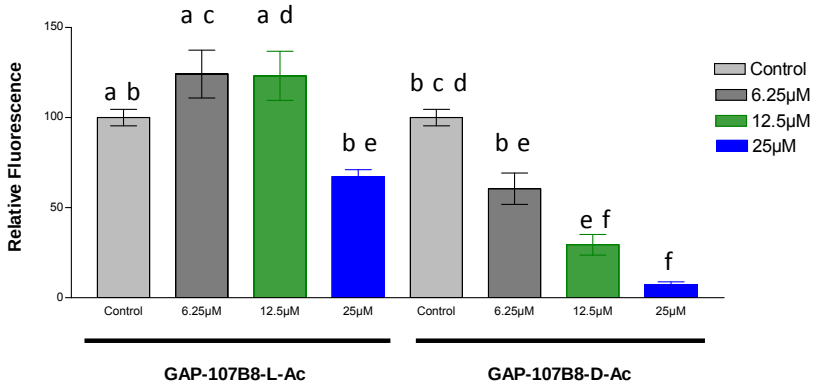

Figure 21. Inhibition of cell viability of A2780cp, OCC1 and OVCAR8 cells in adherent cultures in the presence of GAP-107B8-L-Ac and GAP-107B8-D-Ac. A2780cp cells (**A**), OCC1 cells (**B**) and OVCAR8 cells (**C**) were incubated with the indicated concentrations of GAP-107B8-L-Ac or GAP-107B8-D-Ac for 48 hours. All data bars represent the means of three experiments performed in triplicate with values normalized to yield a mean control value equal to 100. Error bars show the standard error of the mean (SEM). Means with different letters indicate statistical differences (Bonferroni, $p<0.05$). Note: GAP-107B8-D-TFA was used only in treating OCC1 cells grown in adherent cultures.

Ac are shown in **Table 7** with all three cell lines showing a greater than 85% reduction over 48 hours when treated with the GAP-107B8-D-Ac.

3.4.2 GAP-107B8-L-Ac and GAP-107B8-D-Ac effect on cell viability in anchorage independent cell cultures

Reductions in growth of three ovarian cancer cell lines in soft agar following treatment with GAP-107B8-D-Ac and GAP-107B8-L-Ac are summarized in **Figure 22**. **Figure 22A** shows the inhibition of cell viability of A2780cp cells after 5 days in soft agar treated with 6.25 and 12.5 μM GAP-107B8-D-Ac and 12.5 and 25 μM GAP-107B8-L-Ac. **Figures 22B** and **22C** show the effects on cell viability in soft agar of OCC1 and OVCAR8 cells, respectively, after 10 days of culture treated with 12.5 and 25 μM of both GAP-107B8-D-Ac and GAP-107B8-L-Ac.

The inhibition of cell viability in anchorage independent cultures was significant only in the OVCAR8 and OCC1 cells when they were treated with the higher dose (25 μM) of GAP-107B8-L-Ac, whereas A2780cp cells were strongly inhibited at both doses ($p<0.05$). Treatment with GAP-107B8-D-Ac caused a significant inhibition of cell viability of all three cell lines and at all concentrations used ($p<0.05$). The mean percent reductions in cell numbers are summarized in **Table 7**. All comparisons were performed using one-way ANOVA.

Table 7. Percent reduction of cell viability of cells treated with GAP-107B8-L-Ac or GAP-107B8-D-Ac

	GAP-107B8-L-Ac		GAP-107B8-D-Ac	
	Cell Viability		Cell Viability	
	Adherent	Agar	Adherent	Agar
A2780cp	61%	75%	95%	82%
OCC1	52%	26%	86%	95%
OVCAR8	33	80%	91%	93%

The mean percentage reduction shown is based on three independent experiments done in triplicate. Statistically significant values ($p<0.05$) are highlighted. The concentration used for all (yellow) highlighted values was 25 μM and for (green) highlighted values was 12.5 μM.

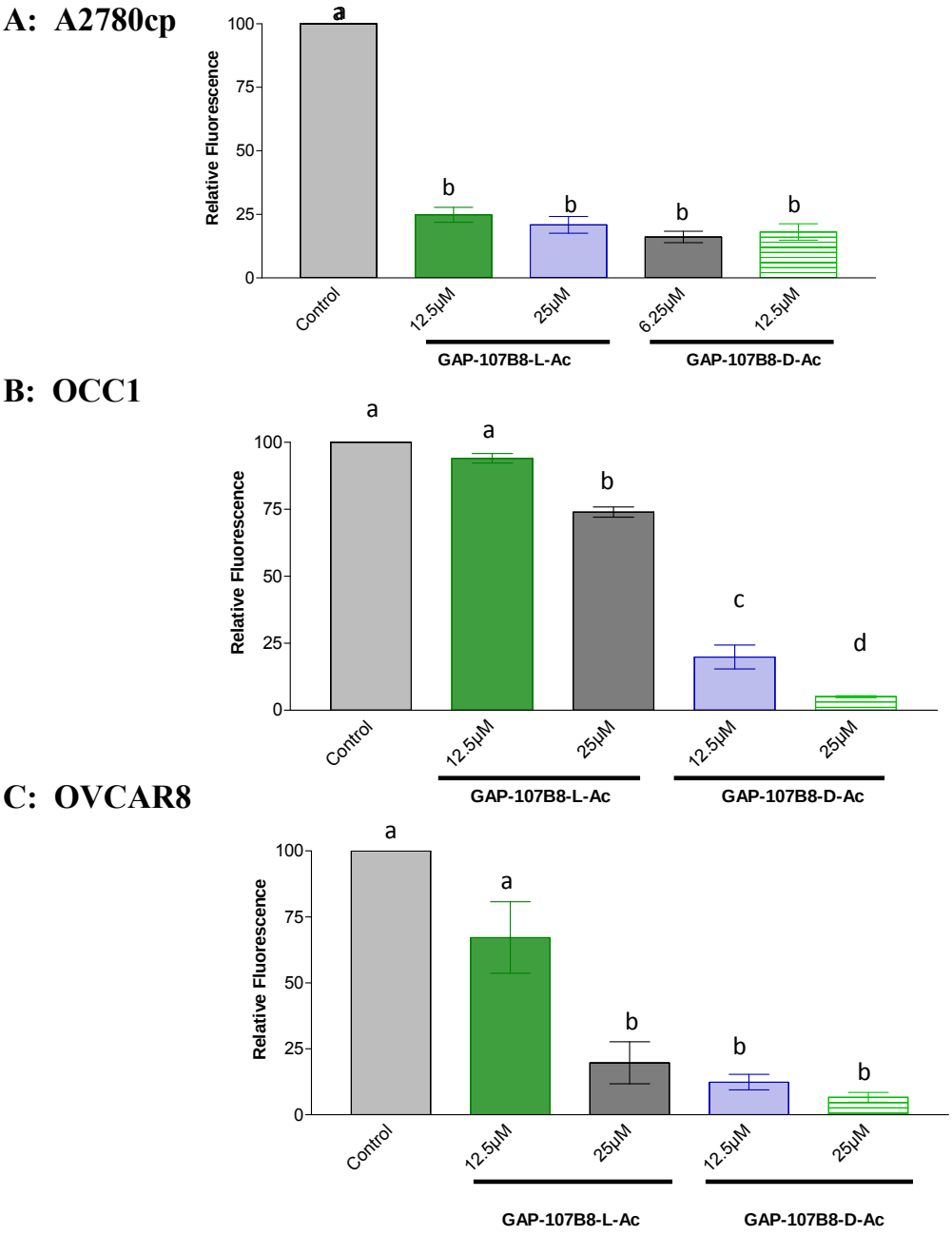

Figure 22. Inhibition of cell viability of A2780cp, OCC1 and OVCAR8 cells in anchorage independent cultures in the presence of GAP-107B8-L-Ac and GAP-107B8-D-Ac A2780cp cells (**A**), OCC1 cells (**B**) and OVCAR8 cells (**C**) were incubated with the indicated concentrations of GAP-107B8-L-Ac or GAP-107B8-D-Ac for 5 days (**A**: A2780cp cells) or 10 days (**B**: OCC1 cells, and **C**: OVCAR8 cells). All data bars represent the means of three experiments performed in triplicate with values normalized to yield a mean control value equal to 100. Error bars show the standard error of the mean (SEM). Means with different letters indicate statistical differences (Bonferroni, $p<0.05$).

3.4.3 Comparing treatment of A2780cp cells with GAP-107B8-L-Ac, GAP-107B8-D-Ac or Wortmannin

Wortmannin is a PI3K inhibitor and comparing treatment of both GAP-107B8-L-Ac or GAP-107B8-D-Ac with Wortmannin may help to determine whether either GAP-107B8 isomer is acting on targets other than Akt. **Figure 23A** showed the minimal dose of GAP-107B8-L-Ac causing downregulation of pAkt is 1μM and so this dose was used to assess the effects on cell viability. As seen in **Figure 23B**, pAkt is downregulated by both GAP-107B8-L-Ac and GAP-107B8-D-Ac isomer, as well as by Wortmannin. However, as seen in **Figure 24,** no impact on cell viability was observed in either condition and the combination therapy of carboplatin and GAP-107B8-L-Ac, Wortmannin, and GAP-107B8-D-Ac did not result in synergistic cell killing.

3.4.4 Determining the MTD of treatment of intraperitoneal xenograft tumours with GAP-107B8-L-Ac and GAP-107B8-D-Ac

Based on the above *in vitro* results (**Figures 21 and 22**), GAP-107B8–D-Ac was shown to be more potent than GAP-107B8-L-Ac (L-Isomer) in the ce ll lines tested. Previous experiments determined the MTD of GAP-107B8-L-TFA (**Figure 6**) to be 20 mg/kg, with 160 mg/kg being a lethal dose. However, in those experiments, the peptide was dissolved in DMSO and it was noted that DMSO could be a confounding factor in assessing the toxicity of the drug. Therefore, this experiment was repeated to determine the MTD of GAP-107B8-L-Ac and GAP-107B8-D-Ac in SCID mice. As described in **Table 8**, mice in the 80mg/kg GAP-107B8-L-Ac group exhibited signs of pain and loss of wellness after the first day of administration of that dose. One mouse did not survive the

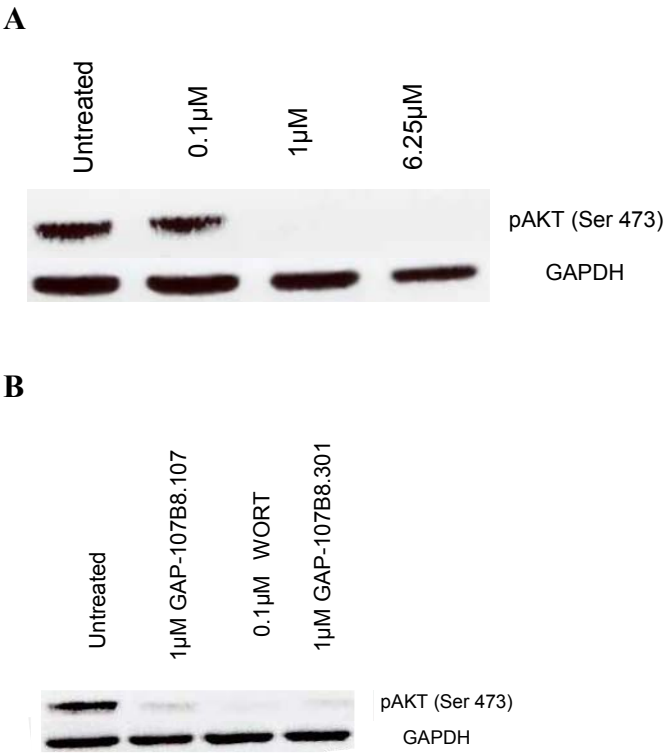

Figure 23. Western blot analysis of pAkt status in A2780cp cells after treatment with decreasing concentrations of GAP-107B8-L-Ac (A) or with GAP-107B8-L-Ac, Wortmannin, or GAP-107B8-D-Ac (B). A) Western blot analysis of pAkt status in A2780cp cells after 1hr after treatment with GAP-107B8-L-Ac. Cells were lysed and 40µg of total cell extracts of untreated and treated samples were resolved by SDS-PAGE, transferred to nitrocellulose membrane and probed with an antibody to pAkt and GAPDH. GAPDH was used as a loading control. Data is from one experiment. **B)** Western blot analysis of pAkt status in A2780cp cells was performed after treatment with GAP-107B8-L-Ac, Wortmannin, or GAP-107B8-D-Ac for 90 minutes. Cells were lysed and 30µg of total cell extracts of untreated and treated samples were resolved by SDS-PAGE, transferred to nitrocellulose membrane and probed with an antibody to pAkt and GAPDH. GAPDH was used as a loading control. Data is representative of two independent experiments for each condition except treatment with 1µM GAP-107B8-D-Ac, which was performed once.

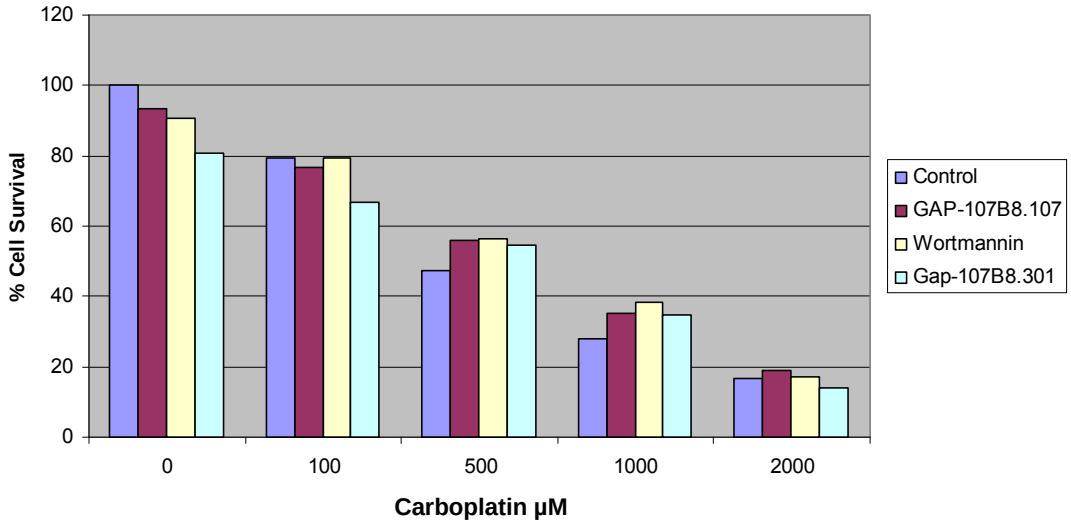

Figure 24. **A2780cp cells were treated with either GAP-107B8-L-Ac, GAP-107B8-D-Ac or Wortmannin in the presence of an increasing dose of carboplatin.** Cells were plated and allowed to grow for 24 hours. Cells were then pre-treated for 1 hour with GAP-107B8-L-Ac or Wortmannin or GAP-107B8-D-Ac and then treated with carboplatin for 48 hours before cells were quantified. Data from A2780cp cells treated with GAP-107B8-D-Ac was performed once in duplicate. All other data is from two independent experiments, once performed in triplicate and once in duplicate.

Table 8. Health status of SCID mice in each group during the course of the GAP-107B8-L-Ac and GAP-107B8-D-Ac MTD study.

GAP-107B8-L-Ac

Group	Status
Group1 (5mg/kg)	Well hydrated throughout study, normal behavior
Group2 (10mg/kg)	Well hydrated throughout study, normal behavior
Group3 (20mg/kg)	Appeared to behave normally throughout the study. The immediate response to each injection was crowding in a corner, eyes squinting, and hunching although it was transient and by the next injection, the mice had recovered and returned to normal. Fairly well hydrated throughout. Did not appear worse as the injection schedule neared completion.
Group4 (40mg/kg)	Appeared to behave normally throughout the study. The immediate response to each injection was crowding in a corner, eyes squinting, and hunching although it was transient and by the next injection, the mice had recovered and returned to normal. Fairly well hydrated throughout. Did not appear worse as the injection schedule neared completion.
Group5 (80mg/kg)	Beginning on Day 6 of the injection schedule, these mice exhibited the usual characteristics as mentioned above after the first injection and were struggling to survive the second dose given in the afternoon that day. 1 of the 4 mice in this group did not survive the night. The remaining mice were not well enough to receive their injections the following day and were euthanized on Day 3.

GAP-107B8-D-Ac

Group	Status
Group1 (5mg/kg)	Well hydrated throughout study, normal behavior
Group2 (10mg/kg)	Appeared to behave normally throughout the study. The immediate response to each injection was crowding in a corner, eyes squinting, and hunching although it was transient and by the next injection, the mice had recovered and returned to normal. Fairly well hydrated throughout. Did not appear worse as the injection schedule neared completion.
Group3 (20mg/kg)	Appeared to behave normally throughout the study. The immediate response to each injection was crowding in a corner, eyes squinting, and hunching although it was transient and by the next injection, the mice had recovered and returned to normal. Fairly well hydrated throughout. Did not appear worse as the injection schedule neared completion.
Group4 (40mg/kg)	Beginning on Day 2 of the injection schedule, the mice exhibited the usual characteristics as mentioned above after the first injection and were struggling to survive the second dose given in the afternoon that day. 2 of the 4 mice in this group did not survive the night. The remaining mice were not well enough to receive their injections the following morning but did receive injections on the afternoon of Day 2. However, the following day, these mice were not able to receive any doses due to being unwell and were euthanized on the night of Day 3.
Group5 (80mg/kg)	Not performed due to toxicity observed in the 40mg/kg group.

Mice were allowed to accommodate in the animal facility for five days. Subsequently, the thirty mice were separated into groups of 3 (5, 10 and 20mg/kg groups) or 4 (40 and 80mg/kg groups) and each mouse was injected twice daily IP with a dose of GAP-107B8-L-Ac or GAP-107B8-D-Ac for 7 days.

first day of injections and the rest of the mice were euthanized on the third day of injection of GAP-107B8-L-Ac. Similarly, mice in the 40mg/kg GAP-107B8-D-Ac group exhibited loss of wellness at that dose after the first day of administration. Two mice did not survive the first day of injections and the rest of the mice were euthanized on the third day of injection of GAP-107B8-D-Ac. Therefore, the MTD was determined to be 40 mg/kg for GAP-107B8-L-Ac and 20 mg/kg for GAP-107B8-D-Ac.

3.4.5 Treatment of intraperitoneal xenograft tumours with GAP-107B8-L-Ac and GAP-107B8-D-Ac

Using the MTD values, the ability of GAP-107B8-L and GAP-107B8-D to inhibit cancer cell viability IP *in vivo* and reduce tumour burden was investigated. The OCC1 cell line was chosen for this xenograft study due to its *in vitro* sensitivity to the treatment with GAP-107B8-L-Ac and the propensity of SCID mice xenografted with OCC1 cells to develop peritoneal ascites and small nodular tumours. The mice were given GAP-107B8-L-Ac and GAP-107B8-D-Ac injections IP twice daily for 13 days (5 days on, 2 days off). During the course of treatment of this study, mice in both the GAP-107B8-L-Ac and GAP-107B8-D-Ac treated groups developed a mild hunched posture during daily wellness checks that was not evident in the first few days of treatment nor evident at any time in the control untreated xenografted mice. After 13 days elapsed, all mice were euthanized.

As shown in **Figure 25A**, there was no significant difference in the mean total tumour burden of the mice treated with GAP-107B8-L-Ac or GAP-107B8-D-Ac compared with mice in the control group. However, there appeared to be a trend of decreased mean

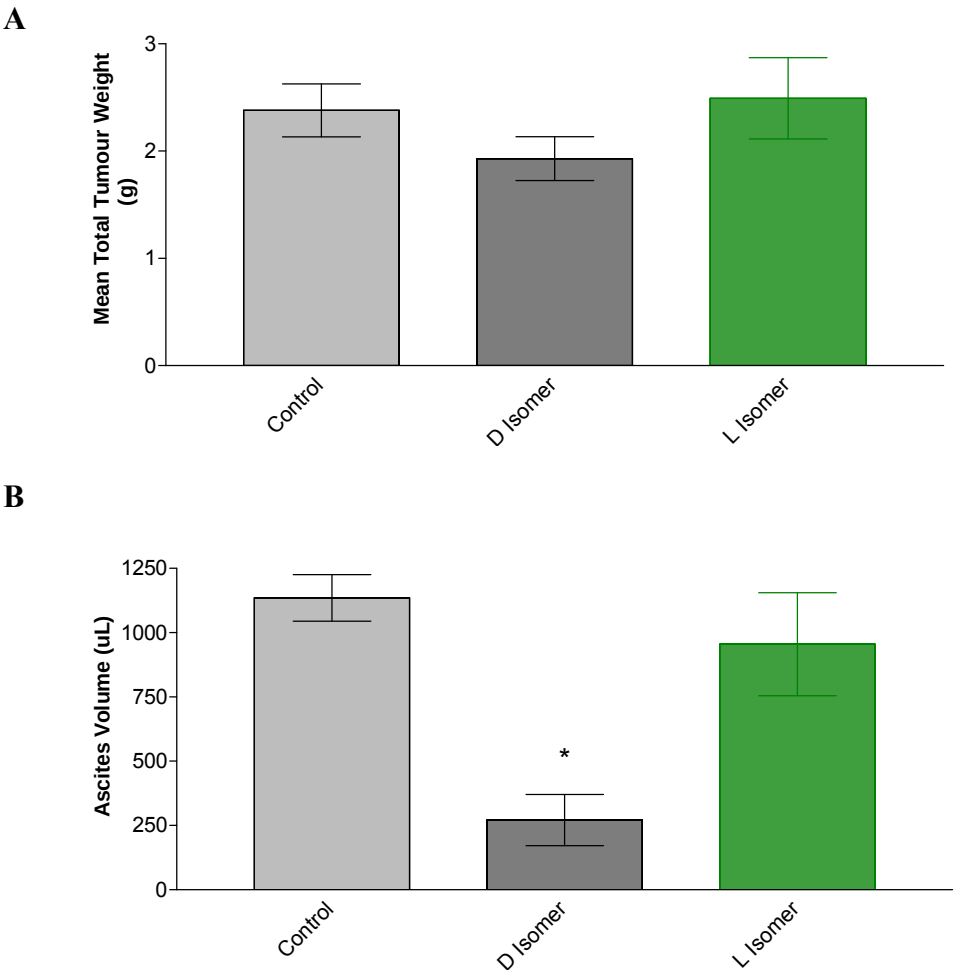

Figure 25. Disease progression in SCID animals xenografted with OCC1 cells IP and treated with GAP-107B8-D-Ac and GAP-107B8-L-Ac IP. Control ($n=6^a$), GAP-107B8-D-Ac ($n=6$), and GAP-107B8-L-Ac (L-isomer) treated mice ($n=6^a$) were monitored for disease progression. In **A,** tumour burden is expressed as mean total tumour weight. There is no significant difference in total tumour burden among any of the groups ($p>0.05$; unpaired t-test). In **B,** mean total ascites volume was quantified. The asterisk (*) indicates a statistical difference in total volume of ascites ($p<0.01$, One-way ANOVA with Bonferroni post-test) between GAP-107B8-D-Ac treated mice and the control mice. There was no significant difference in ascites volume between control mice and those treated with GAP-107B8-L-Ac. Error bars show the standard error of the mean (SEM). [a]Ascites were not present in one control mouse and one GAP-107B8-L-Ac treated mouse, so $n=5$ for those two groups.

tumour burden in the GAP-107B8-D-Ac treated animals compared with control animals ($p=0.19$). Due to the nature of the tumour burden (numerous small nodules in the intestinal mesentery, pancreas and diaphragm), it was not feasible to micro-dissect the tumour nodules from any remnants of normal mesentery, pancreas or diaphragm. As a result, measurements of tumour weight by necessity include the weights of the mesentery, pancreas and diaphragm that are associated with the tumour tissue. Ascites volumes were collected using a 1mL syringe and an $18G1^{1/2}$ gauge needle. Volumes were estimated by comparison to control tubes containing 0-2mLs of water in 0.1mL increments. **Figure 25B** shows that there was a significant difference in the volume of ascites observed between mice treated with vehicle and mice treated with GAP-107B8-D-Ac ($p<0.01$, unpaired t-test), while a slight trend towards decreased total ascites volume was present in mice treated with GAP-107B8-L-Ac ($p=0.63$). **Figure 26** shows a representative image of the tiny tumours adhered to the intestinal mesentery in the mice. **Figure 27** shows a representative image of the ascites fluid present in the peritoneum of the mice. The ascites fluid retrieved was very bloody in appearance in all groups of mice.

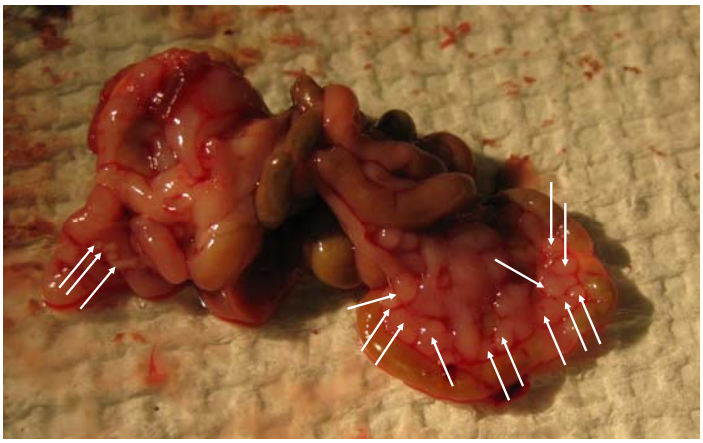

Figure 26. Tumour nodules in SCID mice xenografted IP with OCC1 cells. White arrows indicate the various small nodules adhered to the intestinal mesentery of the mice.

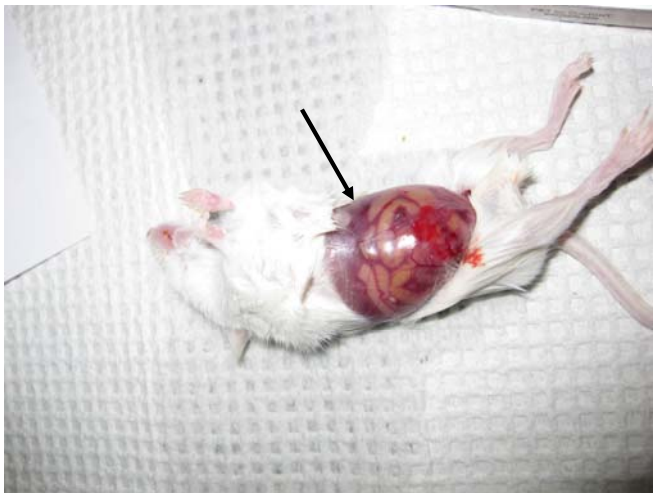

Figure 27. Ascites in SCID mice xenografted with OCC1 cells. The arrow indicates the ascites fluid present in the peritoneum of the mice.

Chapter 4: DISCUSSION

The current standard of care in the treatment of ovarian cancer following surgical debulking is a platinum-paclitaxel combination treatment. While this combination yields high initial response rates, patients often relapse and become resistant to the treatment. Platinum-resistant disease, which is the recurrence of the disease less than 6 months after treatment with platinum chemotherapy, and platinum refractory disease, which is the recurrence of the disease during the platinum chemotherapy, frequently lead to the standard of care being ineffective in managing this disease (Agarwal and Kaye, 2003).

Therefore, a major thrust in ovarian cancer research has been to develop alternative therapies aimed to treat ovarian cancer that is resistant to standard chemotherapy. These targeted therapies include anti-angiogenic agents, monoclonal antibodies, and other small molecule drugs (Agarwal et al., 2006). Targeted therapies are designed to specifically target molecular defects present in cancer cells, and thus are believed to produce less toxic side effects compared to the standard chemotherapy regimen, which non-specifically form adducts with the DNA in cells, or stabilize tubulin polymers.

GAP-107B8 was designed to be a targeted therapeutic against select PKC family members. PKC is a family of several Ser/Thr kinases that are involved in the transduction of signals for cell proliferation, differentiation, angiogenesis, migration and apoptosis. PKC has been implicated in tumourigenesis (Griner and Kazanietz, 2007). Different strategies have been devised in the drug development of PKC inhibitors and these include small molecule kinase inhibitors, peptides, biologic modulators of PKC, and anti-sense oligonucleotides (Ali et al., 2009).

Given the high rate of treatment failure for ovarian cancer, there is an urgency to test and validate new targeted therapeutics such as GAP-107B8. In addition to features designed to target binding and inhibition of PKCs, the GAP-107B8 compound also contains a PTD derived from the HIV tat protein. The PTD moiety, present in GAP-107B8-L-TFA but not in GAP-107X8-L-TFA, was designed to facilitate transport into the target cells. The cytotoxicity of GAP-107B8-L-TFA, which contains the PTD, and the lack of observed cytotoxicity of GAP-107X8-L-TFA, which lacks the PTD, is consistent with the notion that the active components of this compound fail to exert their effects on the intracellular PKC targets unless they can be transported into the target cells.

Our initial tests demonstrated in adherent cultures an acute toxicity of GAP-107B8 to a panel of ovarian cancer cell lines at concentrations $\leq 25\mu M$. The majority of ovarian cancer cell lines displayed an even greater sensitivity to GAP-107B8 when treated in anchorage independent cultures in soft agar. A number of possible explanations exist regarding this observation. One explanation is the plating of single cells without cell-cell contact provides a more favorable situation for GAP-107B8-L-TFA. Differences in initial plating densities were apparent, although more cells were plated in the soft agar assay (10,000 cells) compared to the cells grown in adherent cultures (2000-5000 cells). However, the fact that the cells are plated as single cells in suspension in the soft agar assay where there is no cell-cell contact is also a major difference in assay structure and possibly provides a more favorable environment for GAP-107B8-L-TFA to exert its effects. Even though cancer cells have the ability to grow without contact to other cells

or basement membrane, it is possible that single cells are more susceptible to drug treatment than monolayers of cells with multiple cell contacts.

Alternatively, the difference in sensitivity between the soft agar assay and the adherent cultures assay could also account for the different effects observed. Banasiak *et al.* (1999) compared the survival curves of cells after a dose of radiation using a clonogenic or microtetrazoline (MTT) assay on a series of human bladder cancer cell lines. Similar to our findings, the clonogenic assay was found to be more sensitive in detecting cell survival, particularly at higher doses. Although Carmichael *et al.* (1987) have attributed differences between clonogenic and MTT assays to the presence of dead cells that retain residual dehydrogenase activity, the assay we used precludes this as an explanation since the Cyquant dye binds to the deoxyribonucleic acid (DNA) in cells and does not measure metabolic activity.

Differences in assay end-points could also play a role in explaining discrepancies. The longer duration of the soft agar assay provides more time for cells to interact with GAP-107B8-L-TFA, although this idea assumes the drug is stable for more than 48 hours, which is the amount of time cells were exposed to the drug in the adherent cultures assay. Finally, colony formation relies on cells that maintain the ability to proliferate. Therefore, if the drug affects the cell cycle, cells may be viable and have intact DNA, but will not be recorded in the clonogenic assay.

The encouraging results *in vitro* provided the rationale for the second objective, which was to assess the effect of GAP-107B8 on tumour burden in xenograft models of human ovarian cancer. Xenograft models based on the IP injection of A2780cp cells were used because this generates a phenotype of advanced stage (metastatic) and

chemoresistant disease – the most challenging clinical presentation. IP treatment of advanced ovarian cancer is currently advised by the Gynecologic Oncologists of Canada (Provencher, 2006), whenever it can be tolerated, so we adopted this treatment approach as well. Although we have previously shown that disease progression can be slowed by other experimental treatments (Shaw et al., 2007), mice in this study receiving treatment with twice daily injections of GAP-107B8-L-TFA or GAP-107B8-L-Ac failed to demonstrate any statistically significant difference in mean total tumour burden between the treated and control groups.

A number of possibilities exist as to why no effects were observed. The first issue was how the *in vivo* dose compared to the therapeutic *in vitro* dose. The approximate injected concentration of GAP-107B8-L-TFA and GAP-107B8-L-Ac in the efficacy trials was 200 μM and 400μM, respectively. Even with dilution of the 500μL inoculum in the peritoneum, at least transient exposure of the tumour cells to the *in vitro* therapeutic dose >25 μM would be expected. However, without detailed pharmacokinetic data, it is unclear what initial IP concentration was achieved and how this changed with clearance over time. A second possibility that also could be clarified by detailed pharmacokinetic data is the stability of GAP-107B8 *in vivo*. A short half-life may preclude sufficient dosing of the tumour, especially if the IP dose is unable to quickly access the sites of tumour growth. Finally, the growth of cells *in vivo*, in three dimensions in a distinct environment may alter potential GAP-107B8 targets, decreasing the therapeutic potential.

To address some of the above possibilities, *in vivo* human ovarian cancer xenograft models harbouring a subcutaneous tumour were treated IT with GAP-107B8-L-Ac. Injecting directly into the tumour ensures immediate accessibility of GAP-107B8-L-Ac to the tumour

cells and addresses any changes that might be induced by *in vivo* growth. In addition, even though the length of exposure to stable compound is unknown, the time spent by GAP-107B8-L-Ac acting on the tumour is maximized.

The positive effects observed in reduction of mean tumour size by IT injection of GAP-107B8-L-Ac into subcutaneous A2780cp tumours suggests that GAP-107B8-L-Ac is effective *in vivo* on reducing tumour size when given the maximum time spent at the site of action. Repeating the experiment using a second human ovarian cancer cell line, HEY, showed the effect of reduction on mean tumour size was not a cell-line specific phenomenon, correlating to what was observed *in vitro*.

Even though IT injections are not an applicable delivery method for ovarian cancer treatment, the results of the IT study were important because it demonstrated that the peptide possesses inhibitory activity *in vivo*. The cell lines used were very aggressive according to Shaw *et al.* (2007), who reported in a Kaplan-Meier curve that the A2780cp and HEY cell lines both resulted in a mean survival time of only 24 days in nude mice. These results suggest that improving the stability of the peptide *in vivo* may improve its ability to have a positive effect on reducing tumour burden generated by very aggressive cell lines *in vivo.*

An interesting qualitative observation made in both efficacy studies on A2780cp IP xenografts was the effect of GAP-107B8 treatment on tumour size and number of tumours. It was revealed that despite all mice having similar overall tumour burden, treated mice had significantly fewer, but larger tumours compared to control mice. It was therefore speculated that perhaps GAP-107B8-L-Ac was able to eliminate a number of the smaller tumour nodules at the time of treatment without enhanced growth of more

established, larger tumours. If this were true, and since treatment started one week after injection of the cancer cells, the end result could be the treatment-induced elimination of the smaller tumours, along with the continued growth of the larger, unresponsive tumours present in the mice at the time of initiation of treatment. Alternatively, treatment with GAP-107B8 may have inhibited tumour growth in regions of the peritoneum where the IP injected dose was able to directly access tumour cells resulting in tumours only emerging from regions of the peritoneum not as accessible to IP dosing. However, when this hypothesis was tested in the OCC1 xenograft model, which generates only small tumour nodules, GAP-107B8-L-Ac was unable to reduce mean tumour burden.

Based on our results, it is still quite possible that poor stability of GAP-107B8 may prevent *in vivo* efficacy. Peptides are very susceptible to proteases present in serum and are often degraded quickly *in vivo*. One approach to increasing the stability of peptides is to replace natural amino acids (L-configuration) with D-configuration amino acids. Synthetic enantiomers such as cecropin A and magainin 2 amide have been shown to be resistant to enzymatic degradation and show an activity profile similar to that of their natural form (Westerhoff et al., 1989; Bessalle et al., 1990). Recently, ST100,059, an anti-angiogenic peptide that binds to VEGF was synthesized in the D-conformation due to the L-amino acid version of the peptide having a very short half-life in serum (Rastelli et al., 2011).

Therefore, in consideration of the greater stability afforded by converting L-amino acids to D-amino acids, GAP-107B8 was redesigned such that all possible amino acids were converted to the D-configuration.

It is likely the greater potency of GAP-107B8-D-Ac compared to GAP-107B8-L-Ac in inducing ovarian cancer cell apoptosis *in vitro* may reflect the greater stability of GAP-107B8-D-Ac in culture, allowing prolonged exposure of the cells to the active compound. *In vivo,* IP treatment with the MTD of 20 mg/kg of GAP-107B8-D-Ac in the OCC1 model led to a modest, but not significant decrease in tumour burden, while a slightly negative trend was observed for GAP-107B8-L-Ac. These results suggest that the greater stability afforded by the D-Isomer may explain its enhanced potency *in vitro* and *in vivo.* Based on *in vitro* testing, the A2780cp cells are more sensitive to GAP-107B8 treatment than the OCC1 cell line. This raises the question whether GAP-107B8-D-Ac may have a greater impact on the A2780cp IP xenograft model.

Despite the lack of significant reduction of OCC1 tumour burden following treatment with GAP-107B8-D-Ac, this dose of GAP-107B8-D-Ac did lead to a significant decrease in the accumulation of ascites. The reduction of ascites may have clinical significance due to the high morbidity and poor prognosis associated with the development of ascites in women with ovarian cancer. Ovarian cancer is characterized by rapid growth of peritoneal tumours and frequent accumulation of ascites (Liao et al., 2011).

There are various hypotheses regarding the cause of ascites in women with ovarian cancer. One line of thought is that the blockage of lymphatic ducts by tumour tissue allows the fluid in the peritoneal space to accumulate (Feldman et al., 1972; Hagendoorn et al., 2006). At autopsy, it was observed in our mice that tumours had spread, adhered and covered many areas, including the diaphragm, which possesses many lymphatic vessels and is a major site of peritoneal fluid drainage. It appeared that the diaphragm of both control and treated mice were equally affected. Since there are other sites of drainage all

over the peritoneum and because lower tumour burden in GAP-107B8-D-Ac treated animals compared to the vehicle treated animals was observed, GAP-107B8 may be reducing the tumour cells covering sites other than the diaphragm slightly more in treated mice than control mice, making it possible that the accumulation of ascites fluid may be enhanced by impairment of drainage.

Another cause of ascites production is believed to be increased vascular permeability, a process where VEGF plays a pivotal role. Indeed, Shaw *et al*. (2007) also hypothesized that the OCC1 models likely presented with leaky vasculature due to the animals presenting with severely distended abdomens full of bloody ascites. Previous studies indicate that VEGF acts on the adjacent vascular endothelium through paracrine mechanisms (Bausero et al., 1998; Jackson et al., 2002). This suggests vascular permeability is controlled at least in part, at intercellular junctions. VE-cadherin is one of the major components of the endothelial cell junction that determines the strength of cell-cell adhesion. The location of VE-cadherin at endothelial cell junctions is also the major site of leakage in morphologic studies of tumour vessels (Hashizume et al., 2000). The results of Hu *et al.* (2006) suggest that VEGF increases vascular permeability by rearrangement of the endothelial junctional protein VE-cadherin. They observed that VEGF downregulates expression of VE-cadherin while a VEGF monoclonal antibody inhibits vascular permeability by increasing VE-cadherin expression. Since VEGF is known to be secreted by tumour cells, it is possible that GAP-107B8 is inhibiting the ability of the tumour cells to secrete VEGF, thereby stabilizing vasculature and preventing leakiness.

Because the ascites collected were not analyzed, it is unknown how much of the volume consisted of cancer cells. One way to test this would be to perform a cytospin on the ascites fluid and look for human cells with human specific antibodies, noting that cells in the ascites are likely a variable combination of cancer cells and blood cells, depending on the cause of the ascites. Reports suggest that while some ovarian cancer cells, like OVCAR3, express high levels of VEGF mRNA, OCC1 cells express little VEGF mRNA (Yoneda et al., 1998). Another study (Kim et al., 1993) indicated that HEY A8 and OCC1 cells do not cause ascites. In contrast, this lab has previously determined that when OCC1 cells are injected IP into CD-1 nude mice, they develop mainly ascites along with small tumour nodules ($<0.5cm^3$; Shaw et al., 2007), and our pilot study confirmed this phenotype. Thus, it may be possible that our OCC1 cells express higher levels of VEGF than the cells in published literature. One way to test this hypothesis would be to directly measure VEGF levels or look at VEGF expression in OCC1 cells by quantitative real-time polymerase chain reaction and western blot. Taken together, our results suggest that GAP-107B8-D-Ac may be killing some of the OCC1 cells, and thus not allowing them to produce VEGF. This portion of cells would not have the chance to contribute to the pool of VEGF, resulting in less VEGF, increased expression of VE-cadherin and inhibition of the enhanced vascular permeability that might contribute to ascites formation.

The partial efficacy of GAP-107B8-D-Ac in the OCC1 model may be the result of increased stability; however, results from the *in vivo* MTD study comparing GAP-107B8-L-Ac to GAP-107B8-D-Ac suggest that GAP-107B8-D-Ac is also more toxic. It has been noted that if all amino acid residues are changed to the D-configuration, these

enantiomers may be present for too long and thus cause prolonged toxicity (Hong et al., 1999). One approach to circumvent this problem is to replace only the L-amino acids in the most susceptible sites with D-amino acids. The challenge is to maintain the activity of the peptide by making substitutions at locations where the secondary structure is not affected (Wieprecht et al., 1996). For instance, it was noted that D-amino acid substitutions near the N and C terminus of the antimicrobial peptide KSLK maintained antimicrobial activity while D-amino acid substitutions near the middle of the amino acid sequence disrupted the alpha-helical structure (Hong et al., 1999). Taken together, changing selective amino acids to the D configuration may increase the stability and potency of GAP-107B8 while curbing the toxic effects associated with prolonged stability due to changing all amino acids to the D-conformation.

Other approaches to enhance the stability or protect the peptide can be exploited. For example, advances have been made in identifying pharmaceutical carriers such as liposomes (Gregoriadis, 1998). Long circulating liposomes were created by coating liposomes with a polymer coat that decreased opsonization rate, and vastly increased circulation times (Lasic and Martin, 1995). Therefore, using a polyethylene glycol coated liposome system as a delivery method for the GAP-107B8 peptide is another possible way to improve its stability and delivery to the site of action and may be a promising avenue to achieve greater efficacy *in vivo.*

Animal models represent a very important pre-clinical component of testing new therapeutic drugs. While xenograft models are routinely used for testing of novel therapeutics, they have the limitation of being simply transplanted cancer cells, rather than tumours developing from normal tissues in an immunocompetent host. Transgenic

models of cancer could pose a greater challenge for therapeutic testing because tumour development, including neovasculaturization and immune responses take place within the context of normal tissues. Our lab has developed a mouse model of ovarian cancer, using the plasmid reported by Connolly *et al.* (2003), pMISIIR-TAg, on the FVB/N background. The mice positive for the transgene develop bilateral ovarian tumours with 100% penetrance. Although validation is required that the same targets of the GAP-107B8 are present in the mouse transgenic model, the use of transgenic models in therapeutic testing of GAP-107B8 represents different challenges compared to xenograft models in assessing the effects of GAP-107B8 *in vivo*.

GAP-107B8-L-Ac was shown to lead to the induction of apoptosis in treated cultures as measured by TUNEL, flow cytometry, and analysis of PARP cleavage. It was possible to detect a sub-G_1 population as early as 4 hours after treatment by flow cytometry, cleaved PARP at 8 hours by western blot, and positive TUNEL staining at 30 hours. Detecting breaks in the DNA is a relatively late event in the apoptotic process, and thus explains the lack of observation of TUNEL positive cells prior to 30 hours. While the other methods show more rapid activation of apoptosis, studies have shown that the commencement of the apoptotic process may be very fast. For example, it was shown that two different CD95 signaling pathways that mediate apoptotic cell death showed that caspase-8 and caspase-3 were both activated within 2 hours after stimulation of the CD95 death receptor (Scaffidi et al., 1998). However, this rapid cytotoxicity suggests that even though GAP-107B8 caused a significant reduction in motility in 5 ovarian cancer cell lines, the reductions observed are likely due to cell death rather than inhibition of cell motility.

Mechanisms limiting proliferation may also be involved in the actions of GAP-107B8. Analysis of the cell cycle of cells treated with GAP-107B8-L-Ac for 8 hours revealed delays in the progression of labeled cells through the G_2/M stage of the cell cycle compared to the untreated cells, which had cycled back to the G_1 phase at this time. The delay in progression of the cell cycle is transient as indicated by the 14-hour timepoint, where both the untreated and treated labeled cells are in the G_1 phase of the cell cycle. This may be due either to the presence of a population of cells resistant to GAP-107B8-L-Ac treatment or due to the degradation of GAP-107B8-L-Ac such that it is no longer affecting cells at that point.

One protein whose overexpression has been implicated in the rapid proliferation of ovarian cancer cells is cyclin E. Cyclin E is a cell cycle protein that is responsible for cells to progress from the G_1 to the S phase. The cell cycle phenomena can also be linked to Akt activity. Akt phosphorylates p27kip, which is a negative regulator of cell cycle action. p27 actually binds to cyclin E/cdk-2 complexes, enforcing a G_1 checkpoint (Polyak et al., 1994a,b). While our flow data seems to indicate a delay in progression through G_2/M which would be independent of an effect on cyclin E, it has not been shown whether GAP-107B8 is also able to inhibit cells from progressing from G_1 to the S phase. Our investigation involved labeling cells in the S-phase, and perhaps by the time those cells reached G_1 and return to the S-phase, GAP-107B8 has already been degraded. Therefore, it would be interesting to synchronize cells at G_1 and investigate whether GAP-107B8 is also able to prevent the cells from progressing to the S-phase, possibly mediated by an effect on cyclin E or upstream pathways.

While apoptosis and transient inhibition of the cell cycle have been shown to be actions of GAP-107B8 on the A2780cp cells, other mechanisms may also exist. The rapid response of cells to GAP-107B8 could be due to an autophagic response. For instance, ATP-treated macrophages have been shown to undergo autophagy within 30 minutes of exposure, and this was associated with a subsequent decrease in viability within infected cells (Biswas et al., 2008). Autophagy is characterized by the formation of numerous acidic vesicles called acidic vesicular organelles (Paglin et al., 2001). Previous studies have demonstrated that the PI3K/Akt pathway is involved in regulating autophagy (Zhuang et al., 2009). There are reports that both apoptosis and autophagy can co-occur. For example, carbinol and genistein synergistically induce both processes in human colon cancer HT-29 cells by inhibiting AKT phosphorylation (Nakamura et al., 2009) and synergistic effects of arsenic trioxide and radiation occur in osteosarcoma cells through the induction of both autophagy and apoptosis (Chiu et al., 2011). Our results clearly indicate that apoptosis is one of the mechanisms of decreasing cell viability and inhibition of growth may also play a small role, but other processes such as autophagy may also aid in mediating cell death.

Although we have investigated apoptosis and growth inhibition as mechanisms of cell death, it is important to understand the exact mechanism of action of GAP-107B8. Understanding the mechanism of action of GAP-107B8 is useful for pre-screening of pre-clinical candidates, targeting complementary pathways in cells, and for drug optimization. GAP-107B8 was designed as a PKC inhibitor and initial compound profiling was performed against the PKC family of 10 active PKC targets to determine IC_{50} values. Initial compound profiling resulted in GAP-107B8 having robust effects on 4 targets: PKCζ, PKCμ, PKCι and PKCν with IC_{50} values in the low micromolar range

(SignalChem Compound Profiling Report provided by PharmaGap). These results formed the rationale to investigate the PKC family as potential targets of GAP-107B8 in our human ovarian cancer cell lines.

Inhibition of phosphorylation of PKCι at Thr555 was not observed 1h post-treatment with GAP-107B8. The Thr555 residue of PKC iota is located on the turn-motif (TM) near the C-terminus. Crystallization studies and molecular modeling have shown the phosphate on the TM makes crucial contacts with other residues to help stabilize the core of the kinase (Messerschmidt et al., 2005; Grodsky et al., 2006; Hauge et al., 2007). However, there are conflicting reports as to whether phosphorylation at this residue is indicative of activity for PKCι. One group determined that phosphorylation at the TM was dispensable for PKCι activity by showing that a mutated Thr 555 site resulted in only a 25% reduction in kinase activity (Hauge et al., 2007). On the other hand, treatment of U87MG cells with 20 or 50 μM of pseudosubstrate inhibitor caused a reduction in PKCι activity, assessed by the phosphorylation of the Thr555 (Baldwin et al., 2010). If the Thr555 residue of PKCι is not indicative of activation of PKCι, then it cannot be ruled out that GAP-107B8 is acting through pathways involving PKCι.

PKC isoforms have a number of different roles in tumour biology and both their increased or decreased activity could have anti-tumour implications. Consequently, while GAP-107B8-L-Ac did not appear to inhibit the activity of any of the PKC isoforms investigated in this study, there remains some potential for GAP-107B8 to be enhancing select PKC isoform activity as part of an induction of apoptosis. The phosphorylation status of some isoforms of PKC appeared to show a modest increase in the presence of GAP-107B8-L-Ac. The increase in phosphorylation for PKCα/βII, PKCζ/λ, and PKCδ

are supported from previous studies showing a contributing effect to the induction of apoptosis. For instance, a study in prostate cancer cells showed activation of PKCα promotes dephosphorylation and inactivation of the survival kinase Akt (Guo et al., 2007). In contrast, the activation of PKCβ appears to have anti-apoptotic effects in human leukemia cells (Lee et al., 1996). Nazarenko *et al.* (2010) found that in ovarian cancer cells, PKCζ has a pro-apoptotic function. Their results also indicate that PKCζ might be negatively regulated by the EGFR pathway in a transient manner and can be phosphorylated through clinical EGFR inhibitors like Cetuximab. This is in agreement with literature on PKCδ (Griner and Kazanietz, 2007), which suggests it has pro-apoptotic functions in most cell types. These results indicate that PKC isoforms have varying functions in different cells and that the modest upregulation of the phosphorylated forms of some of these PKCs may be contributing to the apoptosis induced by GAP-107B8.

In the absence of any clear effect of GAP-107B8 on the activation of PKC family members, we decided to examine Akt activation. Akt has been identified as an important molecule in ovarian cancer, particularly the isoform AKT2, which is upregulated in 40% of primary ovarian cancer cases (Yuan et al., 2000). There is much evidence showing that Akt promotes cell survival and suppresses apoptotic cell death (Asselin et al., 2001; Dan et al., 2004; Fraser et al., 2003).

A significant decrease in pAkt was observed in A2780cp cells treated with 25 μM GAP-107B8-L-Ac for 1 to 30 hours. While a dose as low as 6.25 μM or even 1 μM also led to a decrease in pAkt at one hour post treatment, pAkt levels returned to near normal within 4 hours after application of 6.25 μM GAP-107B8. If targeting of Akt is an

important mechanism of GAP-107B8-L-Ac action, then only sustained down-regulation of pAkt with 25 μM GAP-107B8-L-Ac correlates with killing of adherent cells, which required 25 μM GAP-107B8-L-Ac for effective reduction of cell viability. The role of pAkt in GAP-107B8-L-Ac mediated cell killing is also at odds with the expression levels of Akt in ovarian cancer cells. It was previously observed that the OCC1 and HEY cell lines utilized in this study were responsive to GAP-107B8 but did not express detectable amounts of endogenous pAkt (Shaw et al., 2007), suggesting that the observed toxicity of GAP-107B8 in these cell lines is independent of pAkt inhibition. Further evidence for a lack of a role for pAkt in the killing of A2780cp cells comes from treating A2780cp cells with Wortmannin, an irreversible PI3K inhibitor. In this experiment, inhibition of pAkt by Wortmannin did not affect cell viability. These findings suggest mechanisms leading to the inhibition of pAkt alone are unable to explain the cell death in our panel of ovarian cancer cell lines.

Carboplatin is used currently as part of the first-line standard of care treatment after surgery in ovarian cancer patients, and so it was investigated if combining GAP-107B8 with carboplatin would result in synergistic effects on decreasing cell viability. Given that Akt is a central survival molecule in ovarian cancer cells, it was expected that inhibition of pAkt by GAP-107B8 may sensitize the cells to carboplatin treatment. Previous studies using other methods to inhibit pAkt support this hypothesis. Abedini *et al.* (2010) have shown that activation of Akt blocks apoptosis by cisplatin-induced mechanisms, and that suppression of Akt was able to sensitize C13, HEY and OVCA 433 cells to cisplatin-induced apoptosis. Furthermore, dominant-negative Akt (DN-Akt) was able to sensitize the C13 cells to cisplatin (Fraser et al., 2003).

Despite efficient suppression of pAkt by GAP-107B8, the A2780cp cells showed no greater response to carboplatin treatment. The absence of synergistic response in the presence of both GAP-107B8 and carboplatin is difficult to interpret. One explanation for the lack of synergy observed may be due to the p53 status. p53 has been found to be a crucial apoptotic cell death mediator in ovarian cancer cells (Fraser et al., 2003). While C13, HEY and OVCA 433 cells were all able to be sensitized to cisplatin-induced apoptosis upon suppression of Akt, these cell lines all carry wild type (wt) p53 (Abedini et al., 2010), while there is a mutation in the p53 of A2780cp cells (Shaw et al., 2008). Specifically, they showed that in the same cells we used (A2780cp), expression of a DN-Akt failed to sensitize the cells to cisplatin induced apoptosis. These results are consistent with previous data from that lab showing that when A2780cp cells are reconstituted with wt-p53, the cells become sensitive to cisplatin in the presence of DN-Akt (Fraser et al., 2003, 2008; Yang et al., 2006). Furthermore, they found that this response was attenuated when they used a specific inhibitor of p53 function called pifithrin-α-hydrobromide.

Although A2780s, C13, and HEY cells are wt-p53, no synergistic effect was observed when the cells were co-treated with carboplatin in our cell viability assays. In these cell lines, it was not determined whether GAP-107B8 was able to reduce pAKT, and thus it is unclear if the mechanism of action of cell killing is mediated through pAKT in these cell lines. Therefore, it makes sense that future experiments involve treating wt-p53 cell lines with GAP-107B8 to observe if pAKT is downregulated. Taken together, these findings suggest that the lack of synergistic effects observed with the combination treatment of GAP-107B8 and carboplatin are independent of p53 status and that the loss of pAkt function is not sufficient to sensitize the cells to carboplatin-induced apoptosis and that

other pathways are involved in mediating the cell death response.

Akt is activated by two phosphorylation events. Ser 473 is phosphorylated by the mammalian target of rapamycin complex 2 (mTORC2), while Thr 308 is phosphorylated by phosphoinositide-dependent kinase 1 (PDK1; Andjelkovic et al., 1997; Sarbassov et al., 2006). While this study investigated the phosphorylation events at Ser 473, it did not address whether Thr 308 was phosphorylated on Akt and whether the signaling pathway that is involved in that event is also affected by GAP-107B8-L-Ac. However, since full activation of Akt requires both sites to be phosphorylated, the sustained inhibition of Akt in A2780cp cells observed upon treatment of GAP-107B8-L-Ac suggests that inhibiting Akt activity is one of the mechanisms that may contribute to loss of cell viability.

Conclusion

Due to the development of resistance to current chemotherapeutic agents, as well as the toxicity associated with them, the development of new therapeutic strategies is of continued importance. The results of the *in vitro* studies suggest that GAP-107B8 has an impact on reducing cell viability in adherent and anchorage independent cultures. The results of the *in vivo* IT study suggest that GAP-107B8 possesses some therapeutic efficacy in ovarian cancer xenograft models while the results of IP treatment of OCC1 tumours that develop following xenograft into SCID mice suggests that GAP-107B8-D-Ac may be effective at reducing ascites volume. GAP-107B8-L-Ac appears to induce apoptosis in A2780cp cells as determined by flow cytometry, TUNEL staining and detection of cleaved PARP. The induction of apoptosis may be through mechanisms leading to decreased phosphorylation of Akt, although it does not appear that GAP-107B8

targets any PKC isoforms. Finally, GAP-107B8-D-Ac appears to be more potent in inhibiting the proliferation of both adherent and anchorage independent cultures compared to GAP-107B8-L-Ac. The results of *in vitro* and *in vivo* studies suggest that GAP-107B8 has an impact on survival of ovarian cancer cells and on ovarian cancer cell xenograft models and thus should undergo further investigation as a potential treatment for ovarian cancer.

Future formulations of GAP-107B8, including encapsulation in liposomes, may increase the efficacy in our model systems. Equally important is an understanding of the mechanism of action of GAP-107B8. Ideally, a dissection of the various moieties of GAP-107B8 through the generation of the relevant altered compounds can address the role of the PTD domain, the putative PICK1 homology domain and the PNA domain. Given the lack of evidence of direct inhibition of the PKC family members, this type of analysis becomes imperative. In addition, continued efforts examining the mechanism of action might be improved by investigating using more global analyses which pathways are perturbed in GAP-107B8-treated cells. The use of pathway-based arrays may allow the identification of affected pathways which in turn may lead to the identification of direct targets of GAP-107B8. Finally, the identification of direct targets of GAP-107B8 will allow the development of markers of GAP-107B8 function, which will improve the interpretation of pre-clinical trials and potentially offer assays for the development of future generations of this therapeutic agent.

REFERENCES

Abedini, M.R., Muller, E.J., Bergeron, R., Gray, D.A., and Tsang, B.K. (2010). Akt promotes chemoresistance in human ovarian cancer cells by modulating cisplatin-induced, p53-dependent ubiquitination of FLICE-like inhibitory protein Oncogene *29*, 11-25.

Adam, R.A., and Adam, Y.G. (2004). Malignant ascites: past, present, and future. J Am Coll Surg *198*, 999–1011.

Agarwal, R., and Kaye, S.B. (2003). Ovarian cancer:strategies for overcoming resistance to chemotherapy. Nature Rev. Cancer *3*, 502-516.

Agarwal, R., Linch, M., and Kaye, S.B. (2006). Novel therapeutic agents in ovarian cancer. European Journal of Surgical Oncology *32*, 875-886.

Andjelkovic, M., Alessi, D.R., Meier, R., Fernandez, A., Lamb, N.J., Frech, M., Cron, P., Cohen, P., Lucocq, J.M., and Hemmings, B.A. (1997). J. Biol. Chem. *272*, 31515–31524.
Andrews, P.A., and K.D. Albright. (1992). Mitochondrial defects in c/s-diamminedichloroplatinum(II)-resistant human ovarian carcinoma cells, Cancer Res *52*, 1895-1901.

Armstrong, D. K., Bundy, B., Wenzel, L., Huang, H.Q., Baergen, R., Lele, S., Copeland, L. J., Walker, J. L., Burger, R.A. and Gynecologic Oncology Group. (2006). Intraperitoneal cisplatin and paclitaxel in ovarian cancer. The New England Journal of Medicine. *354*, 34-43.

Ashworth, A.A. (2008). Synthetic lethal therapeutic approach: poly (ADP) ribose polymerase inhibitors for the treatment of cancers deficient in DNA double strand break repair. J Clin Oncol *26*, 3785–3790.

Asselin, E., Mills, G.B., and Tsang, B.K. (2001). XIAP regulates Akt activity and caspase-3-dependent cleavage during cisplatin-induced apoptosis in human ovarian epithelial cancer cells. Cancer Res *61*, 1862–1868.

Auersperg, N., Wong, A.S.T., Choi, K., Kang, S.K., and Leung, P.C.K. (2001). Ovarian surface epithelium: biology, endocrinology, and pathology. Endocrine Reviews *22*, 255-288.

Baldwin, R. M., Barrett, G. M., Parolin, D. A. E., Gillies, J. K., Paget, J.A., Lavictoire, S.J., Gray, D.A., and Lorimer, I.A.J. (2010). Coordination of glioblastoma cell motility by PKCi. Mol. Cancer *9*, 1–13.

Bankhead, C.R., Collins, C., Stokes-Lampard, H., Rose, P., Wilson, S., Clements, A., Mant, D., Kehoe, S.T., and Austoker, J. (2008). Identifying symptoms of ovarian cancer: a qualitative and quantitative study. BJOG *115,* 1008-1014.

Bast Jr, R.C., Feeney, M., Lazarus, H., Nadler, L.M., Colvin, R.B., and Knapp, R.C. (1981). J Clin Invest *68*, 1331–1337.

Bast, R. C. Jr., Klug, T.L., St. John, E., Jenmison, E., Niloff, J.M., Lazarus, H., Berkowitz, R.S., Leavitt, T., Griffiths, T., Parker, L., Zurawski, V.R. Jr., Knapp, R.C. (1983). A radioimmunoassay using a monoclonal antibody to monitor the course of epithelial ovarian cancer. New Engl. J. Med. 309, 883–887.

Bast, R.C., Hennessy, B., and Mills, G.B. (2009). The biology of ovarian cancer: new opportunities for translation. Nat Rev Cancer. *9,* 415-428.

Batist, G., Tulpule, A., Sinha, B.K., Katki, A., Myers, C.E., and Cowan, K.H. (1986). Over expression of a novel anionic glutathione transferase in multidrug resistant human breast cancer cells. J Biol Chem *261,* 15544-15549.

Bausero, P., Cavaille, F., Meduri, G., Freitas, S., and Perrot-Applanat, M. (1998). Paracrine action of vascular endothelial growth factor in the human endometrium: production and target sites, and hormonal regulation. Angiogenesis *2*, 167–182.

Bell, D.A. (2005). Origins and molecular pathology of ovarian cancer. Mod Pathol *18,* S19-S32.

Bessalle, R., Kapitkovsky, A., Gorea, A., Shalit, I., and Fridkin, M. (1990). All-D-magainin: Chirality, antimicrobial activity and proteolytic resistance. FEBS Lett *274*, 151–155.

Biswas, D., Qureshi, O.S., Lee, W.Y., Croudace, J.E., Mura, M., and Lammas, D.A. (2008). ATP-induced autophagy is associated with rapid killing of intracellular mycobacteria within human monocytes/macrophages. BMC Immunol. *9*, 35.

Blagden, S., and Gabra, H. (2009). Promising molecular targets in ovarian cancer. Curr Opin Oncol. *21*, 412-419.

Blay, P., Astudillo, A., Buesa, J.M., Campo, E., Abad, M., García-García, J., Miquel, R., Marco, V., Sierra, M., Losa, R., Lacave, A., Braña, A., Balbín, M., and Freije, J.M. (2004). Protein kinase C theta is highly expressed in gastrointestinal stromal tumors but not in other mesenchymal neoplasias. Clin Cancer Res *10*, 4089-4095.

Bouchard, D., Morisset, D., Bourbonnais, Y., and Tremblay, G.M. (2006) Proteins with whey-acidic protein motifs and cancer. Lancet Oncol. *7*, 167–174.

Bourbon, N.A., Yun, J., and Kester, M. (2000) Ceramide directly activates protein kinase Cζ to regulate a stress-activated protein kinase signaling complex. J Biol Chem *275*: 35617-35623.

Bowtell, D.D. (2010). The genesis and evolution of high-grade serous ovarian cancer. Nat Rev Cancer *10,* 803.

Bozulic, L., Morin, P. Jr., Hunter, T., and Hemmings, B. A. (2007). Sci STKE. 374, pe8.

Bratt, J., Belcher, J., Vercellotti, G.M., and Palmblad, J. (2000). Effects of anti-rheumatic gold salts on NF-κB mobilization and tumour necrosis factor-alpha (TNF-α)-induced neutrophil-dependent cytotoxicity for human endothelial cells. Clinical and Experimental Immunology *120*, 79–84.

Brenner, W., Färber, G., Herget, T., Wiesner, C., Hengstler, J.G., and Thüroff, J.W. (2003). Protein kinase Cη is associated with progression of renal cell carcinoma (RCC). Anticancer Res *23*, 4001–4006.

Buick, R. N., Pullano, R., and Trent, J. M. (1985). Comparative properties of five human ovarian adenocarcinoma cell lines. Cancer Res *45*, 3668 – 3676.

Burger, R.A., Sill, M.W., Monk, B.J., Greer, B.E., and Sorosky, J.I. (2007). Phase II trial of bevacizumab in persistent or recurrent epithelial ovarian cancer or primary peritoneal cancer: a Gynecologic Oncology Group Study. J Clin Oncol. *25,* 5165–5171.

Canadian Cancer Society. (2010). Canadian Cancer Statistics 2010.

Cannistra, S.A., Matulonis, U.A., Penson, R.T., Hambleton, J., Dupont, J., Mackey, H., Douglas, J., Burger, R.A., Armstrong, D., Wenham, R., and McGuire W. (2007). Phase II study of bevacizumab in patients with platinum-resistant ovarian cancer or peritoneal serous cancer. J Clin Oncol *25*, 5180–5186.

Carmichael, J., DeGraff, W.G., Gazdar, A.F., Minna, J.D., Mitchell, J.B. (1987). Evaluation of a tetrazolium-based semiautomated colorimetric assay: assessment of radiosensitivity. Cancer Res *47*, 943–946.

Castagna, M., Takai, Y., Kaibuchi, K., Sano, K., Kikkawa, U., and Nishizuka, Y. (1982). Direct activation of calcium-activated, phospholipid-dependent protein kinase by tumor-promoting phorbol esters. J Biol Chem *257*, 7847–7851.

Chiu, H.W., Lin, W., Ho, S.Y., and Wang, Y.J. (2011). Radiation Research Synergistic Effects of Arsenic Trioxide and Radiation in Osteosarcoma Cells through the Induction of Both Autophagy and Apoptosis. Radiation Research *175*, 547-560.

Colombo, N., Mangili, G., Mammoliti, S., Kalling, M., Tholander, B., Sternas, L., Buzenet, G., and Chamberlain, D. (2008). Aflibercept (VEGF Trap) for

advanced epithelial ovarian cancer (EOC) patients (pts) with symptomatic malignant ascites: preliminary results of a pilot study. J Clin Oncol *26*, 15S.

Connolly, D. C., Bao, R., Nikitin, A. Y., Stephens, K. C., Poole, T. W., Hua, X., Harris, S. S., Vanderhyden, B. C., and Hamilton, T. C. (2003) Female mice chimeric for expression of the simian virus 40 TAg under control of the MISIIR promoter develop epithelial ovarian cancer. Cancer research *63*, 1389-1397.

Cooper, D. A. and Lange, J. M. A. (2004). Lancet Infect Dis *4*, 426–436.

Dan, H.C., Sun, M., Kaneko, S., Feldman, R.I., Nicosia, S.V., Wang, H.G., Tsang, B.K., and Cheng, J.Q. (2004). Akt phosphorylation and stabilization of X-linked inhibitor of apoptosis protein (XIAP). J Biol Chem *279*, 5405-5412.

Das, P. M. and Bast, R. C. Jr. (2008). Early detection of ovarian cancer. Biomarkers Med *2*, 291–303.

Dekker, L.V. and Parker, P.J. (1994). Protein kinase C-α question of specificity. Trends in Biochemical Scienece *19*, 73-77.

Dekker, L.V. (2004). Protein kinase C: molecular biology intelligence unit. Landes Biosciences Inc.

Detjen, K.M., Brembeck, F.H., Welzel, M., Kaiser, A., Haller, H., Wiedenmann, B., and Rosewicz, S.(2000). Activation of protein kinase Cα inhibits growth of pancreatic cancer cells via p21(cip)-mediated G(1) arrest. J Cell Sci *113*, 3025–3035.

DiSaia, P. J., Sinkovics, J. G., Rutledge, F. N., and Smith, J. P. (1972). Cell-mediated immunity to human malignant cells: a brief review and further studies with two gynecologic tumors. Am. J. Obstet. Gynecol. *114*, 979 – 989.

D'Souza, T., Indig, F. E., and Morin, P.J. (2007). Phosphorylation of claudin-4 by PKCe regulates tight junction barrier function in ovarian cancer cells. Experimental Cell Research 313, 3364-3375.

Eder, A.M., Sui, X., Rosen, D.G., Nolden, L.K., Cheng, K.W., Lahad, J.P., Kango-Singh, M., Lu, K.H., Warneke, C.L., Atkinson, E.N., Bedrosian, I., Keyomarsi, K., Kuo, W.L., Gray, J.W., Yin, J.C., Liu, J., Halder, G., and Mills, G.B. (2005). Atypical PKCiota contributes to poor prognosis through loss of apical-basal polarity and cyclin E overexpression in ovarian cancer. Proc Natl Acad Sci USA *102*, 12519–12524.

Eichler, J. (2008). Curr Opin Chem Biol *12*, 707–713.

El-Rayes, B.F., Ali, S., Philip, P.A., and Sarkar, F.H. (2008). Protein kinase C: a target for therapy in pancreatic cancer. Pancreas *36*, 346–352.

Eva, A., Robbins, K.C., Andersen, P.R., Srinivasan, A., Tronick, S.R., Reddy, E.P., Ellmore, E.W., Galen, A.T., Lautenberger, J.A., Papas, T.S., Westin, E.H., Wong-Staal, F., Gallo, R.C., and Aaronson, S.A. (1982). Cellular genes analogous to retroviral *onc* genes are transcribed in human tumour cells. Nature *295*, 116-119

Feldman, G.B., Knapp, R.C., Order, S.E., and Hellman, S. (1972). The role of lymphatic obstruction in the formation of ascites in a murine ovarian carcinoma. Cancer Res *32*, 1663-1666.

Fields, A.P. and Gustafson, W.C. (2003). Protein kinase C in disease: cancer. Methods Mol Biol *233*, 519–537.

Foerg, C. and Merkle, H.P. (2008). On the biomedical promise of cell penetrating peptides: limits versus prospects. J Pharm Sci *97*,144-162.

Fogh, J., and Trempe, G. (1975). New Human Tumor Cell Lines. 115–159.

Fong, P.C., Boss, D.S., Carden, C.P., Roelvink, M., De Greve, J., Gourley, C.M., Carmichael, J., De Bono, J.S., Schellens, J.H., and Kaye, S.B. (2008). AZD2281 (KU-0059436), a PARP (poly ADP-ribose polymerase) inhibitor with single agent anticancer activity in patients with BRCA deficient ovarian cancer: results from a phase I study. J Clin Oncol *26*, 15S.

Fournier, D.B., Chisamore, M., Lurain, J.R., Rademaker, A.W., Jordan, V.C., and Tonetti, D.A. (2001). Protein kinase C alpha expression is inversely related to ER status in endometrial carcinoma: possible role in AP-1-mediated proliferation of ER-negative endometrial cancer. Gynecol Oncol *81*, 366–372.

Fraser, M., Leung, B.M., Yan, X., Dan, H.C., Cheng, J.Q., and Tsang, B.K. (2003). p53 is a determinant of X-linked inhibitor of apoptosis protein/Akt-mediated chemoresistance in human ovarian cancer cells. Cancer Res *63*, 7081–7088.

Fraser, M., Bai, T., Tsang, B.K. (2008). Akt promotes cisplatin resistance in human ovarian cancer cells through inhibition of p53 phosphorylation and nuclear function. Int J Cancer *122*, 534–546.

Frederick, P.J., Straughn, J.M., Alvarez, R.D., Buchsbaum, D.J. (2009). Preclinical studies and clinical utilization of monoclonal antibodies in epithelial ovarian cancer. Gynecol Oncol *113*, 384–390.

Garrison, R.N., Galloway, R.H., and Heuser, L.S. (1987). Mechanisms of malignant ascites production. J Surg Res *42*, 126–132.

Gokmen-Polar, Y., Murray, N.R., Velasco, M.A., Gatalica, Z., and Fields, A.P. (2001). Elevated protein kinase C betaII is an early promotive event in colon carcinogenesis. Cancer Res *61*, 1375–1381.

Goodman, S. L., Holzemann, G., Sulyok, G. A. G., and Kessler, H. (2002).
J Med Chem *45*, 1045–1051.
Gregoriadis, G. (1988). Liposomes as Drug Carriers. Wiley p279.

Griner, E.M. and Kazanietz, M.G. (2007). Protein kinase C and other diacylglycerol effectors in cancer. Nat Rev Cancer *7*, 281-294.

Grodsky, N., Li, Y., Bouzida, D., Love, R., Jensen, J., Nodes, B., Nonomiya, J., and Grant S. (2006). Structure of the catalytic domain of human protein kinase C beta II complexed with a bisindolylmaleimide inhibitor. Biochemistry *45*, 13970-13981.

Guo, J., Zhu, T., Xiao, Z.X., and Chen, C.Y. (2007). Modulation of intracellular signaling pathways to induce apoptosis in prostate cancer cells. J Biol Chem *282*, 24364–24372.

Hagendoorn, J., Tong, R., Fukumura, D., Lin, Q., Lobo, J., Padera, T.P., Xu, L., Kucherlapati, R., Jain, R.K. (2006). Onset of abnormal blood and lymphatic vessel function and interstitial hypertension in early stages of carcinogenesis. Cancer Res *66*, 3360-3364.

Hamilton, T.C., Young, R.C., McKoy, W.M., Grotzinger, K.R., Green, J.A., Chu, E.W., Whang-Peng, J., Rogan, A.M., Green, W.R., and Ozols, R.F. (1983). Characterization of a human ovarian carcinoma cell line (NIH:OVCAR-3) with androgen and estrogen receptors. Cancer Res *43*, 5379-5389.

Hanahan, D., and Folkman, J. (1996). Patterns and emerging mechanisms of the angiogenic switch during tumorigenesis. Cell *86*, 353–364.

Harrison, S., Das, K., Karim, F., Maclean, D., and Mendel, D. (2008). Expert Opin Drug Discov *3*, 761–774.

Hashizume, H., Baluk, P., Morikawa, S., McLean, J.W., Thurston, G., Roberge, S., Jain, R.K., and McDonald, D.M. (2000). Openings between defective endothelial cells explain tumor vessel leakiness. Am J Pathol *156*, 1363–1380.

Hauge, C., Antal, T.L., Hirschberg, D., Doehn, U., Thorup, K., Idrissova, L., Hansen, K., Jensen, O.N., Jørgensen, T.J., Biondi, R.M., and Frödin, M. (2007). Mechanism for activation of the growth factor-activated AGC kinases by turn motif phosphorylation. EMBO J *26*, 2251-2261.

Henderson, G., and Bradley, M. (2007). Curr Opin Biotechnol *18*, 326–330.

Hong, H. Y., Lee, H. Y., Kwak, W., Yoo, J., Na, M. H., So, I. S., Kwon, T. H., Park, H. S., Huh, S., Oh, G. T., Kwon, I. C., Kim, I. S., and Lee, B. H. (2008). Phage Display Selection of Peptides that Home to Atherosclerotic Plaques: IL-4 Receptor as a Candidate Target in Atherosclerosis. J Cell Mol Med *12*, 2003–2014.

Hong, S.Y., Oh, J.E., and Lee, K.H. (1999). Effect of D-amino acid substitution on the stability, the secondary structure, and the activity of membrane-active peptide. Biochem. Pharmacol *58*, 1775-1780.

Hu, L., Hofmann, J., Lu, Y., Mills, G. B. and Jaffe, R. B. (2002). Inhibition of phophatidylinositol 3′ kinase increases efficacy of paclitaxel in *in vitro* and *in vivo* ovarian cancer models. Cancer Res *62*, 1087–1092.

Hu, L., Ferrara, N., and Jaffe, R.B. (2006). Paracrine VEGF/VE-Cadherin action on ovarian cancer permeability. Exp Biol Med *231*, 1646–1652.

Hurwitz, H., Fehrenbacher, L., Novotny, W., Cartwright, T., Hainsworth, J., Heim, W., Berlin, J., Baron, A., Griffing, S., Holmgren, E., Ferrara, N., Fyfe, G., Rogers, B., Ross, R., and Kabbinavar, F. (2004). Bevacizumab plus irinotecan, fluorouracil, and leucovorin for metastatic colorectal cancer. N Engl J Med *350*, 2335–2342.

Inoue, M., Kishimoto, A., Takai, Y., and Nishizuka, Y. (1977). J Biol Chem *252*, 7610−7616.

Ito, T., Matsui, Y., Ago, T., Ota, K., and Sumimoto, H. (2001). Novel modular domain PB1 recognizes PC motif to mediate functional protein–protein interactions. EMBO J *20*, 3938–3946.

Jackson, M.W., Roberts, J.S., Heckford, S.E., Ricciardelli, C., Stahl, J., Choong, C., Horsfall, D.J., and Tilley, W.D. (2002). A potential autocrine role for vascular endothelial growth factor in prostate cancer. Cancer Res *62*, 854–859.
Jeon, K.I., Jeong, J.Y., and Jue, D.M. (2000). Thiol-reactive metal compounds inhibit NF-kappa B activation by blocking I kappa B kinase. J Immunol *164***,** 5981–5989.

Ji, J., Forsti, A., Sundquist, J., Lenner, P., and Hemminki, K. (2008). Survival in ovarian cancer patients by histology and family history. Acta Oncol *47,* 1133-1139.

Jiang, X.H., Lam, S.K., Lin, M.C., Jiang, S.H., Kung, H.F., Slosberg, E.D., Soh, J.W., Weinstein, I.B., and Wong, B.C. (2002). Novel target for induction of apoptosis by cyclo-oxygenase-2 inhibitor SC-236 through a protein kinase C-beta(1)-dependent pathway. Oncogene *21*, 6113–6122.

Kahl-Rainer, P., Karner-Hanusch, J., Weiss, W., and Marian, B. (1994). Five of six protein kinase C isoenzymes present in normal mucosa show reduced protein levels during tumor development in the human colon. Carcinogenesis *15*, 779–782.

Kerfoot, C., Huang, W. D., and Rotenberg, S. A. (2004). Immunohistochemical analysis of advanced human breast carcinomas reveals downregulation of protein kinase Cα. J Histochem Cytochem *52*, 419–422.

Kim, K.J., Li, B., Winner, J., Armanini, M., Gillett, N., Phillips, H.S., and Ferrara, N. (1993). Inhibition of vascular endothelial growth factor-induced angiogenesis suppresses tumor growth. Nature *362*, 841–844.

Kobel, M., Kalloger, S.E., Boyd, N., McKinney, S., Mehl, E., Palmer, C., Leung, S., Bowen, N.J., Ionescu, D.N., Rajput, A., Prentice, L.M., Miller, D., Santos, J., Swenerton, K., Gilks, C.B., and Huntsman, D. (2008). Ovarian carcinoma subtypes are different diseases: implications for biomarker studies. PLoS Med *5*, e232.

Kobold, S., Hegewisch-Becker, S., Oechsle, K., Jordan, K., Bokemeyer, C., and Atanackovic, D. (2009). Intraperitoneal VEGF inhibition using bevacizumab: a potential approach for the symptomatic treatment of malignant ascites? Oncologist *14*, 1242–1251.

Konstantinopoulos, P.A., Spentzos, D., and Cannistra, S.A. (2008). Gene-expression profiling in epithelial ovarian cancer. Nat Clin Pract Oncol 5, 577–587.

Koren, R., Ben Meir, D., Langzam, L., Dekel, Y., Konichezky, M., Baniel, J., Livne, P.M., Gal, R., and Sampson, S.R. (2004). Expression of protein kinase C isoenzymes in benign hyperplasia and carcinoma of prostate. Oncol Rep *11*, 321–326.

Kunnumakkara, A.B., Anand, P., and Aggarwal, B.B. (2008). Curcumin inhibits proliferation, invasion, angiogenesis and metastasis of different cancers through interaction with multiple cell signaling proteins. Cancer Lett *269*, 199-225.

Lahn, M., Sundell, K., and Kohler, G. (2006). The role of protein kinase C-alpha in hematologic malignancies. Acta Haematol *115*, 1–8.

Lasic, D., and Martin, F. (1995). (Eds.) Stealth Liposomes. CRC Press, Boca Raton.

Lau, D. H., Lewis, A. D., Ehsan, M. N., and Sikic, B. I. (1991). Multifactorial mechanisms associated with broad cross-resistance of ovarian carcinoma cells selected by cyanomorpholino doxorubicin. Cancer Res *51*, 5181 – 5187.

Lee, C.W., Bociek, G., and Faught, W. (1998). A survey of practices in management of malignant ascites. J Pain Symptom Manage *16*, 96–101.

Lee, J.Y., Hannun, Y.A., and Obeid, L.M. (1996). Ceramide inactivates cellular protein kinase Calpha. J Biol Chem 271, 13169–13174.

Leseux, L., Laurent, G., Laurent, C., Rigo, M., Blanc, A., Olive, D., and Bezombes, C. (2008). PKC {zeta} mTOR pathway: a new target for rituximab therapy in follicular lymphoma. Blood *111*, 285–291.

Li, H. (2006). Protein kinase C: novel isozyme-selective peptide inhibitors. Expert Opin Ther Patents *16*, 1183 -1187

Liao, S., Liu, J., Lin, P., Shi, T., Jain, R.K., and Xu, L. (2011). TGF-beta blockade controls ascites by preventing abnormalization of lymphatic vessels in orthotopic human ovarian carcinoma models. Clin Cancer Res. *17*, 1415-1424.

Lu, K. H., Patterson, A.P., Wang, L., Marquez, R.T., Atkinson, E.N., Baggerly, K.A., Ramoth, L.R., Rosen, D.G., Liu, J., Hellstrom, I., Smith, D., Hartmann, L., Fishman, D., Berchuck, A., Schmandt, R., Whitaker, R., Gershenson, D.M., Mills, G.B., and Bast, R.C. Jr. (2004). Selection of potential markers for epithelial ovarian cancer with gene expression arrays and recursive descent partition analysis. Clin Cancer Res *10*, 3291–3300.

Masso-Welch, P. A., Winston, J.S., Edge, S., Darcy, K.M., Asch, H., Vaughn, M.M., Ip, M.M. (2001). Altered expression and localization of PKCη in human breast tumors. Breast Cancer Res Treat *68*, 211–223.

Masuda, H., Ozols, R.F., Lai, G.-M., Fojo, A., Rothenberg, M., and Hamilton, T. (1988). Increased DNA repair as a mechanism of acquired resistance to cis-diamminedichloroplatinum(II) in human ovarian cancer cell lines. Cancer Res *48*, 5713 - 5716.

Mazzoni, E., Adam, A., Bal de Kier Joffe, E., and Aguirre-Ghiso, J.A. (2003). Immortalized mammary epithelial cells overexpressing protein kinaseCgamma acquire a malignant phenotype and become tumorigenic in vivo. Mol Cancer Res *1,* 776–787.

McGregor, D.P. (2008). Discovering and improving novel peptide therapeutics. Curr Opin Pharmacol *8,* 616-619.

Menon, U., Gentry Maharaj, A., Hallett, R., Ryan, A., Burnell, M., Sharma, A., Lewis, S., Davies, S., Philpott, S., Lopes, A., Godrey, K., Oram, D., Herod, J., Williamson, K., Seif, M.W., Scott, I., Mould, T., Woolas, R., Murdoch, J., Dobbs, S., Amso, N.N., Leeson, S., Cruickshank, D., Mcguire, A., Campbell, S., Fallowfield, L., Singh, N., Dawnay, A., Skates, S.J., Parmar, M., and Jacobs, I. (2009). Sensitivity and specificity of multimodal and ultrasound screening for ovarian cancer, and stage distribution of detected cancers: results of the prevalence screen of the UK Collaborative Trial of Ovarian Cancer Screening (UKCTOCS). Lancet Oncol *10*, 327–340.

Messerschmidt, A., Macieira, S., Velarde, M., Bädeker, M., Benda, C., Jestel, A., Brandstetter, H., Neuefeind, T., and Blaesse, M. (2005). Crystal structure of the catalytic

domain of human atypical protein kinase C-iota reveals interaction mode of phosphorylation site in turn motif. J Mol Biol *352*, 918-931.

Miller, K., Wang, M., Gralow, J., Dickler, M., Cobleigh, M., Perez, E.A., Shenkier, T., Cella, D., and Davidson, N.E. (2007). Paclitaxel plus bevacizumab versus paclitaxel alone for metastatic breast cancer. N Engl J Med *357*, 2666–2676.

Mischak, H., Goodnight, J.A., Kolch, W., Martiny-Baron, G., Schaechtle, C., Kazanietz, M.G., Blumberg, P.M., Pierce, J.H., and Mushinski, J.F.(1993). Overexpression of protein kinase-C- δ and kinase ε in NIH 3T3 cells induces opposite effects on growth, morphology, anchorage dependence, and tumorigenicity. J Biol Chem *268*, 6090–6096

Murdoch, W.J., and McDonnel, A.C. (2002). Roles of the ovarian surface epithelium in ovulation and carcinogenesis. Reproduction *123,* 743-750.

Murray, N.R., Weems, J., Braun, U., Leitges, M., and Fields, A.P. (2009). Protein kinase C βII and PKCι/λ: collaborating partners in colon cancer promotion and progression. Cancer Res *69,* 656–662.

Nakamura, Y., Yogosawa, S., Izutani, Y., Watanabe, H., Otsuji, E., and Sakai, T. (2009). A combination of indol-3-carbinol and genistein synergistically induces apoptosis in human colon cancer HT-29 cells by inhibiting Akt phosphorylation and progression of autophagy. Mol Cancer *8*, 100.

Nazarenko I., Jenny, M., Keil, J., Gieseler, C., Weisshaupt, K., Sehouli, J., Legewie, S., Herbst, L., Weichert, W., Darb-Esfahani, S., Dietel, M., Schäfer, R., Ueberall, F., and Sers, C. (2010). Atypical protein kinase C zeta exhibits a proapoptotic function in ovarian cancer. Mol .Cancer Res. *8*, 919-934.

Neill, G.W., Ghali, L.R., Green, J.L., Ikram, M.S., Philpott, M.P., and Quinn, A.G.. (2003). Loss of protein kinase C alpha expression may enhance the tumorigenic potential of Gli1 in basal cell carcinoma. Cancer Res *63*, 4692–4697.

Newton, A.C. (1997). Regulation of protein kinase C. Current Opinion in Cell Biology *9,* 161-167.

Newton, A.C. (2001) Protein kinase C: structural and spatial regulation by phosphorylation, cofactors, and macromolecular interactions. Chem Rev *101*, 2353–2364.

Nishizuka, Y. (1986). Studies and perspectives of protein kinase C. Science *233*, 305-312.

Paglin, S., Hollister, T., Delohery, T., Hackett, N., McMahill, M., Sphicas, E., Domingo, D., and Yahalom, J. (2001). A novel response of cancer cells to radiation involves autophagy and formation of acidic vesicles. Cancer Res *61*, 439–444.

Pan, Q., Bao, L.W., Kleer, C.G., Sabel, M.S., Griffith, K.A., Teknos, T.N., and Merajver, S.D. (2005). Protein kinase C epsilon is a predictive biomarker of aggressive breast cancer and a validated target for RNA interference anticancer therapy. Cancer Res *65*, 8366-8371.

Parker, P.J., Coussens, L., Totty, N., Rhee, L., Young, S., Chen, E., Stabel, S., Waterfield, M.D., and Ullrich, A. (1986). The complete primary structure of protein kinase C-the major phorbol ester receptor. Science *233*, 859-866.

Pears, C., Stable, S., and Cazaubon, S. (1992). Studies on the phosphorylation of protein kinase C-alpha. Biochemical Journal *283*, 515-518.

Peng, Y., Sigua, C.A., Gallagher, S.F., Murr, M.M. (2007). Protein kinase C-zeta is critical in pancreatitis-induced apoptosis of Kupffer cells. J Gastrointest Surg *11*, 1253–1261.

Provencher, D.M. (2006). GOC Position Statement on IP Chemotherapy. http://www.g-o-c.org/en/news/positionstatements/ip_en.aspx. June 25th 2011.

Pepio, A.M., and Sossin, W.S. (2001). Membrane translocation of novel protein kinase Cs is regulated by phosphorylation of the C2 domain. The Journal of Biological Chemistry *276*, 3846-3855.

Philip, P.A., and Zonder, J.A. (1999). Pharmacology and clinical experience with bryostatin 1: a novel anticancer drug. Expert Opin Invest Drug *8*, 2189–2199.

Polyak, K., Kato, J.-Y., Solomon, M.J., Sherr, C.J., Massagué, J., Roberts, J.M., and Koff, A. (1994a). p27*Kip1*, a cyclin-cdk inhibitor, links transforming growth factor-b and contact inhibition to cell cycle arrest. Genes and Dev 8, 9–22.

Polyak, K., Lee, M.-H., Erdjument-Bromage, H., Koff, A., Roberts, J.M., Tempst, P. and Massagué, J. (1994b). Cloning of p27Kip1, a cyclin-dependent kinase inhibitor and a potential mediator of extracellular antimitogenic signals. Cell *78,* 59–66.

Qvit, N., Reuveni, H., Gazal, S., Zundelevich, A., Blum, G., Niv, M. Y., Feldstein, A., Meushar, S., Shalev, D. E., Friedler, A., and Gilon, C. (2008). Synthesis of a novel macrocyclic library: discovery of an IGF-1R inhibitor. J Comb Chem *10*, 256–266.

Rastelli, L., Valentino, M.L., Minderman, M.C., Landin, J., Malyankar, U.M., Lescoe, M.K., Kitson, R., Brunson, K., Souan, L., Forenza, S., Goldfarb, R.H., and Rabbani, S.A. (2011). A KDR-binding peptide (ST100,059) can block angiogenesis, melanoma tumor growth and metastasis in vitro and in vivo. Int J Oncol *39*, 401-408.

Regala, R.P., Weems, C., Jamieson, L., Copland, J.A., Thompson, E.A., Fields, A.P. (2005). Atypical Protein Kinase C{iota} Plays a Critical Role in Human Lung Cancer Cell Growth and Tumorigenicity. J Biol Chem *280*, 31109–31115.

Rizvi, M.A., Ghias, K., Davies, K.M., Ma, C., Weinberg, F., Munshi, H.G., Krett, N.L., and Rosen, S.T. (2006). Enzastaurin (LY317615), a protein kinase Cbeta inhibitor, inhibits the AKT pathway and induces apoptosis in multiple myeloma cell lines. Mol Cancer Ther *5*, 1783–1789.

Roffey, J., Rosse, C., Linch, M., Hibbert, A., McDonald, N.Q., and Parker, P.J. (2009). Protein kinase C intervention: the state of play. Curr Opin Cell Biol *21*, 268–279.

Rubinstein, M., and Niv, M.Y. (2009). Peptidic modulators of protein-protein interactions: progress and challenges in computational design. Biopolymers *91*, 505–513.

Runyon, B.A. (1994). Care of patients with ascites. N Engl J Med *330*, 337–342.

Sanz, L., Sanchez, P., Lallena, M.J., Diaz-Meco, M.T., Moscat, J. (1999). The interaction of p62 with RIP links the atypical PKCs to NF-kappaB activation. Embo J *11*, 3044–53.

Saras, J., and Heldin, C.H. (1996). PDZ domains bind carboxy-terminal sequences of target proteins. Trends Biochem Sci *21***,** 455–458

Sarbassov, D.D., Guertin, D.A., Ali, S.M., and Sabatini, D.M. (2005). Phosphorylation and regulation of Akt/PKB by the rictor-mTOR complex. Science *307*, 1098–1101**.**

Scotti, M.L., Bamlet, W.R., Smyrk, T.C., Fields, A.P., and Murray, N.R. (2010). Protein kinase Ciota is required for pancreatic cancer cell transformed growth and tumorigenesis. Cancer Res *70*, 2064–2074.

Sebolt-Leopold, J. S. and English, J. M. (2006). Nature *441*, 457–462.

Seidman, J.D., Horkayne-Szakaly, I., Cosin, J.A., Ryu, H.S., Haiba, M., Boice, C.R., and Yemelyanova, A.V. (2006). Testing of two binary grading systems for FIGO stage III serous carcinoma of the ovary and peritoneum. Gynecol Oncol *103,* 703-708.

Senger, D.R., Galli, S.J., Dvorak, A.M., Perruzzi, C.A., Harvey, V.S., and Dvorak, H.F. (1983). Tumor cells secrete a vascular permeability factor that promotes accumulation of ascites fluid. Science *219*, 983–985.

Sharif, T.R., and Sharif, M. (1999). Overexpression of protein kinase C epsilon in astroglial brain tumor derived cell lines and primary tumor samples. Int J Oncol *15***,** 237-243.

Shih, L., and Kurman, R.J. (2004). Ovarian tumorigenesis: a proposed model based on morphological and molecular genetic analysis. Am J Pathol *164,* 1511-1518.

Shaw, T.J. and Vanderhyden, B.C. (2007). AKT mediates the pro-survival effects of KIT in ovarian cancer cells and is a determinant of sensitivity to imatinib mesylate. Gynecol Oncol *1,* 122-131.

Shaw TJ, Lacasse EC, Durkin JP, Vanderhyden BC. Downregulation of XIAP expression in ovarian cancer cells induces cell death in vitro and in vivo. Int J Cancer 2008;122:1430–4.

Sheng, M. and Sala, C. (2001). PDZ domains and the organizationof supramolecular complexes. Annu Rev Neurosci *24*, 1–29.

Slosberg, E.D., Klein, M.G., Yao, Y., Han, E.K., Schieren, I., and Weinstein, I.B. (1999). The α isoform of protein kinase C mediates phorbol ester-induced growth inhibition and p21cip1 induction in HC11 mammary epithelial cells. Oncogene *18*, 6658–6666.

Smith, J.B., Smith, L., and Pettit, G.R. (1985). Bryostatins: potent, new mitogens that mimic phorbol ester tumor promoters. Biochem Biophys Res Commun *132*, 939–945.

Sowter, H.M., and Ashworth, A. (2005). BRCA1 and BRCA2 as ovarian cancer susceptibility genes. Carcinogenesis *26*, 1651–1656.

Staudinger, J., Zhou, J., Burgess, R., Elledge, S.J., and Olson, E.N. (1995). PICK1: a perinuclear binding protein and substrate for protein kinase C isolated by the yeast two-hybrid system. J Cell Biol *128*, 263–271

Staudinger, J., Lu, J., and Olson, E.N. (1997). Specific interaction of the PDZ domain protein PICK1 with the COOH terminus of protein kinase C-α. J Biol Chem *272*, 32019–32024.

Ströhlein, M.A., Siegel, R., Jäger, M., Lindhofer, H., Karl-Walter, J., and Heiss, M.M. (2009). Induction of anti-tumor immunity by trifunctional antibodies in patients with peritoneal carcinomatosis. J Exp Clin Cancer Res *28*, 18.

Taylor, S.S., Knighton, D.R., Zheng, J., Sowadski, J.M., Gibbs, C.S., Zoller, M.J. (1993). A template for the protein kinase family. Trends Biochem Sci *18*, 84 -89.

Traxler, P. (2003). Tyrosine kinases as targets in cancer therapy – successes and failures. Expert Opin Ther Targets *7***,** 215-234.

Tsai, J.H., Tsai, M.T., Su, W.W., Chen, Y.L.,Wu, T.T., Hsieh, Y.S., Huang, C.Y., Yeh, K.T., and Liu, J.Y. (2005). Expression of protein kinase C alpha in biopsies and surgical specimens of human hepatocellular carcinoma. Chin J Physiol *48*, 139–143.

Tutt, A.N.J., Lord, C.J., McCabe, N., Farmer, H., Turner, N., Martin, N.M., Jackson, S.P., Smith, G.C.M., Ashworth, A. (2005). Exploiting the DNA repair defect in BRCA

mutant cells in the design of new therapeutic strategies for cancer," Cold Spring Harbor Symposia on Quantitative Biology 70, 139–148.

Vang, R., Shih, I., and Kurman, R.J. (2009). Ovarian low-grade and high-grade serous carcinoma: pathogenesis, clinicopathologic and molecular biologic features, and diagnostic problems. Adv Anat Pathol *16,* 267-282.

Varga, A., Czifra, G., Tallai, B., Nemeth, T., Kovacs, I., Kovacs, L., and Biro, T. (2004). Tumor grade-dependent alterations in the protein kinase C isoform pattern in urinary bladder carcinomas. Eur Urol *46*, 462–465.

Walsh, D.A., Ashby, C.D., Gonzalez, C., Calkins, D., Fischer, E.H, and Krebs, E.G. (1971). Purifi cation and characterization of a protein inhibitor of adenosine 3.′,5.′-monophosphate-dependent protein kinases. J Biol Chem *246*, 1977 -1985.

Waldron, R. T., and Rozengurt, E. (2003). Protein kinase C phosphorylates protein kinase D activation loop Ser744 and Ser748 and releases autoinhibition by the pleckstrin homology domain J Biol Chem *278*, 154-163.

Wang, Y., Cortez, D., and Yazdi, P. (2000). BASC, a super complex of BRCA1-associated proteins involved in the recognition and repair of aberrant DNA structures. Genes Dev *14*, 927–939.

Westerhoff, H.V., Hendler, R.W., Zasloff, M. and Juretic, D. (1989). Interactions between a new class of eukaryotic antimicrobial agents and isolated rat liver mitochondria. Biochim Biophys Acta *975***,** 361–369.

Weisberg, E., and Griffin, J.D. (2001). Mechanisms of resistance imatinib (STI571) in preclinical models and in leukemia patients. Drug Resist Update *4*, 22–28.

Wieprecht, T., Dathe, M., Schumann, M., Krause, E., Beyermann, M., and Bienert M. (1996). Conformational and functional study of magainin 2 in model membrane environments using the new approach of systematic double-D-amino acid replacement. Biochemistry *35***,** 10844–10853.

Wong, W. S., Wong, Y.F., Ng, Y.T., Huang, P., Chew, E.C., Ho, T.H., and Chang, M.Z. (1990). Establishment and characterization of a new human cell line derived from ovarian clear cell carcinoma. Gynecol Oncol *38*, 37 – 45.

Wood, C.D., Kelly, A.P., Matthews, S.A., and Cantrell, D.A. (2007). Phosphoinositide-dependent protein kinase-1 (PDK1)-independent activation of the protein kinase C substrate, protein kinase D. FEBS Lett *581*, 3494-3498.

Xia, J., Zhang, X., Staudinger, J., and Huganir, R.L. (1999). Clustering of AMPA receptors by the synaptic PDZ domain-containing protein PICK1. Neuron *22*, 179–187.

Xing, H., Weng, D., Chen, G., Tao, W., Zhu, T., Yang, X., Meng, L., Wang, S., Lu, Y., and Ma, D. (2008). Activation of fibronectin/PI-3K/Akt2 leads to chemoresistance to docetaxel by regulating survivin protein expression in ovarian and breast cancer cells. Cancer Lett *261*, 108–119.

Xu, J. and Xia, J. (2007). Structure and Function of PICK1. Neurosignals *15,* 190-201.

Yamashita, M., Ashino, S., Oshima, Y., Kawamura, S., Ohuchi, K., and Takayanagi, M. (2003). Inhibition of TPAinduced NF-kappaB nuclear translocation and production of NO and PGE2 by the anti-rheumatic gold compounds. J Pharm Pharmacol *55*, 245–251.

Yang, X., Fraser, M., Moll, U.M., Basak, A., and Tsang, B.K. (2006). Akt-mediated cisplatin resistance in ovarian cancer: modulation of p53 action on caspase-dependent mitochondrial death pathway. Cancer Res *66*, 3126–3136.

Yap TA, Boss DS, Fong PC, Roelvink, M., Tutt, A., Carmichael, J., O'Connor, M.J., Kaye, S.B., Schellens, J.H., de Bono, J.S. (2007). First in human phase I pharmacokinetic (PK) and pharmacodynamic (PD) study of KU-0059436 (Ku), a small molecule inhibitor of poly ADP-ribose polymerase (PARP) in cancer patients (p), including BRCA1/2 mutation carriers. J Clin Oncol *25*, (18S).

Yuan, Z.Q., Sun, M., Feldman, R.I., Wang, G., Ma, X., Jiang, C., Coppola, D., Nicosia, S.V., and Cheng, J.Q. (2000). Frequent activation of AKT2 and induction of apoptosis by inhibition of phosphoinositide-3-OH kinase/Akt pathway in human ovarian cancer. Oncogene. *19*, 2324–2330.

Yoneda, J., Kuniyasu, H., Crispens, M.A., Price, J.E., Bucana, C.D., Fidler, I.J. (1998). Expression of angiogenesis-related genes and progression of human ovarian carcinomas in nude mice. J Natl Cancer Inst *90*, 447–454.

Zhang, L., Huang, J., Yang, N., Liang, S., Barchetti, A., Giannakakis, A., Cadungog, M.G., O'Brien-Jenkins, A., Massobrio, M., Roby, K.F., Katsaros, D., Gimotty, P., Butzow, R., Weber, B.L., and Coukos, G. (2006). Integrative genomic analysis of protein kinase C (PKC) family identifies PKCiota as a biomarker and potential oncogene in ovarian carcinoma. Cancer Res *66***,** 4627–4635.

Zhuang, W., Qin, Z., and Liang, Z. (2009). The role of autophagy in sensitizing malignant glioma cells to radiation therapy. Acta Biochim Biophys Sin *41*, 341–351.

Zimmermann, P., Meerschaert, K., Reekmans, G., Leenaerts, I., Small, J.V., Vandekerckhove, J., and Gettemans, J. (2002). PIP 2 -PDZ domain binding controls the association of syntenin with the plasma membrane. Mol Cell *9*, 1215–1225.